NREL
NATIONAL RENEWABLE ENERGY LABORATORY

Development and Analysis of Desiccant Enhanced Evaporative Air Conditioner Prototype

Eric Kozubal, Jason Woods, and Ron Judkoff

NREL is a national laboratory of the U.S. Department of Energy, Office of Energy Efficiency & Renewable Energy, operated by the Alliance for Sustainable Energy, LLC.

Technical Report
NREL/TP-5500-54755
April 2012

Contract No. DE-AC36-08GO28308

NREL
NATIONAL RENEWABLE ENERGY LABORATORY

Development and Analysis of Desiccant Enhanced Evaporative Air Conditioner Prototype

Eric Kozubal, Jason Woods, and Ron Judkoff

Prepared under Task No. BEC7.1302

National Renewable Energy Laboratory
15013 Denver West Parkway
Golden, Colorado 80401
303-275-3000 • www.nrel.gov

Technical Report
NREL/TP-5500-54755
April 2012

Contract No. DE-AC36-08GO28308

NOTICE

Available electronically at http://www.osti.gov/bridge

Available for a processing fee to U.S. Department of Energy
and its contractors, in paper, from:

U.S. Department of Energy
Office of Scientific and Technical Information
P.O. Box 62
Oak Ridge, TN 37831-0062
phone: 865.576.8401
fax: 865.576.5728
email: mailto:reports@adonis.osti.gov

Available for sale to the public, in paper, from:

U.S. Department of Commerce
National Technical Information Service
5285 Port Royal Road
Springfield, VA 22161
phone: 800.553.6847
fax: 703.605.6900
email: orders@ntis.fedworld.gov
online ordering: http://www.ntis.gov/help/ordermethods.aspx

Cover Photos: (left to right) PIX 16416, PIX 17423, PIX 16560, PIX 17613, PIX 17436, PIX 17721

Printed on paper containing at least 50% wastepaper, including 10% post consumer waste.

Acknowledgments

We wish to acknowledge the efforts of many industry experts who provided valuable knowledge and support in developing the prototype desiccant enhanced evaporative air conditioner (DEVAP AC):

We would like to acknowledge Andrew Lowenstein from AIL Research for participating in project planning, design, and prototype development. Throughout the project, Andrew provided invaluable guidance and supporting analysis. His expertise was instrumental in the success of this project.

We would like to acknowledge Dylan Garrett, Ian Graves, and Redwood Stephens from Synapse Product Development for participating in a design and prototype development. Throughout the project, the Synapse team provided excellent guidance in manufacturing design. Their design team was instrumental to the success of this project.

We would like to acknowledge John Pellegrino from the University of Colorado at Boulder for his extensive knowledge of design and testing of membrane systems, Dave Paulson from Water Think Tank for his insight into the membrane component manufacturing industry and selection of industry vendors, and Michael Brandemuehl from the University of Colorado at Boulder for his experience with heating, ventilation, and air-conditioning systems and desiccants.

We would like to acknowledge Jay Burch for his guidance in planning and executing this project.

We would like to acknowledge Aaron Boranian for his assistance in analysis of the two-stage regenerator.

We would like to acknowledge Jordan Clark from the University of Texas for his analysis of air flow through the second-stage heat and mass exchanger using computational fluid dynamics.

We would like to thank the NREL peer review team: Bill Livingood, Michael Deru, Paul Torcellini, Dane Christiansen, and Ren Anderson.

We would like to thank Stephanie Woodward for her editorial review.

We would like to thank Alexis Abramson, Colin McCormick, and Tony Bouza from the U.S. Department of Energy for their support of the DEVAP prototype project.

Executive Summary

In FY 2010, the National Renewable Energy Laboratory (NREL) used numerical models and building energy simulations to analyze the performance of a DEVAP AC for residential and commercial buildings. For commercial buildings, the building energy simulations showed 80% and 40% source energy savings in a typical office building in Phoenix and Houston, respectively, compared to a high-efficiency vapor compression AC (Kozubal et al. 2011).

In FY 2011, NREL was tasked to design and build a prototype DEVAP AC for testing at NREL's Advanced Heating, Ventilation, and Air-Conditioning (HVAC) Systems Laboratory. The purposes of this effort were to:

1. Construct a DEVAP prototype.
2. Validate DEVAP cycle performance used to predict energy savings.
3. Validate numerical model and design tools to predict performance of future designs.
4. Improve cost, weight, and size estimates of future designs.

The design approach used the previously developed numerical model to investigate many variables and find near-optimal designs of small size (and therefore low cost) and with high energy efficiency. Two vendors (AIL Research and Synapse Product Development) were selected competitively to construct the DEVAP prototypes. They proposed changes to the near-optimal designs developed by NREL to fit their manufacturing techniques and their use of off-the-shelf components. Future work will focus on achieving smaller size and better efficiency.

Experimental Approach

The two DEVAP prototypes were delivered in two distinct heat and mass exchangers: a first-stage dehumidifier and a second-stage indirect evaporative cooler. They were assembled with a previously developed desiccant regenerator now being used in AIL Research's commercially available low-flow liquid desiccant AC. We tested the prototype system at NREL's Advanced HVAC Systems Laboratory. A number of tests, sufficient for characterizing performance, were conducted at various airflow rates, liquid desiccant concentrations and flow rates, and a range of return air and outdoor air psychrometric conditions.

Results

An effective integrated energy efficiency ratio ($IEER_{effective}$) was calculated to be 23.2 for the DEVAP AC, based on test standard 340/360 (AHRI 2007) for rating AC performance. For comparison, typical high-efficiency vapor compression AC achieves IEERs up to 15.4. DOE's goal in their high performance rooftop unit challenge (DOE 2012) is an IEER of 18, a level requiring state of the air technology. The American Society of Heating, Refrigerating and Air-Conditioning Engineers standard 90.1 2010 specifies a minimum of 11.2 for a 10-ton commercially packaged air-cooled unit (ASHRAE 2010). Energy savings are expected to be greater than indicated by the $IEER_{effective}$ measurement, because this standardized test does not fully account for the savings potential for desiccant and evaporative cooling technologies. Annual building energy simulations provide the best comparison of actual energy performance between a DEVAP and a vapor compression AC. Most test results agreed with our numerical model to within ±10% in cooling capacity, electricity use, thermal energy use, and water

evaporation rate. The AIL Research first-stage heat and mass exchanger had known issues that reduced its latent cooling capacity by 22%, which affects size but not efficiency.

Conclusions

The agreement in efficiency, measured by the coefficient of performance (COP), between the numerical model and the experiments (Figure ES–1) adds confidence to our previous building energy simulation results (Figure ES–2). It also empowers the model as a tool for future designs. A second-generation DEVAP AC was designed with this model, which showed significant size reductions and additional optimized design features. These features were based on a parametric analysis with the model and lessons learned from the two first-generation prototypes. The result is a smaller, lower cost second-generation prototype design. We estimate the footprint and weight to be equal to a vapor compression unit with an IEER of 14.5, except the DEVAP unit would have an $IEER_{effective}$ of 23.2. We estimate the retail cost to be 28% higher. Based on the estimated cost premium and the simulated energy savings, we estimate a simple payback of less than two years in Phoenix and less than three years in Houston.

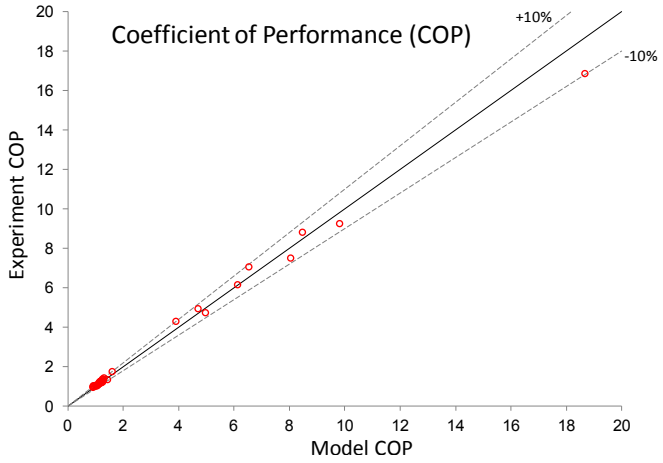

Figure ES–1 Model-experiment agreement of cooling efficiency (coefficient of performance)

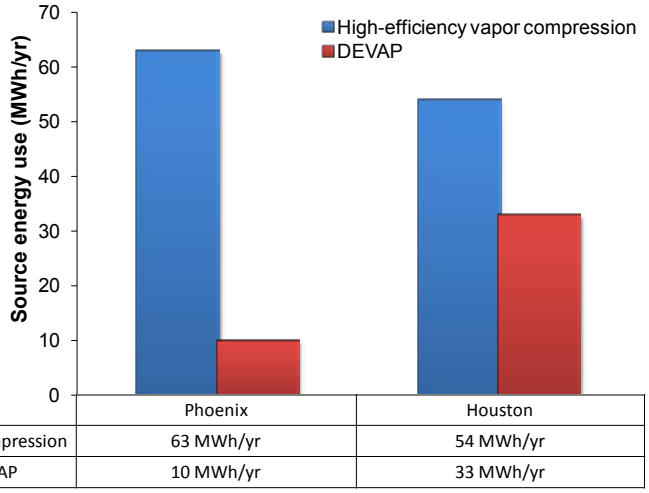

	Phoenix	Houston
Vapor compression	63 MWh/yr	54 MWh/yr
DEVAP	10 MWh/yr	33 MWh/yr

Figure ES–2 Source energy use estimate for a small office building from previous research (Kozubal et al. 2011)

Nomenclature

A	heat transfer area (ft^2/ton)
AHRI	Air-Conditioning, Heating, and Refrigeration Institute
AC	air conditioning or air conditioner
CAD	computer-aided design
C_{LD}	liquid desiccant concentration ($kg_{salt}/kg_{solution}$)
COP	coefficient of performance
COP_{latent}	water removal source COP by the regenerator
COP_{space}	total space cooling source COP
COP_{unit}	total cooling source COP
DEVAP	desiccant enhanced evaporative
DH	dehumidification mode
EA	exhaust air
EER	energy efficiency ratio (Btu/Wh)
Gen-1	generation 1
Gen-2	generation 2
gpm	gallons per minute
H	height
H_{e1}	stage 1 exhaust air channel height
H_{e2}	stage 2 exhaust air channel height
H_{s1}	stage 1 supply air channel height
H_{s2}	stage 2 supply air channel height
HMX	heat and mass exchanger
HVAC	heating, ventilation, and air conditioning
ICHX	interchange heat exchanger
IEC	indirect evaporative cooler or indirect evaporative cooling
IEER	integrated energy efficiency ratio (Btu/Wh)
$IEER_{effective}$	integrated energy efficiency ratio of the DEVAP AC using the calculation method described in Section 3.3 (Btu/Wh)
LD	liquid desiccant
LDAC	liquid desiccant air conditioner
NREL	National Renewable Energy Laboratory
OA	outdoor air
P_{amb}	ambient pressure (psi)
P_{fan}	fan power (kW)

PP	polypropylene
$Q_{cooling}$	total cooling (kW or Btu/h)
Q_{latent}	latent cooling (kW or Btu/h)
$Q_{sensible}$	sensible cooling (kW or Btu/h)
Q_{th}	thermal power (kW)
RA	return air
SA	supply air
S1	airstream state 1 – inlet mixed airstream to conditioner
S1.5	airstream state 1.5 – airstream at the state between the first- and second-stage conditioner sections
S2	airstream state 2 – supply airstream from conditioner
S3	airstream state 3 – purge air inlet to first-stage conditioner
S4	airstream state 4 – exhaust air outlet from first-stage conditioner
S5	airstream state 5 – exhaust air outlet from second-stage conditioner
SCFM	standard cubic feet per minute
T_{db}	dry bulb temperature (°F)
$T_{db,in}$	inlet dry bulb temperature (°F)
T_{dp}	dew point temperature (°F)
T_{OA}	outdoor air dry bulb temperature (°F)
$T_{OA,wb}$	outdoor air wet bulb temperature (°F)
T_{SA}	supply air dry bulb temperature (°F)
T_{wb}	wet bulb temperature (°F)
$T_{wb,in}$	inlet wet bulb temperature (°F)

Greek symbols

ε_{wb}	wet bulb effectiveness: $\varepsilon_{wb} = \frac{T_{db,in} - T_{SA}}{T_{db,in} - T_{wb,in}}$
Δh	change in enthalpy (Btu/lb_m)
ΔP	change in pressure (in H_2O)
ΔT	change in temperature (°F)
ω	humidity ratio (lb_m/lb_m)
$\Delta\omega$	change in humidity ratio (lb_m/lb_m)

Contents

Figures and Tables

Figures

Tables

1.0 Introduction

This report documents the design of a desiccant enhanced evaporative air conditioner (DEVAP AC) prototype and the testing to prove its performance. Previous numerical modeling and building energy simulations indicate a DEVAP AC can save significant energy compared to a conventional vapor compression AC (Kozubal et al. 2011). The purposes of this research were to build DEVAP prototypes, test them to validate the numerical model, and identify potential commercialization barriers.

The prototypes were built with two vendors: AIL Research and Synapse Product Development (Synapse). An iterative process consisting of collaborative design, numerical modeling, and component testing transformed the conceptual design criteria into two working prototypes. Pursuing two independent design approaches provided us the opportunity to incorporate the best features of both into a second-generation (Gen-2) prototype.

The prototypes were tested at the National Renewable Energy Laboratory's (NREL) Advanced Heating, Ventilation, and Air-Conditioning (HVAC) Systems Laboratory (NREL 2005) over a range of operating conditions and inlet air temperatures and humidities. A key barrier to commercializing a DEVAP AC is that the cost and performance tradeoffs associated with changes in product designs cannot be accurately predicted. Prototype testing validated the numerical model making it a design tool that can rapidly—and quite accurately—predict these tradeoffs. This design tool, along with the experience from prototype construction, is used to estimate the cost, weight, and size of a Gen-2 packaged design.

1.1 DEVAP AC Design Innovations

Figure 1–1 shows a schematic of the DEVAP AC and its airflows. A top view of the airflow channels and the thermodynamics of the process are shown in Figure 1–2 and Figure 1–3. Air states are numbered in each graph. We refer to airstreams as moving from one state to the next. For example, airstream 1-1.5 is the stream of air moving from air state 1 (S1) to air state 1.5 (S1.5). The prototypes were designed in two distinct stages: a first-stage dehumidifier and a second-stage indirect evaporative cooler (IEC).

The first-stage dehumidifier is a cross-flow heat and mass exchanger (HMX) between two airstreams (airstreams 1-1.5 and 3-4). Desiccant and water flow vertically and are gravity driven. The desiccant is contained by a polypropylene (PP) microporous membrane (Z-series from Celgard LLC). AIL Research used nozzles to spray a high water flow rate that created a two-phase flow of water and outdoor air (OA) in airstream 3-4. The Synapse design used a low water flow rate that was spread by wicked surfaces in contact with airstream 3-4. Membranes were not used for water containment in either prototype. A waterside membrane was too risky for proper operation and demonstration at this early development phase. However, it may be used in the future for controlling biological growth, because it creates a barrier that prevents organisms from implanting onto wet surfaces.

The second stage is an NREL-designed counterflow IEC with wet bulb effectiveness (ε_{wb}) measured at 120%–128% at the design mass flow rate. For both designs, a low flow rate of water was distributed across the heat transfer surfaces by a wicking material.

Splitting DEVAP into two distinct stages gives HVAC designers many options for placing the two functions in different areas of a building. This strategy thus led to the creation of three potential products:

- Dehumidifier for OA pretreatment (first-stage HMX)
- Evaporative AC only (second-stage HMX)
- DEVAP AC system (combined first- and second-stage HMXs).

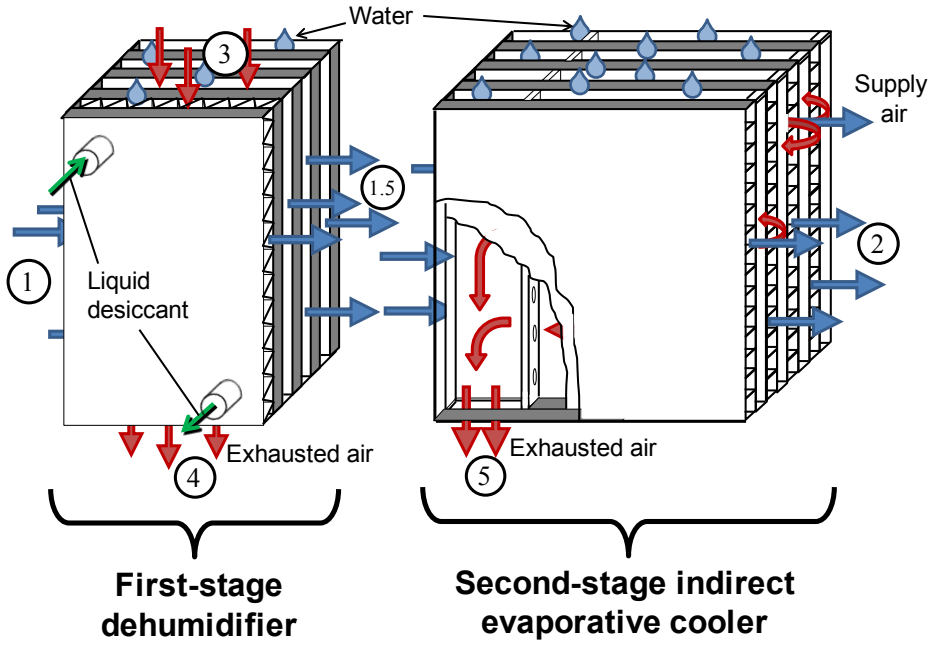

Figure 1–1 Schematic of two-stage DEVAP AC

Illustration by Eric Kozubal and Jason Woods, NREL

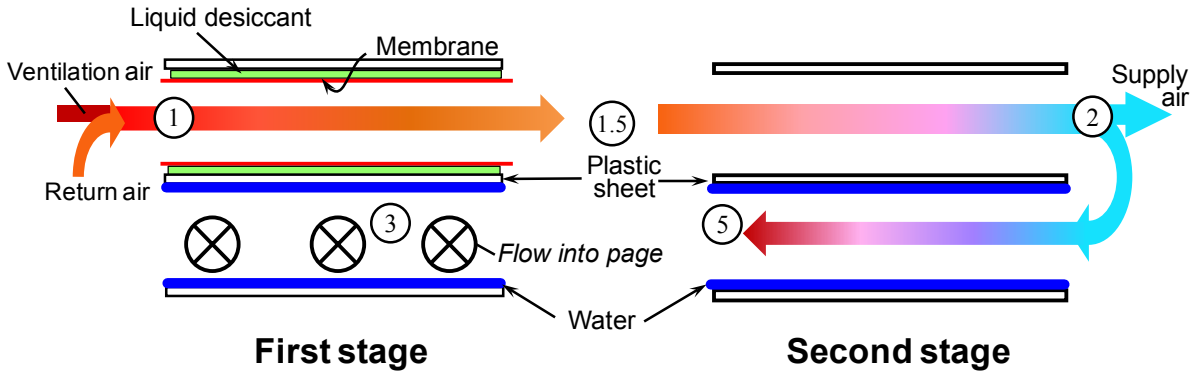

Figure 1–2 Top view of internal air passages in a single channel pair

Illustration by Eric Kozubal and Jason Woods, NREL

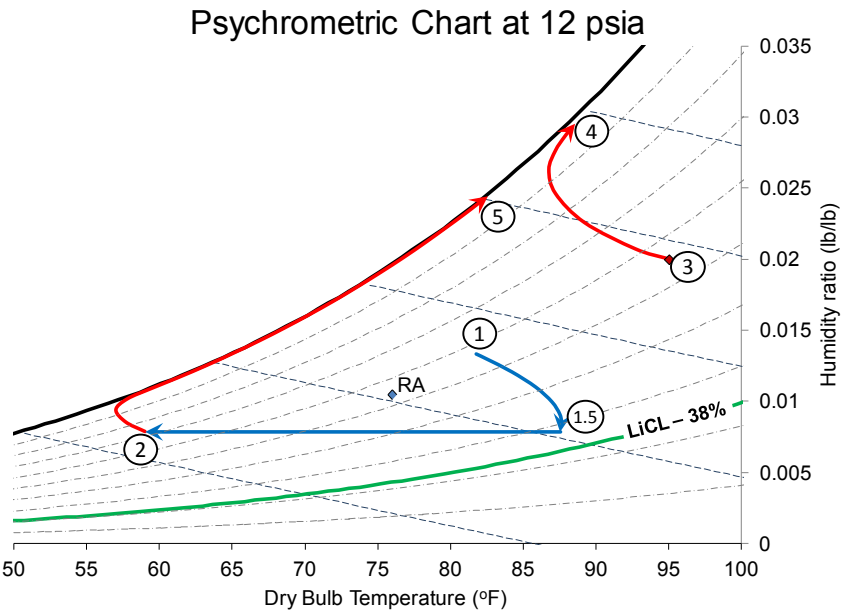

Figure 1–3 Air states shown on a psychrometric chart (RA = return air)

The first-generation (Gen-1) prototypes were built for proof of performance. The project timeline and funding required the following considerations:

- Success depended on the HMXs achieving the predicted performance.
- The design space for a DEVAP AC is large, with many variables and complex interactions that require investigation.
- Independent variables include:
  - Form factor (height, width, length)
  - Airflow channel sizes (height, width)
  - Airflow rate and resulting airflow regime (laminar versus turbulent)
  - Desiccant flow rate
  - Desiccant concentration (salt fraction by weight in solution)
  - Specific cooling rate (enthalpy change of the air)
  - Manufacturing method
  - Material selection, including membrane type and performance.
- Dependent variables include:
  - Size and weight
  - Pressure drop and electrical energy use
  - Cooling efficiency (coefficient of performance or COP)
  - Cost.

- The desiccant was regenerated using a single-effect scavenging air regenerator already being commercialized by AIL Research in its low-flow liquid desiccant air conditioner (LDAC) product (see Section 2.3). Energy performance was estimated using a two-stage regenerator model that was validated for a sample of points (see Section 3.0).
- The system would be configured without packaging that would normally be required in a product.
    - Fans were not included. Fan power was estimated using laboratory pressure loss data and nominal efficiency.
    - Pumping power was not indicative of an actual product because of the prototype's small size and added liquid sensors. Thus, this power was also calculated using head pressure and nominal pump efficiency.

Having two vendors enabled us to develop two design strategies, manufacturing methods, and material choices. Given the many variables and time constraints, some aspects of both designs had to use off-the-shelf components, which meant these first prototypes would not be optimized for performance, size, weight, and cost. Instead, the project focused on validating the numerical model, which could then be used to create future designs, including a Gen-2 design that incorporates the best features of the AIL Research and Synapse prototypes.

2.0 Design Optimization

At the start of the project, we developed design criteria from a parametric analysis with our thermodynamics-based numerical model. These criteria set the geometric parameters, materials, and manufacturing methods. With this basic blueprint, we sought expert manufacturing vendors to develop a prototype. We contracted with Dave Paulson from Water Think Tank and John Pellegrino from the University of Colorado, Boulder to create selection criteria and identify candidate companies. We identified eight companies and ultimately chose AIL Research (www.ailr.com) and Synapse Product Development (www.synapse.com).

AIL Research previously developed the low-flow LDAC with NREL and has expertise in the manufacture of prototype desiccant systems. Its founder, Andrew Lowenstein, is widely regarded as a top expert in the field of liquid desiccant (LD) cooling. Synapse designs products for other entities that do not have the necessary staff and prototyping capabilities. Synapse uses many manufacturing partnerships for rapid prototype development. Its engineering staff has designed plate-and-frame membrane systems with similar requirements to a DEVAP prototype.

Figure 2–1 outlines the method used to develop the two prototypes. NREL and the two vendors used an iterative process to design the Gen-1 prototype. This process involved numerical modeling, component testing, experience from NREL about desired design features, and experience from the vendors about manufacturing methods.

The iterative process starts with the numerical modeling. The design goal was to optimize the conditioner to provide efficient space cooling, which was calculated from return air (RA) to supply air (SA). The system uses 0%-30% OA to provide the necessary airflow for the second-stage HMX, and by doing so creates a 0%–30% guaranteed ventilation rate. However, to properly converge on efficient space cooling performance, the cooling required to bring the OA to room neutral conditions was not included. This ensures that the process converges on a design that provides efficient space cooling, and not one that only provides efficient ventilation. We used the following peak design conditions:

- OA at a 95°F, humidity ratio (ω) = 0.020 lb/lb
- RA at 76°F, ω = 0.010 lb/lb
- SA flow rate = 380 SCFM/space cooling ton
- First-stage exhaust air (EA) ratio = 0%–50%
- Second-stage EA ratio = 0%–40%
- Design OA fraction = 30%
- SA change relative to RA: enthalpy change = 7 Btu/lb, sensible heat ratio = 0.6 (SA = 59°F, ω = 0.0077 lb/lb)
- Desiccant inlet and outlet concentration = 38% and 36% by weight of lithium chloride resulting in a flow rate = 0.34 gpm/space cooling ton.

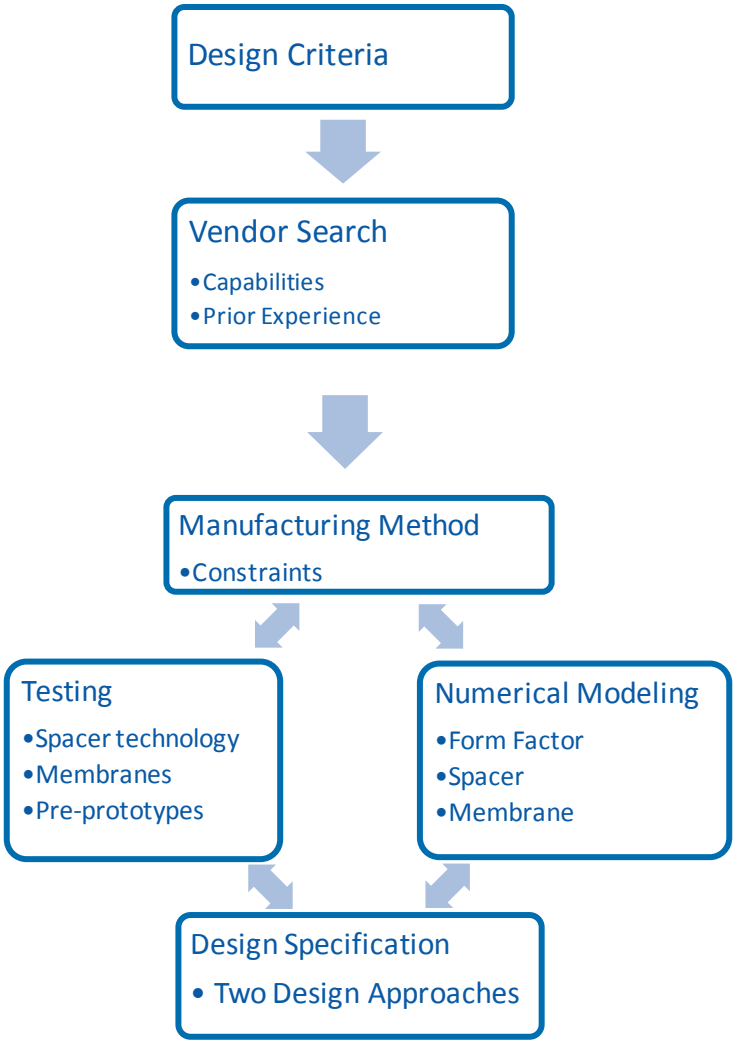

Figure 2–1 Design approach flow diagram

The numerical modeling determined the performance based on a range of independent variable combinations. We developed routines to determine near-optimal designs that balance source energy space cooling COP (COP_{space}), size, and material costs given the constraints on manufacturing methods and available off-the-shelf parts. Figure 2–2 and Figure 2–3 show how the process was used to explore the sensitivity and interaction between channel heights (H): stage 1 SA (H_{s1}), stage 2 SA (H_{s2}), stage 1 EA (H_{e1}), and stage 2 EA (H_{e2}). In these two charts, our method seeks a design in the upper left corner. This results in high efficiency with minimal heat transfer area, a surrogate for size, weight, and cost. Cost was not used explicitly because this surrogate is sufficient for this stage of development.

We started with a design at the intersection of all the sensitivity lines (diamond point). We used the sensitivity shown in Figure 2–2 to find the path that maximizes COP_{space} at a reduced area. This leads to the next iterative point in Figure 2–3. This process defines the "knee" in the curve where smaller heat transfer area results in significantly reduced COP_{space}. We then used our engineering judgment to choose a near-optimal design with heat transfer area and COP_{space} near this "knee". We discuss only the interactions of channel heights in this report; however, in

practice we accounted for the interactions of all factors listed. Section 4.0 discusses COP_{space} versus heat transfer area for each prototype and a proposed Gen-2 design.

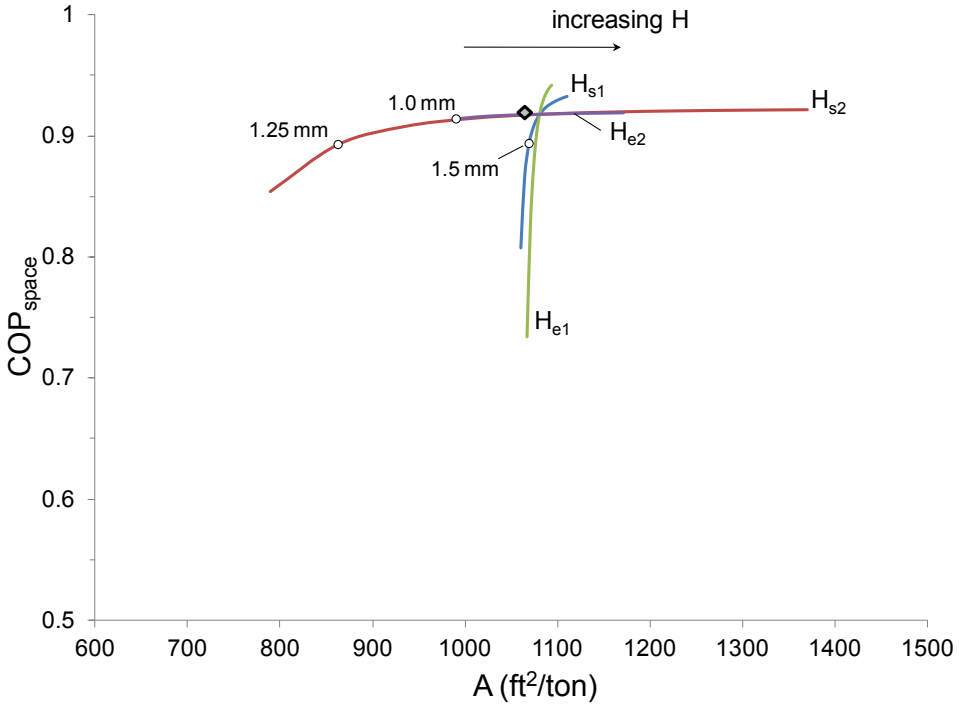

Figure 2–2 Example of interaction between channel heights, heat transfer area, and COP_{space}

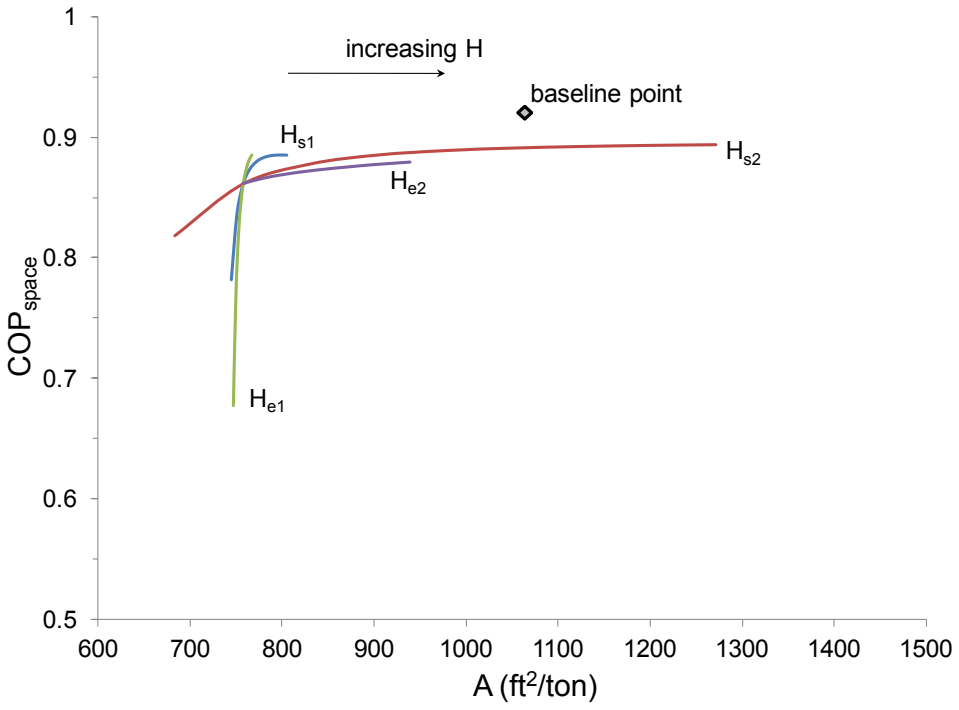

Figure 2–3 Example of interaction between channel heights, heat transfer area, and COP_{space} showing next iterative point

The optimization process was used at the start of the project to determine an initial conceptual design. With this in mind, we began an independent collaborative design process with each vendor in which ideas about manufacturing methods and their effects on performance were exchanged. The vendors focused on construction methods. NREL focused on achieving higher heat and mass transfer and uniform air flow. This led us to focus on the development of two critical features: a support spacer for the air gaps, and a membrane for desiccant containment.

The spacer performs two functions: (1) it maintains airflow gap geometry; and (2) it enhances heat and mass transfer without excessive friction loss (pressure drop).

To find suitable spacers, we tested off-the-shelf and newly constructed components. We then developed evaluation techniques. This involved the construction of an air channel test apparatus for air to liquid flow evaluation. Heat and mass transfer in this the DEVAP geometry is not well developed in industry, and literature searches turned up little information. Our work on characterizing the pressure drop and heat transfer performance of these spacers was submitted to the journal *Applied Thermal Engineering* (Woods and Kozubal 2012b).

We identified the microporous PP membrane from Celgard LLC as a good candidate for use in DEVAP. This membrane came with the option of a nonwoven PP adhered backing, which improves tear resistance, but reduces the diffusion coefficient. We used data from the manufacturer and from nitrogen gas permeation tests to estimate the water vapor diffusion coefficient for the unbacked and backed versions, then used these estimates in the numerical model to calculate vapor transport through the membrane.

The DEVAP design evolved with these new performance data for the spacers and the membrane and with input from the vendors. We adjusted the design as constraints and data on manufacturing methods, materials, geometry, and membrane and spacer performance became apparent. Two 1/10-scale pre-prototypes were then created, built, and delivered for testing at NREL's Advanced HVAC Systems Laboratory. After testing, we conducted a redesign review with each firm to determine areas for improvement. We then collaborated on two full-scale prototypes with nominal capacity of 1 ton at Air-Conditioning, Heating, and Refrigeration Institute (AHRI) standard conditions.

2.1 AIL Research Prototype Description

The construction of the AIL Research prototype revolved around extruded PP plastic made by Coroplast (Figure 2–4). A computer-aided design (CAD) rendering of the first- and second-stage DEVAP HMXs is shown in Figure 2–5. Numbers in the figure indicate airstreams in and out of the device as described in Figure 1–1. A photo of the assembled first-stage HMX is shown in Figure 2–6.

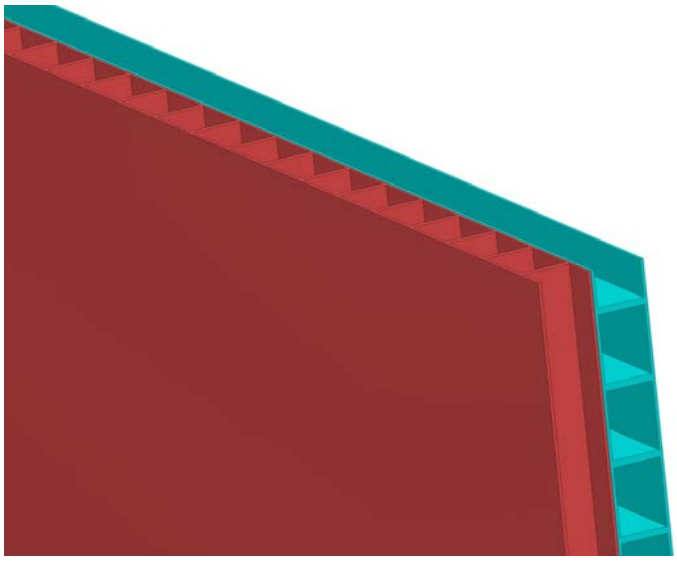

Figure 2–4 Example of extruded PP sheets

Illustration by Andrew Lowenstein, AIL Research, used by permission

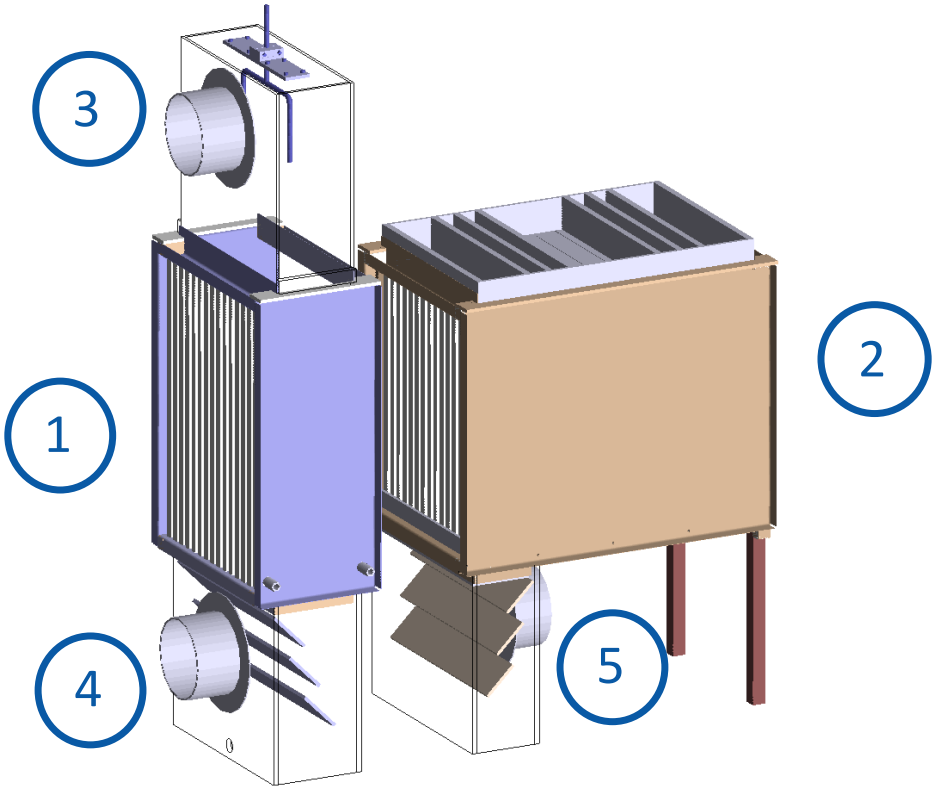

Figure 2–5 CAD rendering of the AIL Research DEVAP AC showing first- and second-stage HMXs in the enclosure. Airstream numbers are also shown.

Illustration by Andrew Lowenstein, AIL Research, used by permission

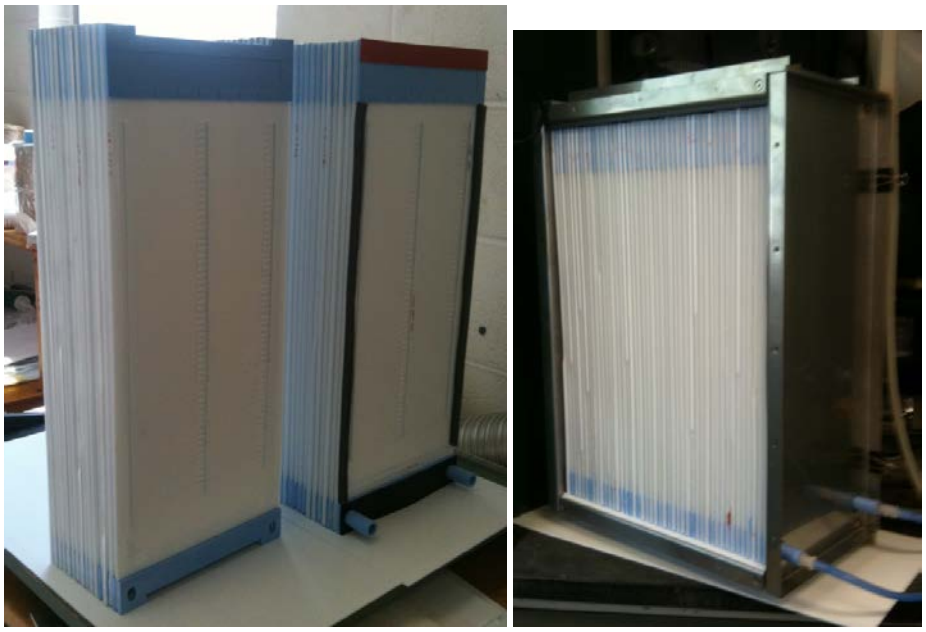

Figure 2–6 Subassembly and fully assembled view of AIL Research first-stage conditioner

Photo from Andrew Lowenstein, AIL Research, used by permission

In the first-stage, AIL Research used the flutes created by the Coroplast extrusion to form the coolant airstream 3-4. Water was distributed via flow nozzles at the top of the HMXs (shown in the airstream 3 plenum) and mixed with airstream 3-4, which ran vertically downward. Some water evaporated as it traveled through the HMX, but most was collected at the bottom of the airstream 4 plenum. Louvers shown in this plenum were used to separate the water droplets from the airstream. Because this design did not have a method to hold up the water internal to the flutes (e.g., wicked surfaces), this configuration requires a water flow rate that is significantly higher than the water evaporation rate. Thus, a water reservoir and pump are required to return the water from the collection sump to the top flow nozzles.

The unbacked Celgard PP membrane was welded to the Coroplast extrusions using techniques developed by AIL Research. A liquid manifold design (proprietary to AIL Research) distributed desiccant to the space between the membrane and Coroplast. Air gaps on airstream 1-1.5 were maintained by strips of Coroplast spacers with the extruded flutes oriented parallel to the airflow. The design also incorporated proprietary AIL Research spacers that mix the airstream to enhance heat and mass transfer.

A photo of the assembled second-stage HMX is shown in Figure 2–7. AIL Research used the Coroplast flutes to form the SA channels (airstream 1.5-2). A nylon wick was applied to the outer walls of the PP. These subassemblies were then stacked with spacers between each to form the EA channels (airstream 2-5). A low flow of water was distributed into the second-stage EA channels from the top. The nylon wick had sufficient water upkeep to allow this flow rate to be marginally above the water evaporation rate. Thus, a solenoid valve controlling domestic cold water is the only mechanism required to distribute water. Purge water was collected at the bottom of the EA plenum (airstream 5), at which point it was directed to a drain.

Figure 2–7 Fully assembled view of AIL Research second-stage conditioner (outlet airstream 2 shown)

Photo by Eric Kozubal, NREL

Wicked surfaces provide the following advantages for IECs:

- The wicking ensures that the walls are fully wetted and there is no lost evaporation area.
- The water feed rate can be held to a factor of 1.25-2 times that of the evaporation rate. This technique allows for "once-through" water use. The water that drains off the HMX is concentrated with minerals and can then be drained away. A sump and pumping system are no longer required, which improves energy performance and eliminates sump-borne biological growth.
- A simple controller in the AC can periodically use fresh (low concentration) water to rinse the HMX and clear any built-up minerals.

Airstreams 1.5-2 and 2-5 are in counterflow in the second-stage HMX. A sensitivity analysis showed that the cooling effectiveness could be reduced by as much as 20% if proper counterflow was not achieved. Airstream 1.5-2 flowed straight, through extruded flutes, but airstream 2-5 required a 90-degree turn before exiting the HMX. NREL used computational fluid dynamics software to design an air restrictor to ensure proper counterflow of airstream 2-5. Figure 2–8 shows the resulting stream lines of the EA stream with this air restrictor. Both vendors incorporated this technique in their final designs.

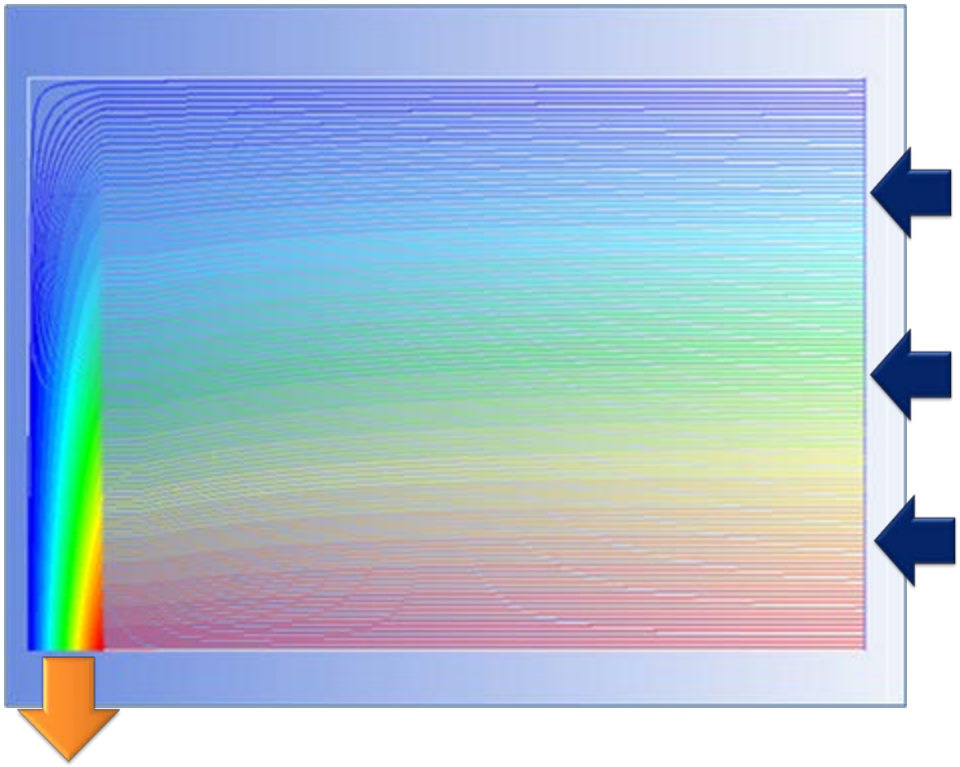

Figure 2–8 Stream lines from computational fluid dynamics software showing the airflow pattern in airstream 2-5. The color map represents the stream function values. Areas with sharp color transitions indicate higher velocity flow.

2.2 Synapse Prototype Description

The construction of the Synapse prototype revolved around laminated layers of polyethylene terephthalate (PET) plastic that were adhered with layers of acrylic pressure-sensitive adhesive (see Figure 2–9). Although this assembly method cannot easily be scaled to high-volume manufacturing, the achievable geometries are nearly ideal and therefore appropriate for prototypes. This enabled us to create a prototype with parallel plate geometry and to include airside turbulators to enhance heat and mass transfer on airstreams 1-1.5 and 3-4.

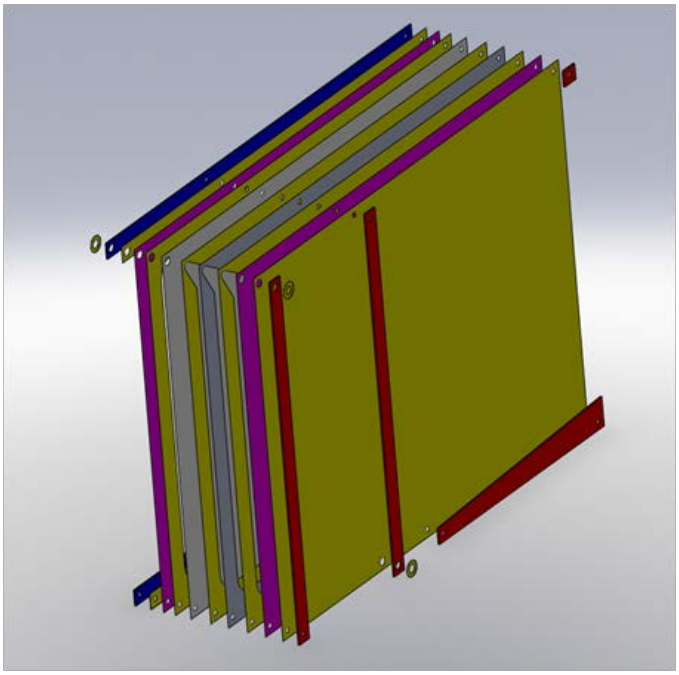

Figure 2–9 Example CAD rendering of laminated design approach showing layers of polyethylene terephthalate plastic, membrane, and pressure-sensitive adhesive

Illustration by Ian Graves, Synapse, used by permission

For the first-stage, the laminated layers enabled us to use wicked surfaces in the airstream 3-4 channels. For the spacer, we adapted an off-the-shelf expanded aluminum grating made by Permatron, because an optimized solution was not feasible in the project schedule. The spacer created airflow channels that were larger than optimum and would not be used in a future product design. This spacer was used in airstream 1-1.5 and airstream 3-4.

The Synapse design used the same expanded PP hydrophobic membrane from Celgard, but was backed with a nonwoven PP fabric to add strength. The backing reduces vapor diffusion through the membrane, but increases tear resistance. Synapse oriented the backing to the airside gap, where tears can originate from abrasion by foreign objects or the aluminum spacer.

Synapse developed a desiccant manifold that used laminated layers of plastic and adhesive to effectively and evenly distribute LD behind the membrane. Distribution was verified using dyed water flowing through a sample assembly as a method of flow visualization.

The Synapse second stage used laminated construction, but with minimal spacers to create laminar flow, parallel plate air channels. The design used Coroplast strips as airflow spacers and wicked surfaces on the wet side of the HMX.

The Synapse first- and second-stage HMXs are shown together in Figure 2–10 and Figure 2–11. Numbers in the figure indicate airstreams in and out of the device as described in Figure 1–1

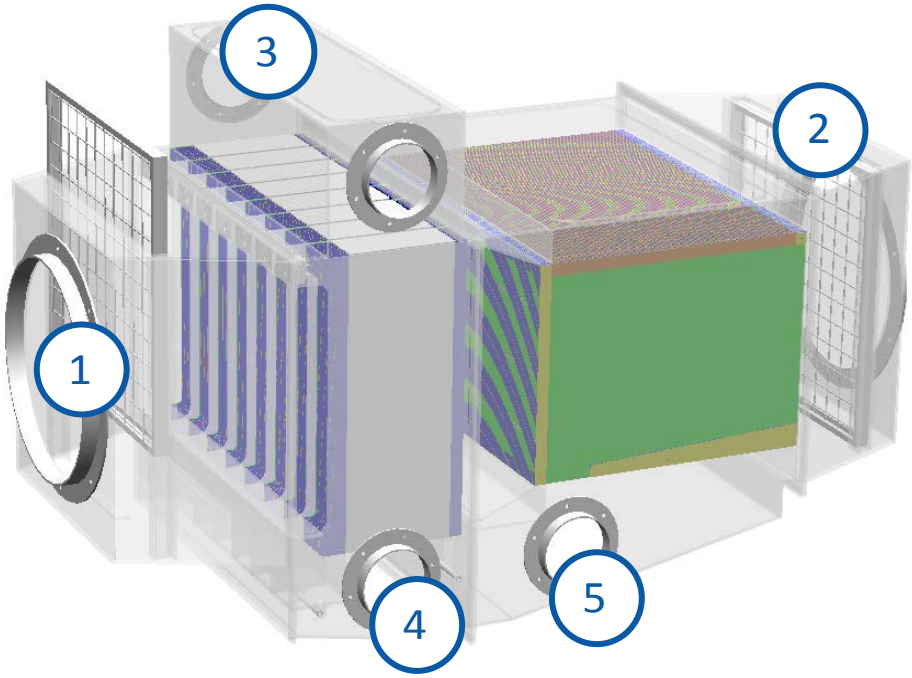

Figure 2–10 CAD rendering of the Synapse DEVAP AC showing first- and second-stage HMXs in the enclosure. Airstream numbers are also shown.

Illustration by Ian Graves, Synapse, used by permission

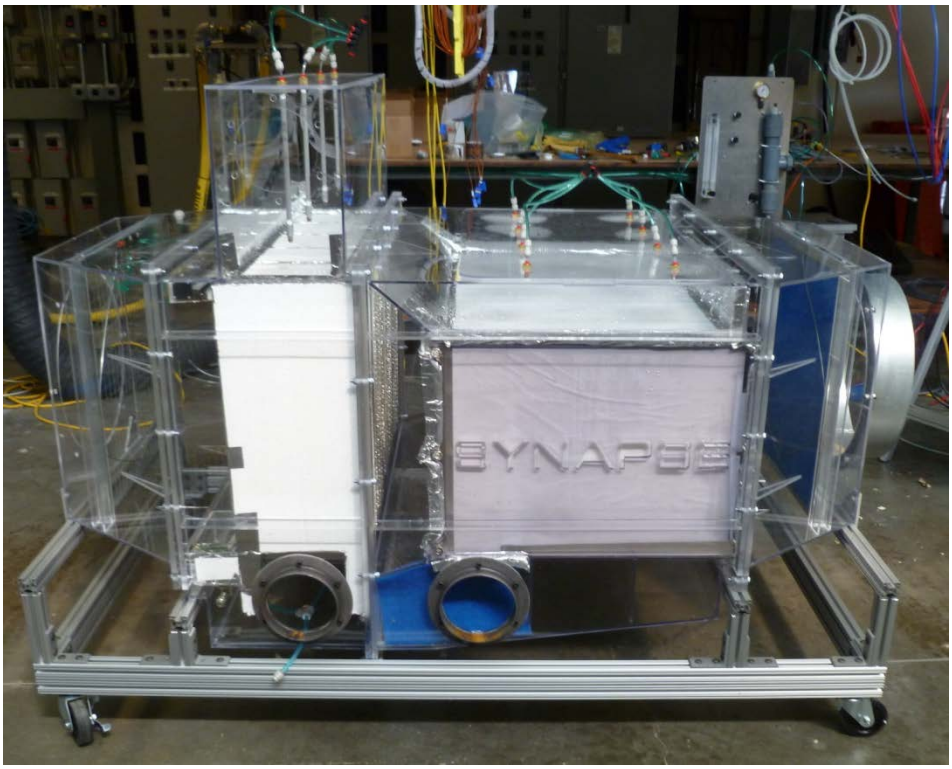

Figure 2–11 Photo showing the Synapse HMXs at the NREL HVAC laboratory

Photo by Eric Kozubal, NREL

2.3 Balance of System Description

In addition to the two prototype DEVAP conditioners, NREL assembled the balance of system in the laboratory for testing. We used a scavenging air LD regenerator developed for NREL by AIL Research (Lowenstein et al. 2006) (see Figure 2–12). This regenerator, shown in Figure 5 of Lowenstein's report, was delivered to NREL in 2006. For this project, we sent the regenerator back to AIL Research to refurbish it for use with the DEVAP AC. The delivered unit had the following characteristics:

- Two-ton (about 24 lb/h) low-flow LD regenerator that accepts approximately 8 gpm of hot water. Hot water was supplied by the boiler system at NREL's laboratory.
- LD storage tank, designed specifically for DEVAP desiccant concentration working range.
- Interchange heat exchanger (ICHX) to improve regeneration efficiency.
- A desiccant pump and fittings to circulate desiccant from the tank to the scavenging air regenerator component.

We connected the regenerator and conditioner with off-the-shelf components PP desiccant storage tank, Kynar tube fittings, polyvinyl chloride tubing for liquid delivery, and a magnetic drive centrifugal pump from March Pumps). Two toroidal conductivity sensors from Analytical Technology Inc. (ATI Q45CT) measured the salt concentration of the lithium chloride solution from Kathabar. These sensors were used to measure inlet and outlet concentrations from the DEVAP AC. A schematic of the system configuration is shown in Appendix A, Figure A–1.

We connected the airstreams to the HVAC laboratory to measure all inlet and outlet airflow rates, temperatures, and humidities. The laboratory control software maintained set points for the inlet airstreams and controlled the water feed rate to the systems by modulating a control valve. The software maintained inlet desiccant concentration to a typical dead band of two percentage points by modulating the desiccant regenerator on and off.

The regenerator operation is similar to the low-flow LDAC, with the following adaptations for operating with DEVAP:

- The regenerator operated at a concentration increase of 6 to 8 percentage points, up to 43% concentration.
- The desiccant was stratified to avoid mixing strong and weak desiccant by carefully returning weak desiccant to the top of the tank and strong desiccant to the correct vertical location by means of natural density stratification.
- System control is based on desiccant concentration directly rather than on SA humidity.

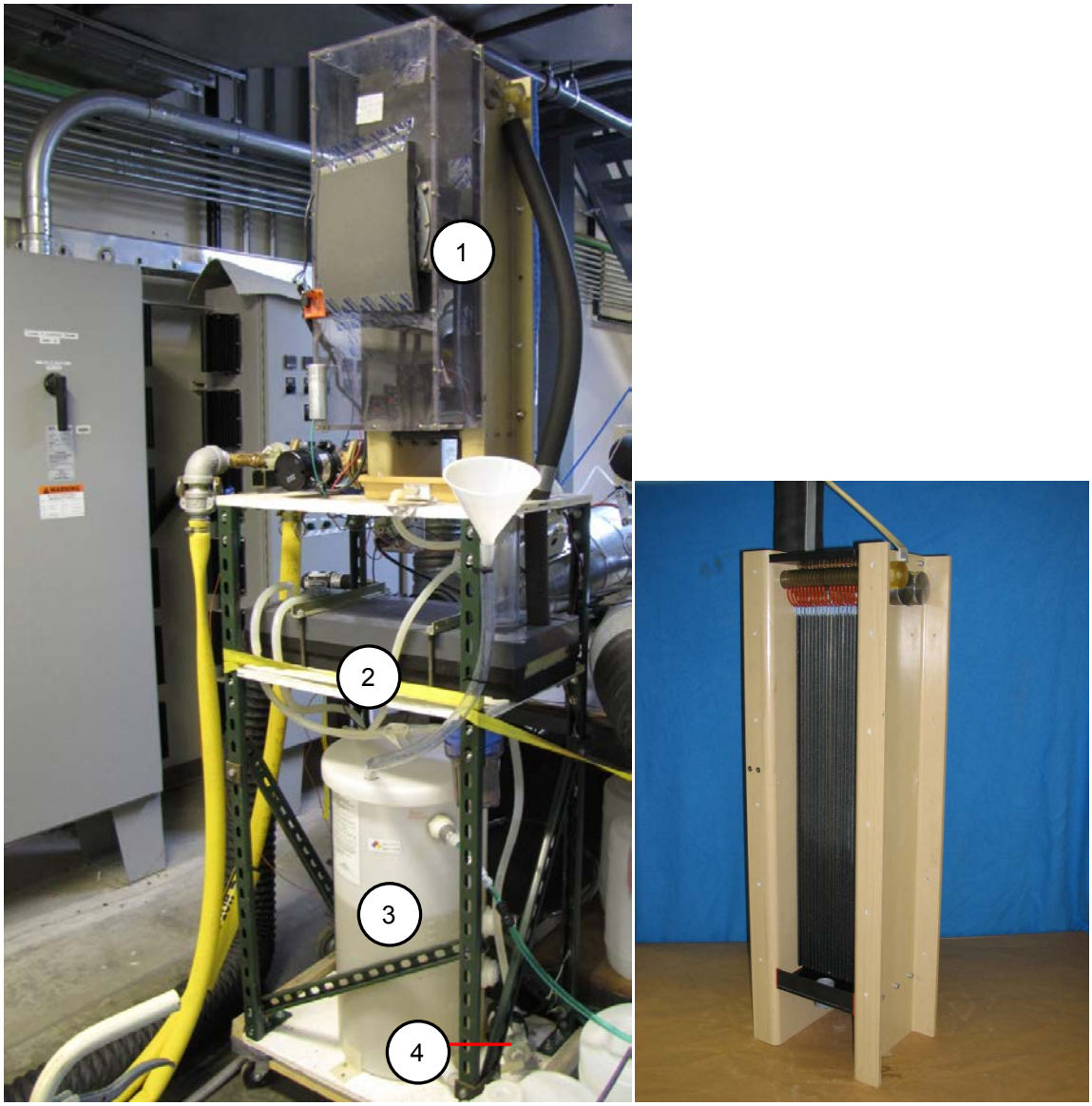

Figure 2–12 Left: (1) Scavenging air regenerator, (2) ICHX, (3) desiccant tank, and (4) desiccant pump set up at the NREL HVAC laboratory. Right: Scavenging air regenerator delivered to NREL in 2006.

Left Photo by Jason Woods, NREL; Right Photo by Andrew Lowenstein, AIL Research, used by permission

3.0 Laboratory Testing and Results

We tested the cooling and dehumidification performance of the first-stage, second-stage, and the two stages combined in NREL's HVAC Laboratory. Table 3–1 lists the measured parameters.

Table 3–1 Measured Parameters

	Measurement
Global measurements	Ambient temperature, ambient pressure in laboratory
Airstreams 1, 2, 3, 4, and 5	Temperature, dew point temperature, mass flow rate, pressure
LD inlet and outlet streams	Temperature, electrical conductivity
Water flow	Nozzle flow rate, duty cycle, temperature
Scavenging air regenerator	Inlet water temperature, duty cycle

The DEVAP AC numerical model comprises three smaller, integrated numerical models: the first- and second-stage HMXs, and a desiccant regenerator. Our focus was to validate the first- and second-stage HMX numerical models, based onWoods and Kozubal (2012a), with the experimental prototypes. The single- and two-stage regenerators have been under development through separate project funding. Ultimately, to determine the efficiency of the DEVAP AC with a two-stage regenerator, we must use the experimental data for the first- and second-stage HMXs and combine them with a two-stage regenerator numerical model.

We did not test the DEVAP conditioner with the two-stage regenerator in the laboratory, because it could not be developed for this smaller scale testing with the allotted time and resources. However, AIL Research has developed a two-stage regenerator through separate NREL-funded projects (Lowenstein 2006). In Figure 3–1, we compare the performance of this Gen-1 regenerator to NREL's two-stage regenerator model. The graph shows the water removal source energy efficiency (COP_{latent}) versus desiccant concentration change. Higher COPs are achieved with lower inlet concentrations and with a high change in desiccant concentration across the regenerator. High concentration change results in lower heat losses because of the lower desiccant flow rate. The DEVAP working range is shown on the graph, along with two data points from AIL Research (Lowenstein 2006). The data show that the modeled COP_{latent} is less than the measured values and is therefore conservative. More data points that cover a greater range of operating conditions would fully validate the two-stage regenerator model, but are not available until AIL Research completes the fabrication of a Gen-2 regenerator and measures its performance.

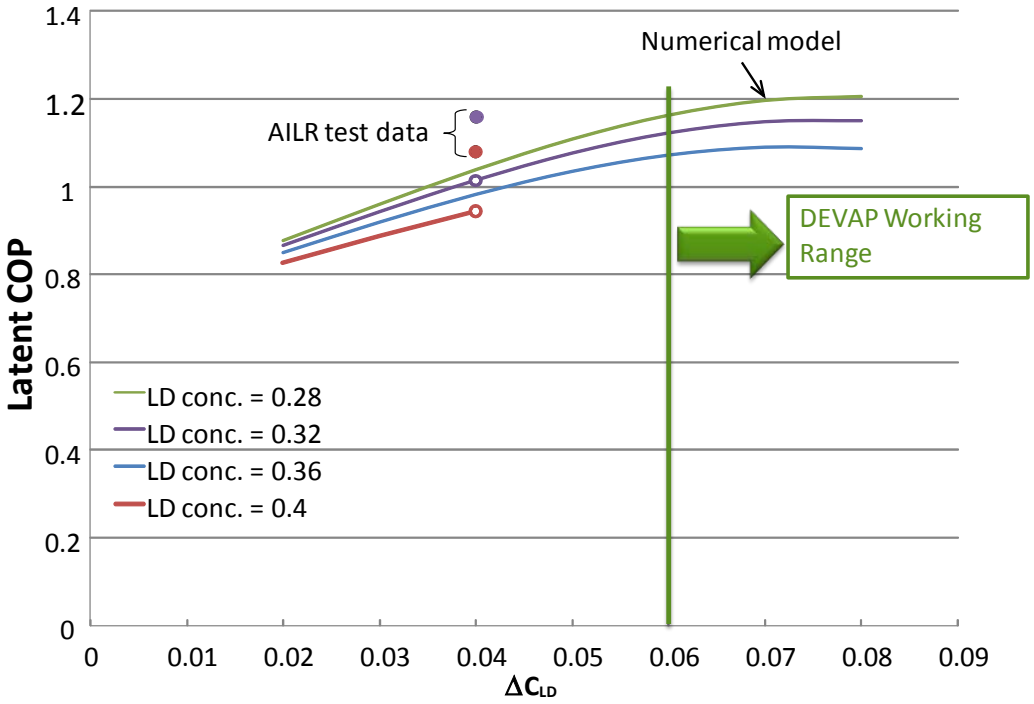

Figure 3–1 Modeled performance of two-stage regenerator with two data points plotted from data obtained by AIL Research

(Lowenstein 2006)

We measured the performance of the AIL Research and Synapse first-stage designs and the AIL Research second-stage design. During our evaluation of the Synapse second-stage design, we determined that the construction technique used inadequate spacers, which led to inconsistent air channel geometry. These air channels did not have sufficient support to maintain geometrical tolerance, a problem that degraded cooling capacity by about 20%. We concluded that the short project timeline would prevent us from resolving this performance issue.

3.1 Test Interpretation

In this section, we describe key test points that illustrate the operation of the DEVAP AC. We show the test points on psychrometric charts and show the model predictions against the measured data. The full dataset can be found in Appendix B, which shows both measured and modeled data used to create the figures in this section. Details of the numerical model can be found in Woods and Kozubal (2012a), which also shows test data from the Synapse first-stage and the AIL Research second-stage HMXs. Appendix C shows similar information for the AIL Research first-stage HMX.

3.1.1 First-Stage HMX Performance (AIL and Synapse Units)

Tests were performed at AHRI standard rating conditions (AHRI 2007). Figure 3–2 shows the performance of the AIL Research and Synapse first-stage HMX using the AHRI RA and OA conditions as the inlet air states for S1 and S3, respectively. The measured outlet state (S1.5) is shown against the modeled performance. Figure 3–3 shows the measured versus predicted performance from numerical modeling for all tests on the first-stage (for test points, see Appendix B). The AIL and Synapse HMXs performed on average to about 78% and 98.4% of

the modeled latent capacity, respectively. All data for the Synapse first-stage HMX were within 10% of predicted values.

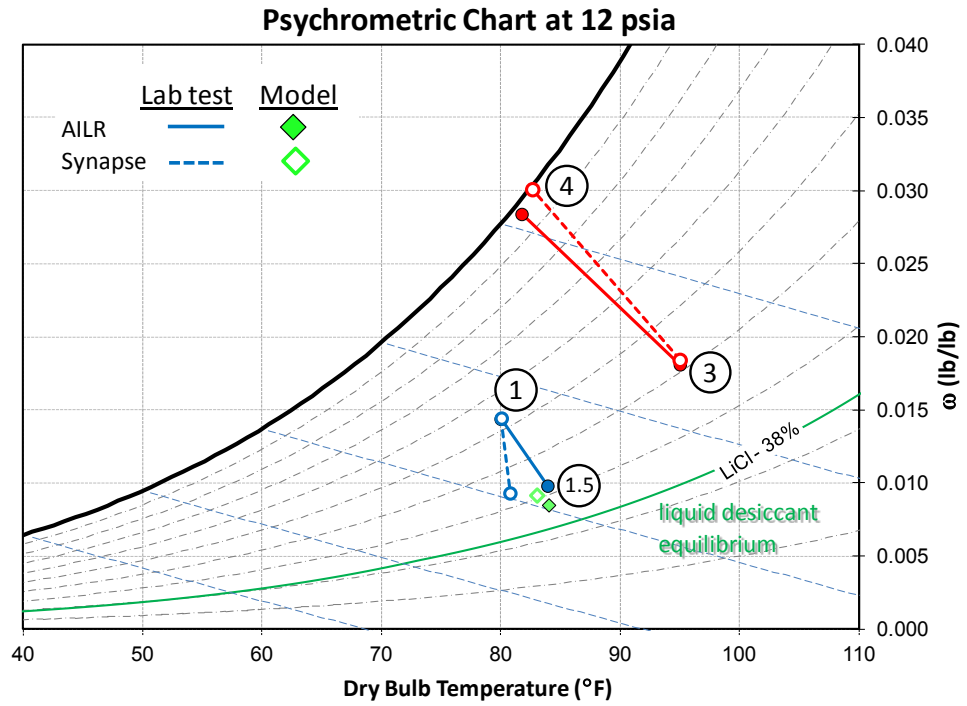

Figure 3–2 Measured performance of AIL Research and Synapse first-stage HMXs at AHRI standard conditions

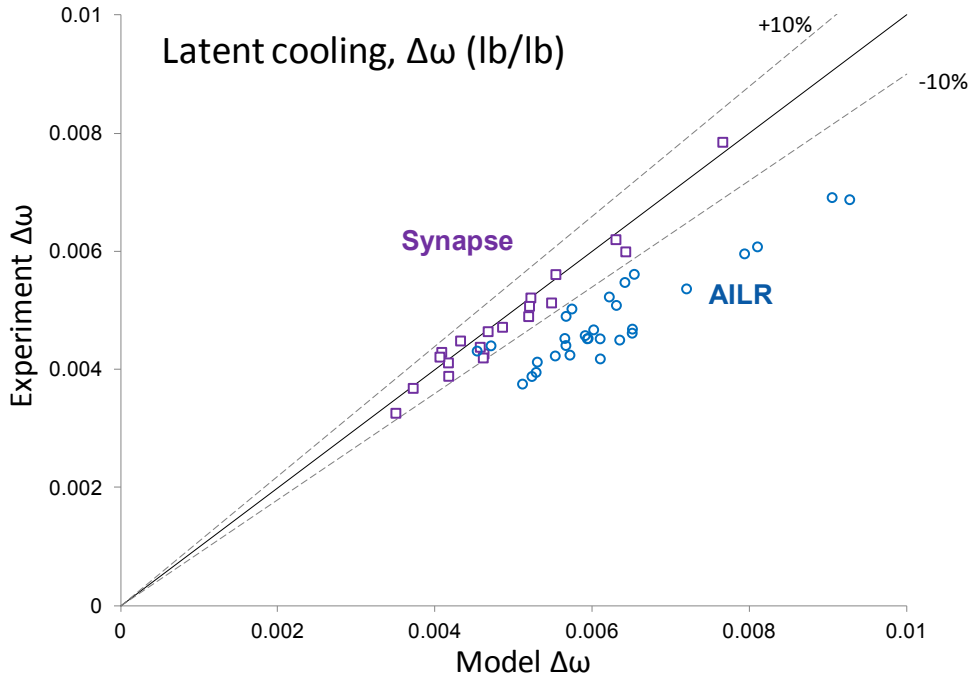

Figure 3–3 Modeled versus experimental measurement of Stage 1 latent cooling

We carefully investigated the performance of the AIL Research first-stage conditioner by using a chilled mirror, dew point hygrometer to measure the latent removal effectiveness of each S1-1.5 air channel. We discovered a large variation from channel to channel; some channels underperformed compared to model prediction. Figure 3–4 shows the latent removal effectiveness of several channels that did not meet the modeled prediction. The cause of this discrepancy was nonuniform desiccant distribution from channel to channel caused by a known manufacturing and design flaw in the desiccant manifold. The data shown are after we spent significant time diagnosing the problem and improving distribution. To help compensate for the deficient desiccant distribution, we increased the total desiccant flow rate by 30% for performance testing.

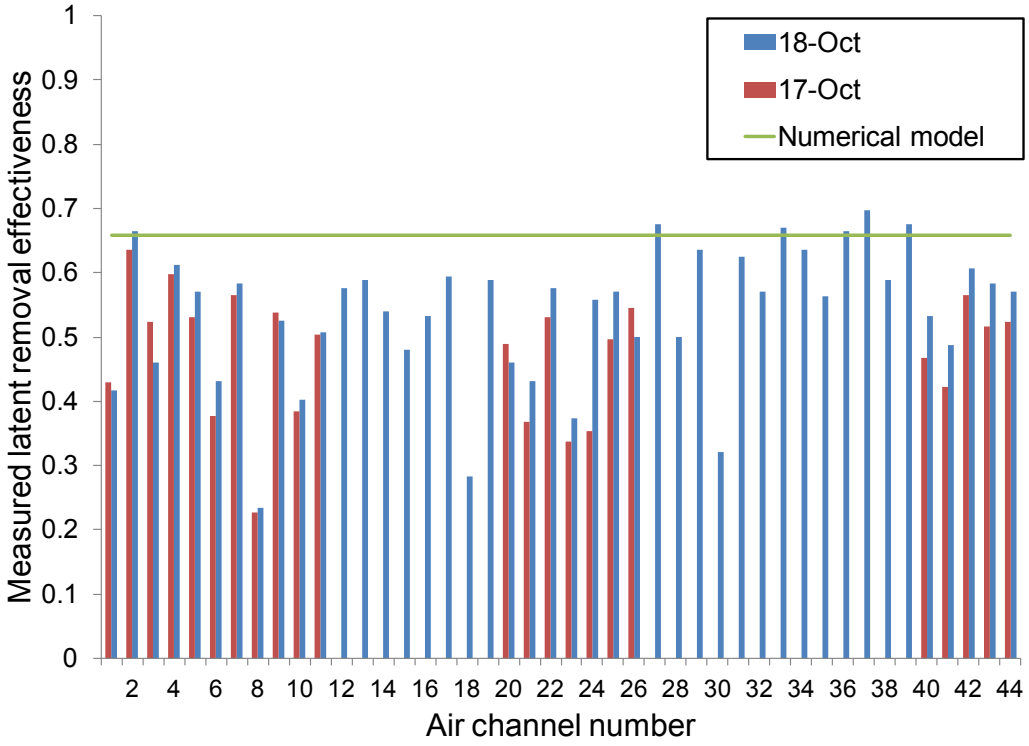

Figure 3–4 Graph of measured latent removal effectiveness per air channel of AIL Research first-stage conditioner

We also performed tests to determine the evaporative cooling performance of the first-stage AIL Research HMX, which showed that the heat transfer was less than predicted. We concluded that the lack of a wicked surface in the flutes of the Coroplast (EA side) contributed significantly to this issue. The flute surfaces were unable to hold a film of water and maintain adequate cooling.

The Synapse first-stage conditioner displayed no significant performance issues, indicating good desiccant flow distribution and good surface wetting on the EA side. The desiccant flow rate is half that of the AIL Research HMX, but achieved the same dehumidification level. We thus conclude that the Synapse method of distributing desiccant is the more reliable approach.

3.1.2 Second-Stage HMX Performance (AIL Research Unit)

Figure 3–5 shows the performance of the AIL Research second-stage HMX with inlet conditions the same as the first-stage outlet from the AHRI test shown in Figure 3–2. Figure 3–6 shows the measured performance versus the modeled prediction for 10 tests. The test points are described in Woods and Kozubal (2012a). This HMX achieved on average 99.7% of sensible capacity compared to the modeled prediction. All measured data points were within 10% of predicted capacity.

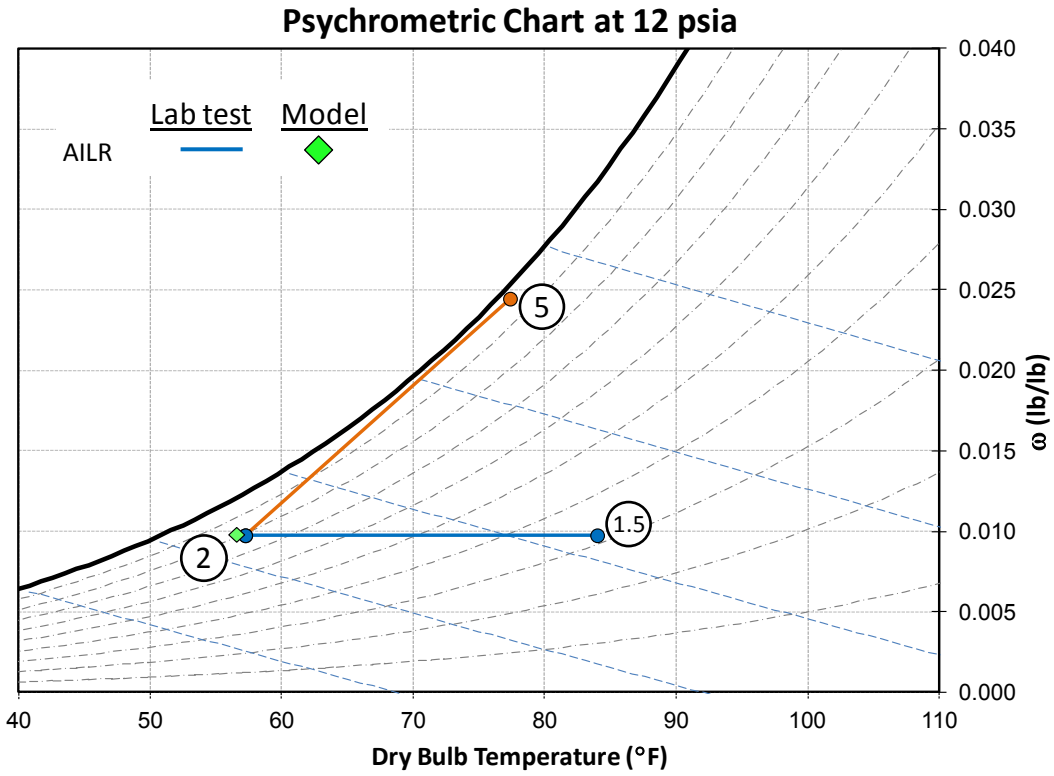

Figure 3–5 Measured performance of AIL Research second-stage HMX at outlet air conditions from the first-stage and AHRI standard conditions

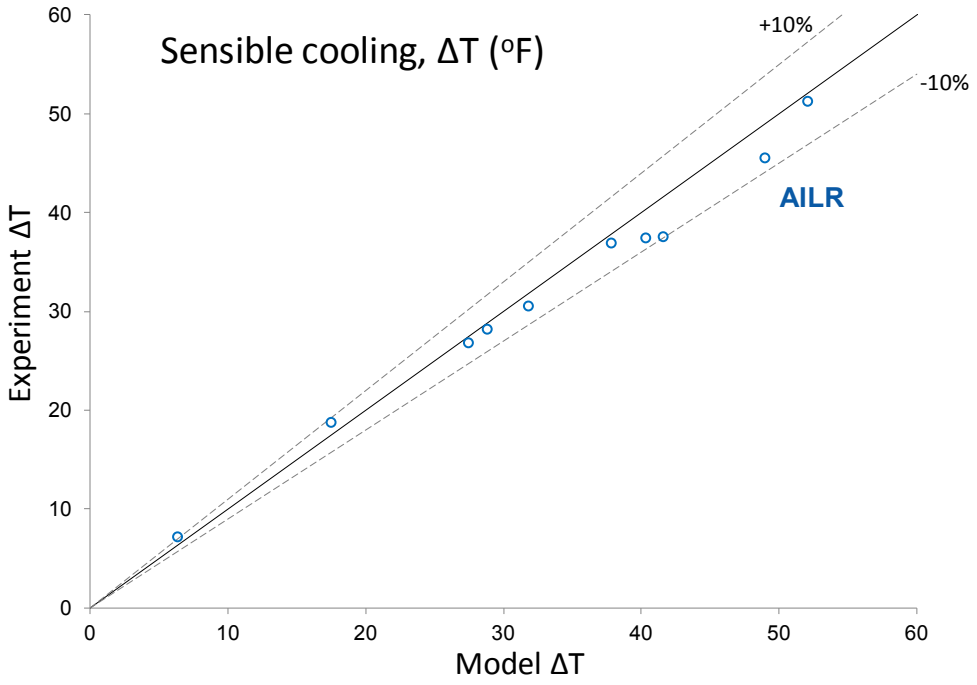

Figure 3–6 Modeled versus experimental measurement of second-stage sensible cooling

3.1.3 First- and Second-Stage HMX Performance (AIL Research Unit)

Figure 3–7 shows the combined performance of the first- and second-stage AIL HMXs at AHRI standard conditions. The difference between measured and predicted performance is due to issues with the first-stage HMX (see Section 3.1.1).

Figure 3–8 and Figure 3–9 show the performance of the first- and second-stage HMXs operating at mild/humid and hot/dry conditions, respectively. These two conditions illustrate how the DEVAP process can adapt to high sensible/low latent and low sensible/high latent conditions. During mild/humid conditions, sensible load is lower and an AC must operate in dehumidification mode (DH). The DEVAP process does this by lowering the second-stage EA flow rate, which reduces the sensible cooling and results in outlet air at a higher temperature. During hot/dry conditions, the first-stage HMX is not used because the second-stage HMX has a wet bulb effectiveness of approximately 125% and can provide air below 59°F. This temperature is low enough to provide space cooling.

As a comparison, an IEC operating in the hot/dry condition with 100% wet bulb effectiveness would provide SA at approximately 70°F, which is too warm to provide sufficient space cooling. Thus, supplemental cooling equipment is needed. As a consequence, evaporative comfort cooling is generally limited to the following applications:

- Dry climates where the ambient wet bulb temperatures are below 65°F
- Applications where backup cooling is available
- Ventilation precooling

Although not designed and optimized to be a dedicated OA system, the DEVAP prototype can supply space cooling at these conditions (Figure 3–10). Again, desiccant distribution issues kept the conditioner from achieving the predicted SA condition. Solving these issues would result in 58°F supply conditions. Creating a higher effective first-stage unit by adding heat exchange area would result in a dedicated outdoor air system that supplies dryer and colder air. This could also reduce the required desiccant concentration, which would improve efficiency.

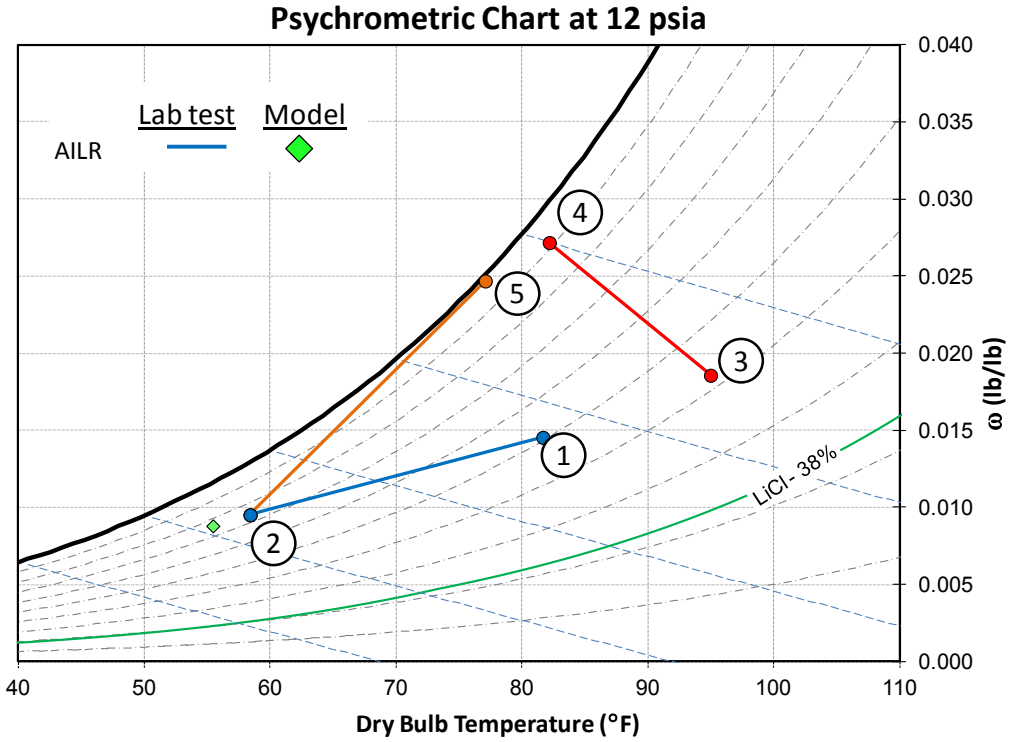

Figure 3–7 Measured performance of AIL Research first- and second-stage HMXs at AHRI standard conditions

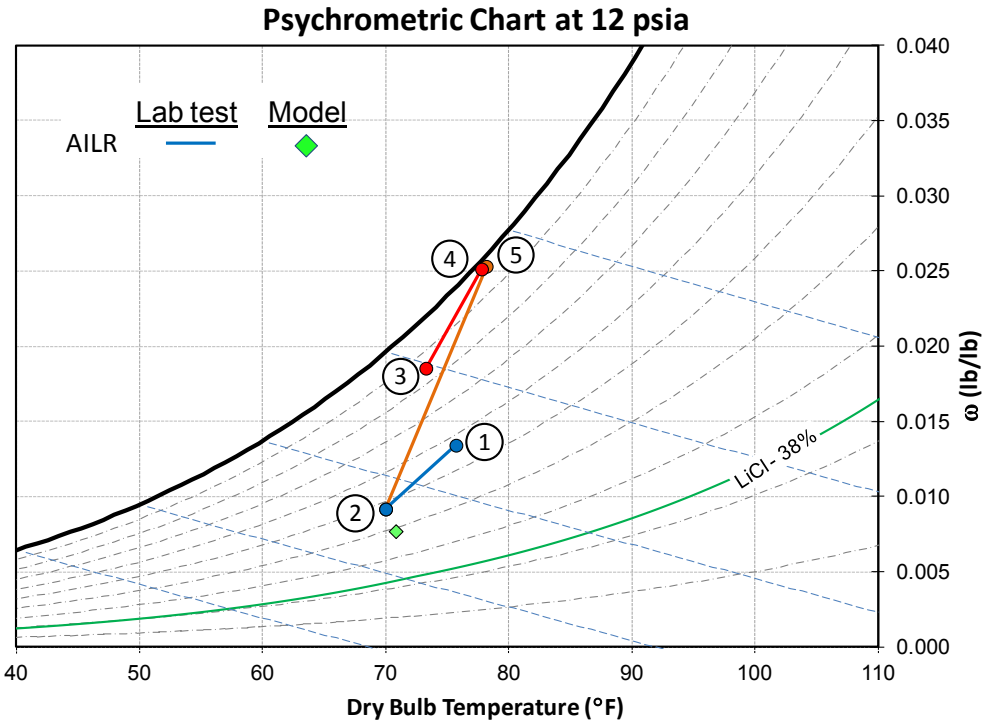

Figure 3–8 Measured performance of AIL Research first- and second-stage HMXs at a mild/ humid condition

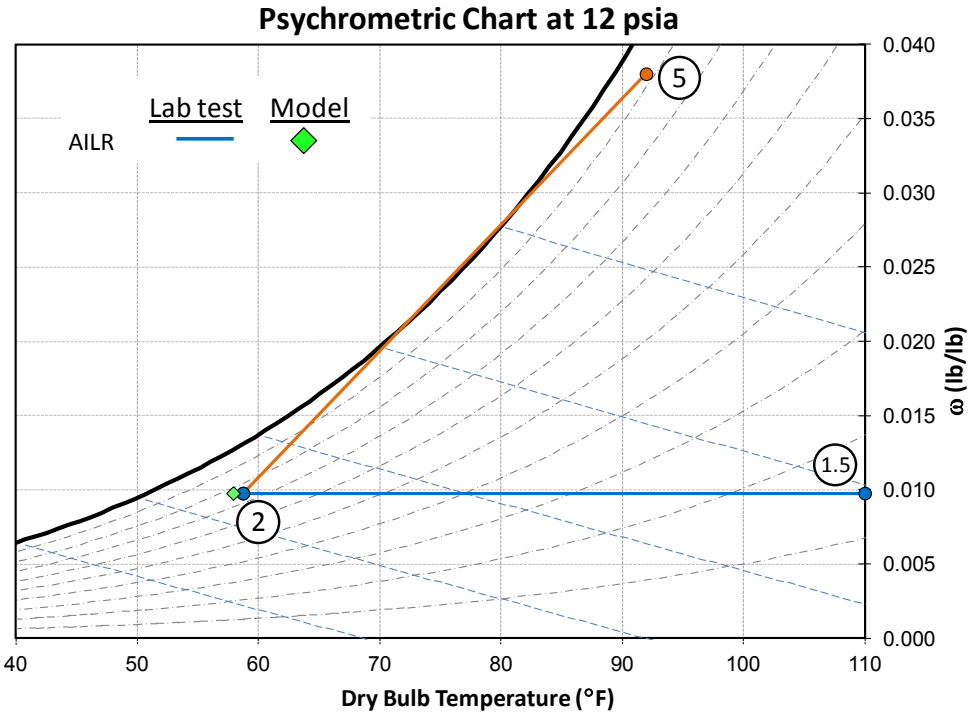

Figure 3–9 Measured performance of AIL Research second-stage HMX at a hot/dry condition

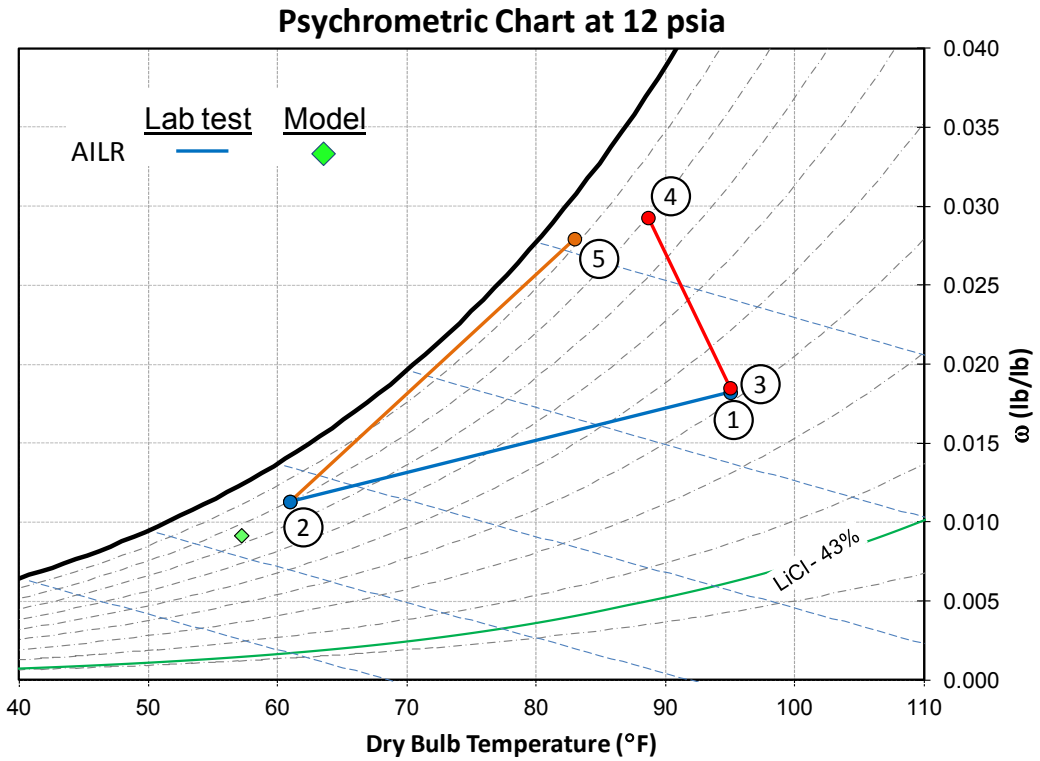

Figure 3–10 Measured performance of AIL Research first- and second-stage HMXs at AHRI condition and 100% OA

3.1.4 Energy Performance

The DEVAP AC energy performance was calculated with the numerical model in Kozubal et al. (2011). We compared this model with the calculated energy use of the two conditioner prototypes for each test we performed. This calculation considers the electric pump and fan energy and the thermal energy required by the regenerator. Assuming 50% efficient fans, we calculated the fan energy used with the measured airflow rate and pressure drop (Figure 3–11). We used the measured dehumidification and airflow rates to compute the required regeneration energy (Figure 3–12), with the regenerator efficiency modeled as described in Section 3.0. Figure 3–12 shows only the DH and standard mode (DH + IEC) of operation when desiccant is flowing and thus thermal energy is required. IEC mode does not require desiccant, and therefore does not require thermal energy. Figure 3–13 shows the source energy efficiency of cooling from S1 to S2 conditions (COP_{unit}). Experimental data use measured pressure drop with a 50% efficient fan, and a two-stage regenerator model to calculate COP_{unit}. The calculation uses site to source energy conversion factors of 1.1 for natural gas and 3.4 for electricity (Deru and Torcellini 2007). The DH + IEC test points are for standard mode, which are shown more closely in Figure 3–14. Explanations of cooling modes and source energy conversion are included in Kozubal et al. (2011). The COP_{unit} of the system improves when dehumidification is turned off (IEC mode). Building energy simulation is required to predict the year-round efficiency of the DEVAP AC, because the system will run in different modes throughout the year. The cooling load and time in each mode are also climate dependent. For example, in drier climates a unit will spend more time in IEC mode.

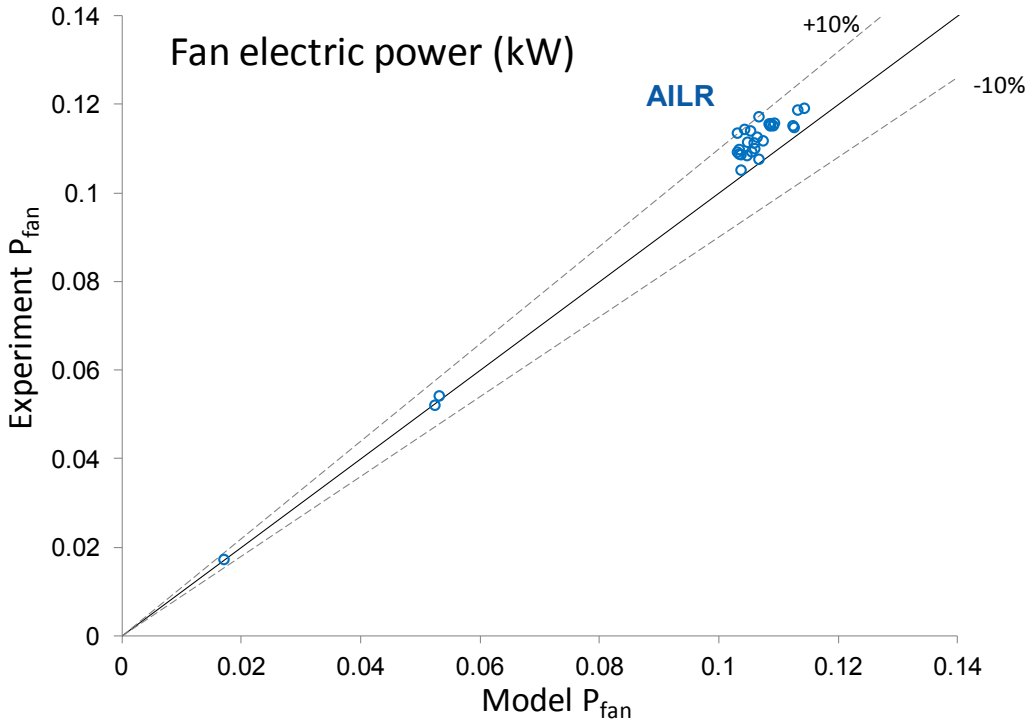

Figure 3–11 Modeled versus experimental measurement of fan power using pressure drop data and a 50% efficient fan

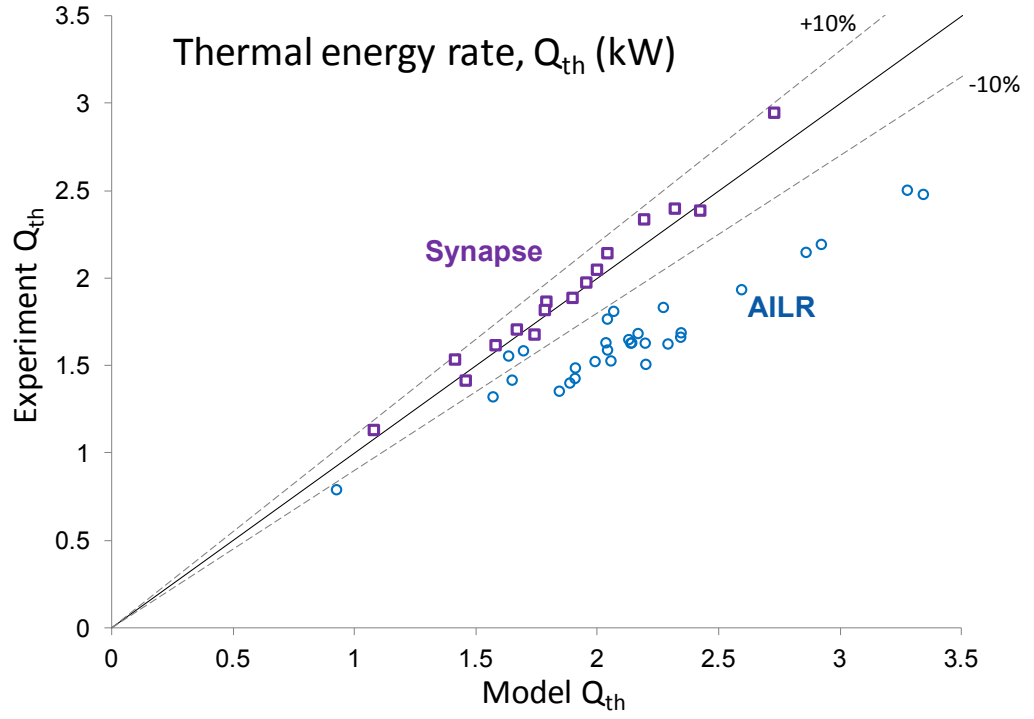

Figure 3–12 Modeled versus experimental measurement of thermal energy rate (Q_{th}) using the two-stage regeneration efficiency model

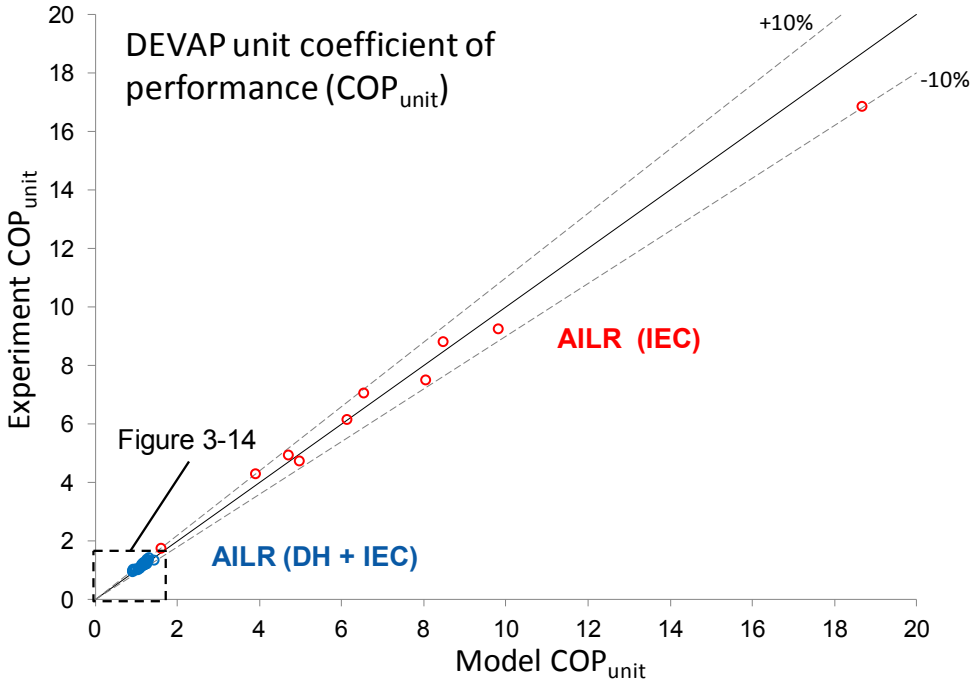

Figure 3–13 Modeled versus experimental measurement of source COP_{unit}.

DH + IEC mode is used when both latent and sensible cooling are required. These points are shown more clearly in Figure 3–14.

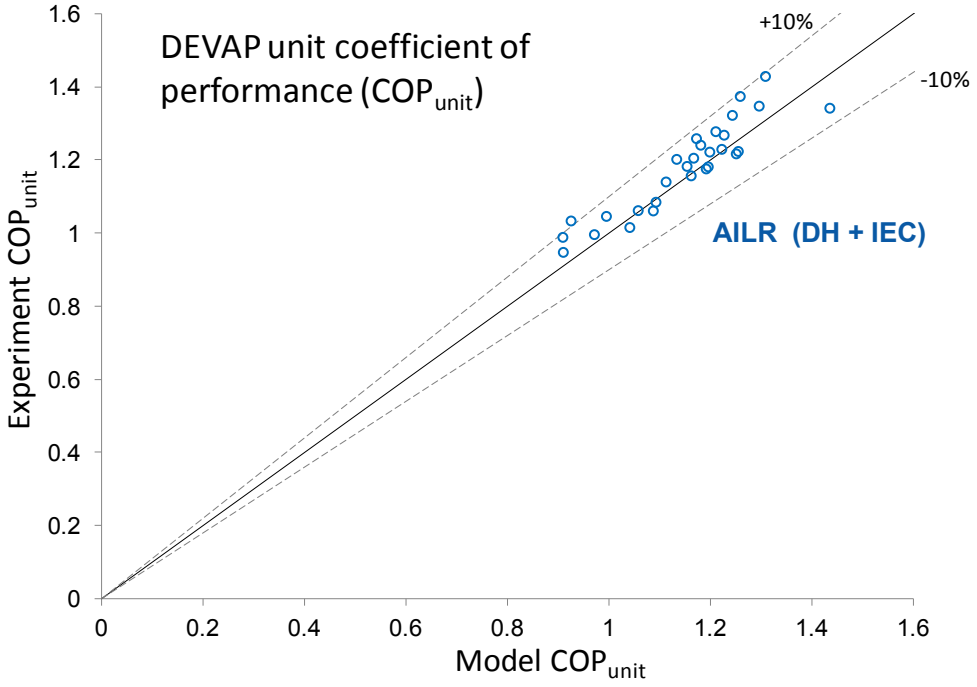

Figure 3–14 Modeled versus experimental measurement of source COP_{unit} for the standard mode of operation (when dehumidification is required).

The source efficiency of the AIL Research first-stage HMX met predicted performance because the lower latent cooling (combined with the lower thermal energy rate) results in the same efficiency. Therefore, the first-stage performance affects only the size and first cost of this component.

3.1.5 Water Use Performance

Figure 3–15 shows the predicted versus measured water use by the AIL Research dehumidifier + IEC HMXs. Measured water use is within 10% of the predicted values.

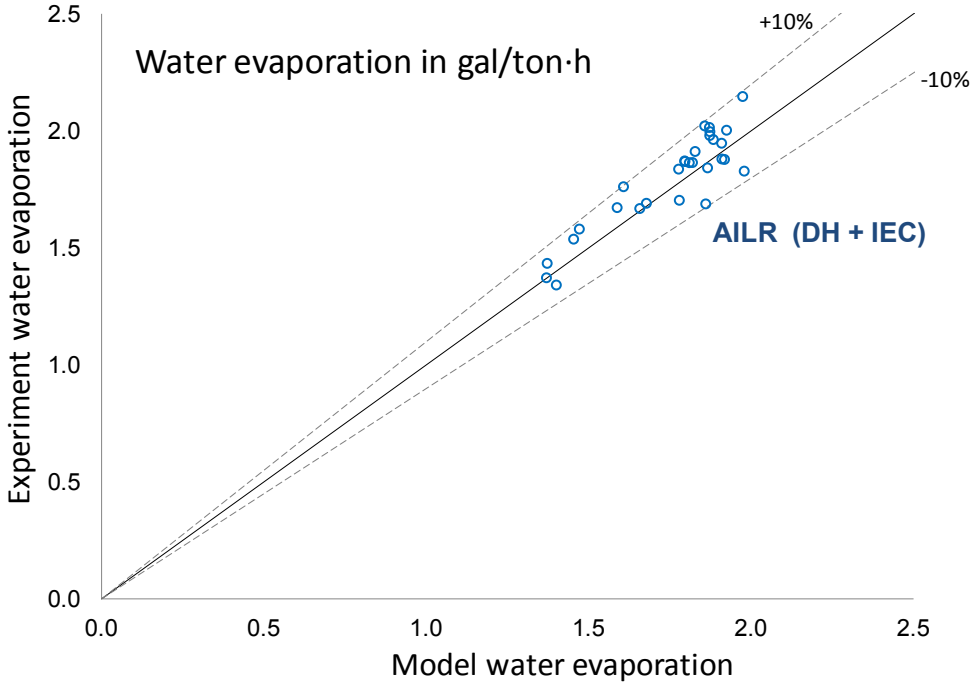

Figure 3–15 Modeled versus experimental measurement of specific water evaporation

3.2 Water Use Strategy Improvements for DEVAP

The second stage of the DEVAP AC is a staged, counterflow IEC. The airflow is staged because airstream 2-5 uses air that passes first through 1.5-2. This ensures an approach to the dew point temperature and is water efficient. The water efficiency approaches the theoretical limit of about 1.36 gal/ton·h of sensible cooling. Figure 3–16 and Figure 3–17 show the measured evaporation rate through the AIL Research second-stage HMX. In contrast, when the first-stage dehumidifier is running without desiccant flow, it operates much like standard cross-flow evaporative coolers. These units inherently use more water, primarily because OA is used for the evaporative cooling sink (airstream S3). As the outdoor wet bulb temperature rises and approaches the entering product airstream (S1) temperature, the water use approaches infinity (gallons evaporated per ton-hour of cooling goes to infinity). Measurements of the DEVAP dehumidifier stage in this configuration showed water use of 2.58–3.81 gal/ ton·h with outdoor conditions at 86°F, a wet bulb temperature of 61°F, and indoor air at 86°F.

The water use was not optimized in the analysis presented by Kozubal et al. (2011). The first-stage HMX was used as an IEC during hot and dry periods. The total yearly water use can be significantly reduced by turning the water off in the first-stage HMX when ambient dew point is lower than 50°F, when the second stage can deliver air at lower than 59°F. Table 3–2 compares the yearly specific water use from Kozubal et al. (2011) (Case 1) to this new strategy (Case 2). The new strategy saves 7% and 30% of the original water use prediction in Houston and Phoenix, respectively.

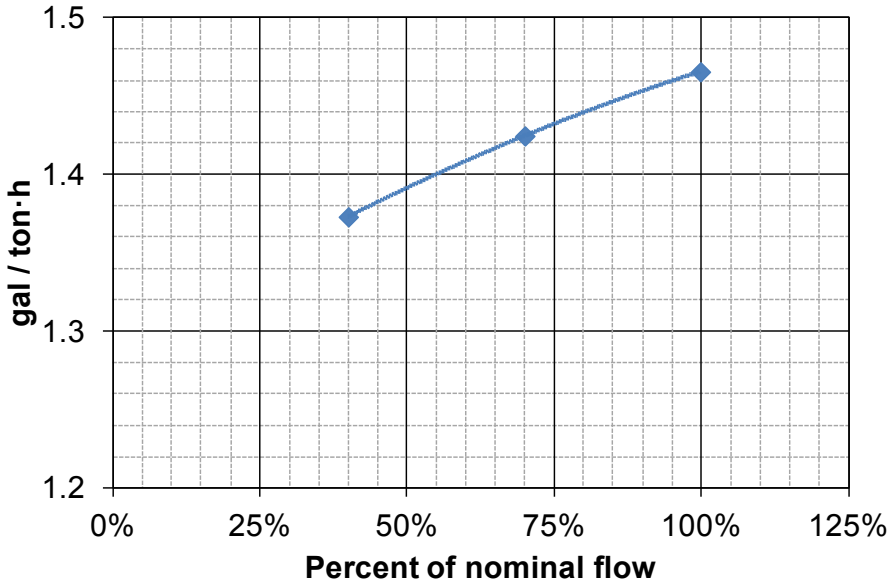

Figure 3–16 Measured water evaporation of the AIL Research second-stage IEC versus airflow

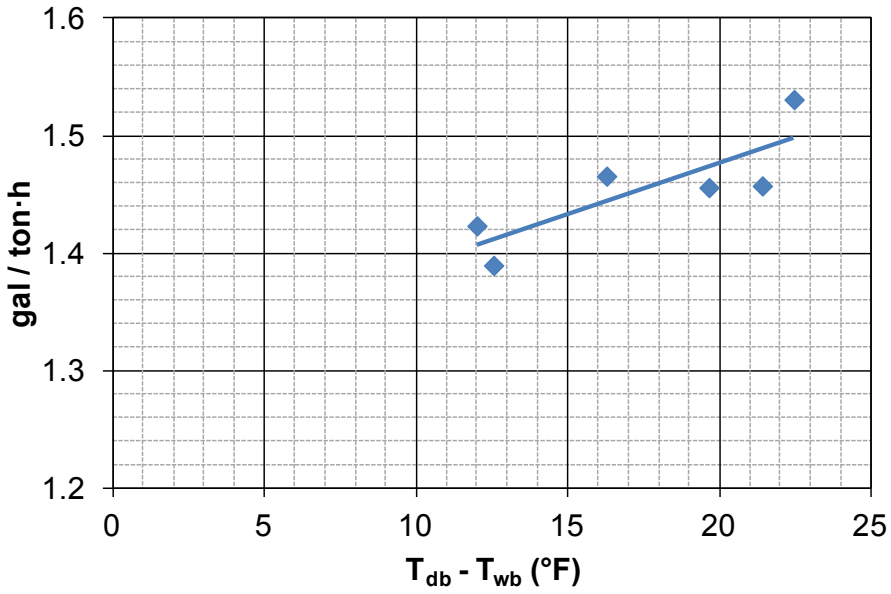

Figure 3–17 Water evaporation of AIL Research second-stage IEC versus wet bulb depression

Table 3–2 Table of yearly total site water evaporation comparing operation with (Case 1) and without (Case 2) the first-stage HMX running below ambient dew point of 50°F

	Case 1 (gal/ton·h)	Case 2 (gal/ton·h)	Percent Difference
Phoenix, Arizona	2.69	1.89	–30%
Houston, Texas	2.08	1.93	–7%

3.3 Performance Metric for Technology Comparison

In an attempt to present a reasonable metric for comparison of the DEVAP AC to other cooling technologies, we tested the AIL Research DEVAP prototype per the AHRI standard 340/360 rating procedure (AHRI 2007). We used the methods in this standard to measure an effective integrated energy efficiency ratio ($IEER_{effective}$) for the DEVAP prototypes because no industry standard rating condition compares vapor compression-based ACs against other technologies. We do not intend this measurement to be a rating of the DEVAP AC, because the IEER method is intended for rating only electrically driven, vapor compression-based ACs. The standard states:

> **2.1.1 Energy Source.** This standard applies only to electrically operated, vapor compression refrigeration systems.

The standard is also not intended to be a measure of actual energy use. The standard states:

> **6.2.1 General.** The IEER is intended to be a measure of merit for the part load performance of the unit. Each building may have different part load performance due to local occupancy schedules, building construction, building location and ventilation requirements. For specific building energy analysis an hour-by-hour analysis program should be used.

We adhered to the standard in all cases for test conditions, except one area. The standard limits the OA flow rate for systems to a maximum of 20% of total SA flow. The DEVAP AC requires 30% OA to obtain its maximum rated capacity. To properly compare it to rated equipment, we calculated its capacity based on a mixed air condition of 30% OA and 70% RA, which results in a lower $IEER_{effective}$ than if 20% OA were used in the calculation. Table 3–3 shows the OA conditions and nominal percent of capacity for each test point. The test conditions are shown in Figure 3–18 on a psychrometric chart. For each test point, the energy efficiency ratio (EER) is calculated with equation 3-1 (the factor 3.4 is used to convert source energy to site electric energy). The table shows two columns where EER is calculated using 50% and 60% fan efficiency.

$$EER = \frac{3.4 \times Capacity}{Source\ Energy\ Use} \qquad (3–1)$$

Table 3–3 Table of EER Values Used To Calculate $IEER_{effective}$ per AHRI Standard 340/360*

	Capacity	T_{OA} (°F)	$T_{wb, OA}$ (°F)	EER – 50% (Btu/Wh)	EER – 60% (Btu/Wh)
Test 1	100%	95.0	75.0	15.3	15.8
Test 2	66%	81.5	65.7	18.2	19.3
Test 3	46%	68.0	57.0	21.5	23.3
Test 4	23%	65.0	52.9	42.7	51.3

* Two sets of EERs are calculated using fan efficiency of 50% and 60% respectively.

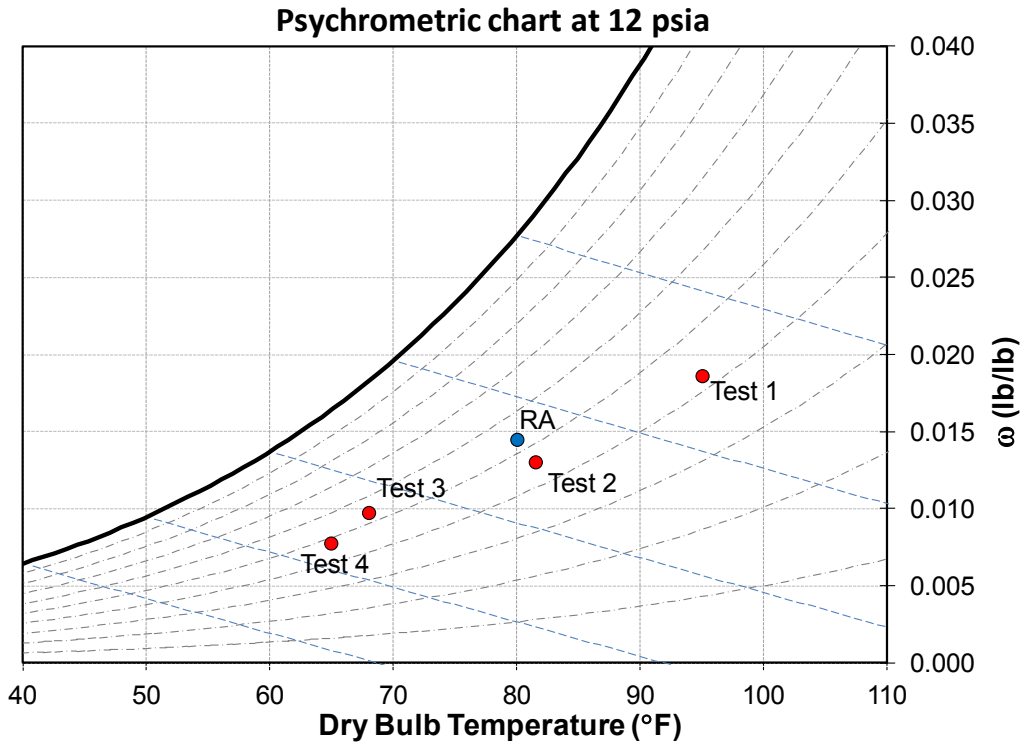

Figure 3–18 Four test conditions and RA condition for measuring $IEER_{effective}$

The $IEER_{effective}$ calculation is taken directly from the standard. The method translates the test data to capacity steps at intervals of 25% of nominal capacity. The use of a constant RA condition at a wet bulb temperature of 67°F is appropriate for rating electrically driven, vapor compression-based ACs. However, this condition does not fully capture the energy savings for the DEVAP AC process. The DEVAP process would normally maintain a lower indoor humidity, which would allow for a higher degree of evaporative cooling operation and a lower degree of dehumidification. As a result, the $IEER_{effective}$ would increase. Using $IEER_{effective}$ to compare DEVAP against vapor compression cooling technologies is imperfect. We identify annual hourly building energy simulations as the best comparison technique.

Table 3–4 shows the EER at these capacity points. Each step is weighted and the sum is the $IEER_{effective}$ value. Again, two values for $IEER_{effective}$ are calculated using 50% and 60% fan efficiency.

Table 3–4 Capacity Step Values Used To Calculate $IEER_{effective}$ per AHRI Standard 340/360*

	Capacity	EER – 50%	EER – 60%
Step 1	100%	15.3	15.8
Step 2	75%	17.4	18.4
Step 3	50%	20.9	21.7
Step 4	25%	40.8	48.8
$IEER_{effective}$		**21.1**	**23.2**

* Two values for $IEER_{effective}$ are calculated using fan efficiency of 50% and 60%, respectively.

4.0 Second-Generation DEVAP Design Description

After testing and validating the DEVAP AC numerical model, we had a third design review with AIL Research and Synapse to determine which aspects of each design worked well. We then developed a Gen-2 design concept for the first- and second-stages. Size and material use are reduced because channels are smaller and heat and mass transfer is enhanced.

For the Gen-2 first-stage design, we incorporated the following aspects from each prototype:

- Laminated layers of membrane, plastic, and nylon wicking fabric to create a simple roll-to-roll approach for attaching membranes
- Desiccant distributor method from the Synapse design (which distributes desiccant evenly across each plate)
- Coroplast frame and spacers with modifications to allow wicking material to be placed on the EA side
- Airside turbulators for airstream 1-1.5 heat and mass transfer enhancement from the AIL Research design.
- Desiccant manifold design from the AIL Research design (which manifolds the desiccant from plate to plate).

For the Gen-2 second-stage design, we removed the extruded flute construction method from the AIL Research design and replaced it with a formed aluminum in a similar airflow arrangement. Aluminum allows heat transfer enhancements to be placed into the air channels, which substantially reduces size.

Numerical modeling of the Gen-2 first- and second-stage concepts shows a reduction in size and weight of nearly 50% with no anticipated change in COP_{space}. Using methods shown in Section 2.0, Figure 4–1 shows how removing the Gen-1 limitations and incorporating the best ideas from each prototype enable us to better optimize the Gen-2 design and improve the COP_{space} versus heat transfer area. This figure also shows how these points compare to the sensitivity analysis in Figure 2–3. The higher heat and mass transfer performance of the Gen-2 design make it much smaller than the two prototypes. It also maintains efficiency by using open channels instead of the flutes in the first-stage EA channel, reducing fan energy use. Replacing the AIL Research fluted channels in the second stage with high conductivity aluminum surfaces improves heat transfer and reduces pressure drop.

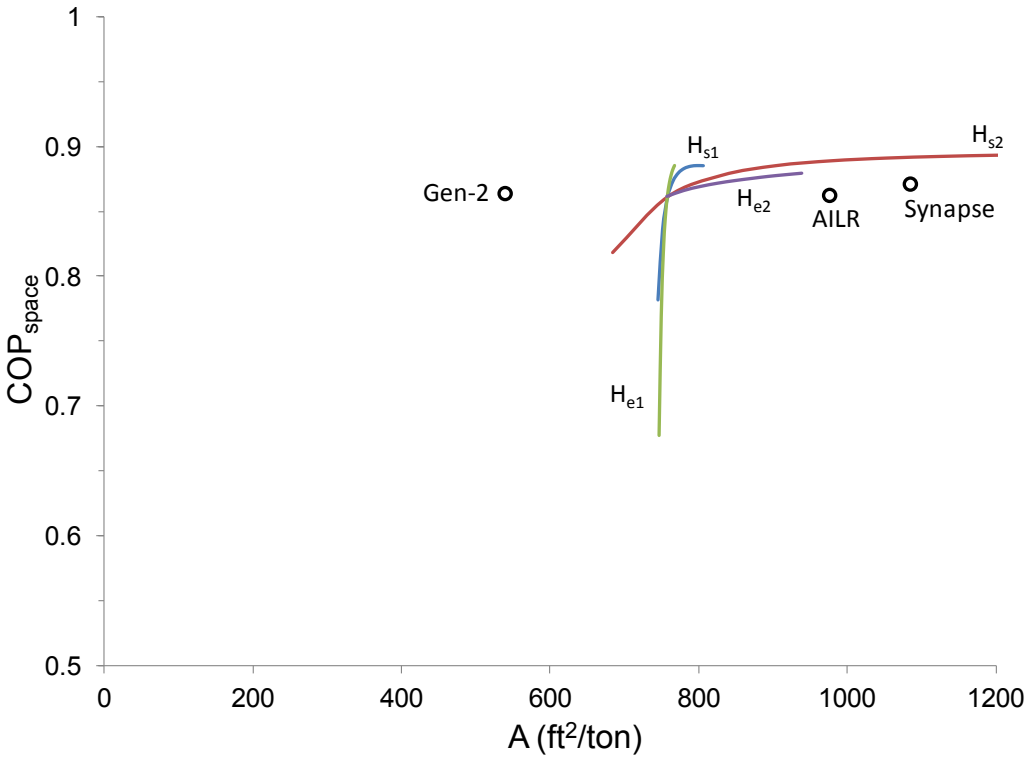

Figure 4–1 COP_{space} and area per space cooling ton of the two prototype designs and the modeled Gen-2 design, along with the effect of channel thicknesses, as shown in Figure 2–3

5.0 Cost, Size, and Weight Estimates

At this point, we shift from discussing performance based on the peak design condition to performance at an AHRI standard condition (test 1 from the $IEER_{effective}$ rating [Table 3–3]) and compare the DEVAP AC against a vapor compression AC. This is used to estimate the per-ton volume and weight of the HMXs of the AIL Research, Synapse, and Gen-2 designs. We then use the current AIL Research design and the Gen-2 design to calculate the dimensions, weight, and cost of a full 10-ton AC. DEVAP size, weight, and cost are conservatively estimated using this metric, because evaporative technologies inherently increase capacity when installed in locations where peak load is hotter than the AHRI standard conditions. In contrast, vapor compression AC capacity will decrease as the ambient temperature increases. The Synapse manufacturing method was sufficient for the prototype phase, but was not viable for a commercial-scale prototype and is therefore not included in the cost analysis.

The volume required for the HMXs, per ton, for each design are shown in Figure 5–1. The reduced size of the Gen-2 design is due to the changes outlined in Section 4.0. This translates to significant weight reduction, as shown in Figure 5–2.

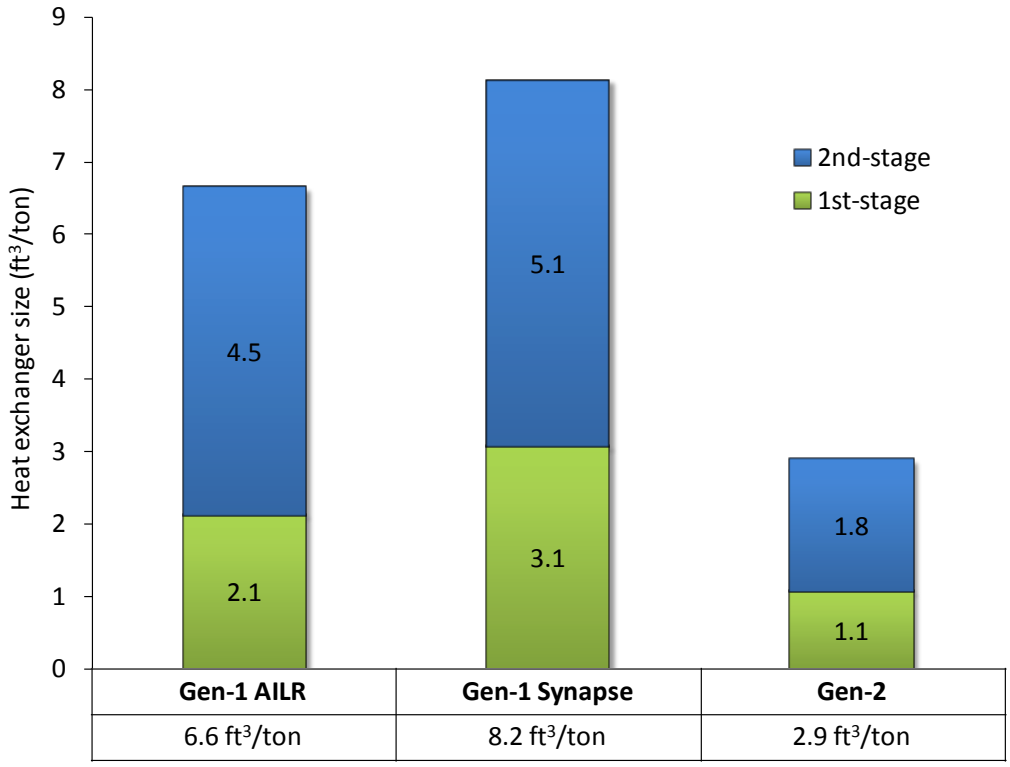

Figure 5–1 Volumetric comparison between the AIL Research and Synapse prototype HMXs and the Gen-2 HMX design

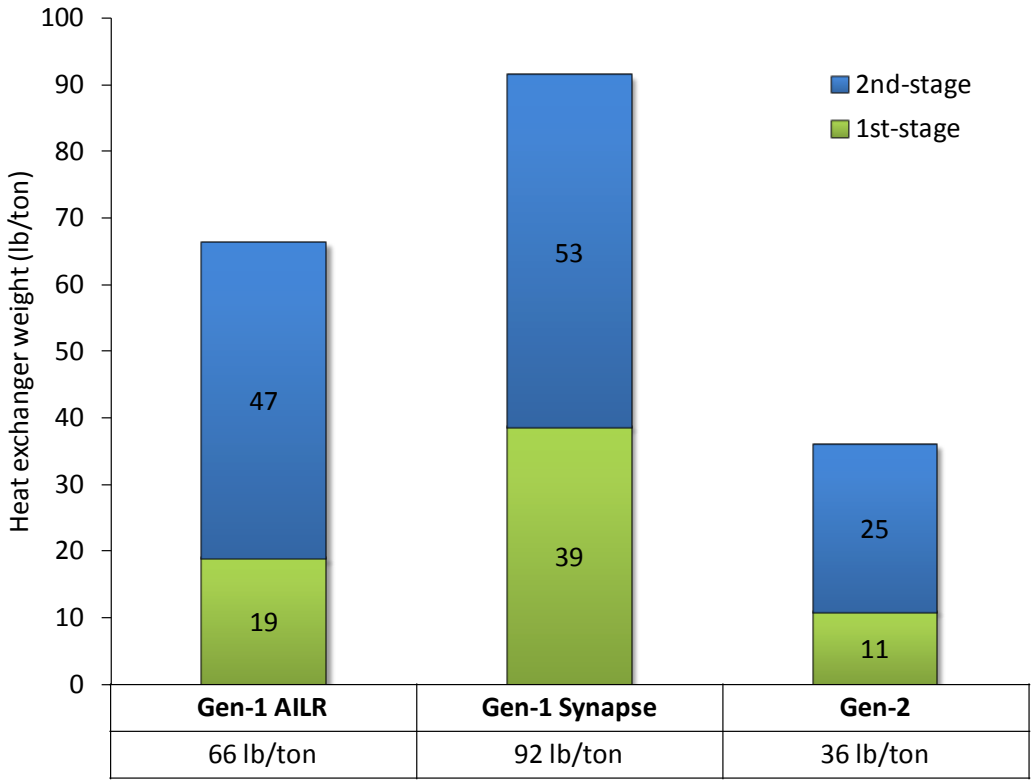

Figure 5–2 Dry weight comparison between the AIL Research and Synapse prototype HMXs and the Gen-2 HMX design

We also calculated weight and cost for a complete, packaged DEVAP AC. These estimates are based on a preliminary packaged design built around the HMXs. Figure 5–3 shows a packaged DEVAP AC based on the size of the Gen-2 HMXs. The optimal packaged arrangement was not explored and the DEVAP package size is based on a first-order attempt to assemble the components. The main components are the first-stage HMX, second-stage HMX, EA fans, airstream S1-2 plenum fan, LD tank, and scavenging and boiler stages of the regenerator. Figure 5–4 (isometric view) and Figure 5–5 (top view) show how these main components fit into the packaged unit. In this arrangement, the HMX cores account for 13% of the total packaged volume. This indicates significant wasted volume in the proposed packaging and that further size, cost, and weight improvements can be made. A similar package of the Gen 1 AIL Research design would be slightly larger because of the larger HMXs.

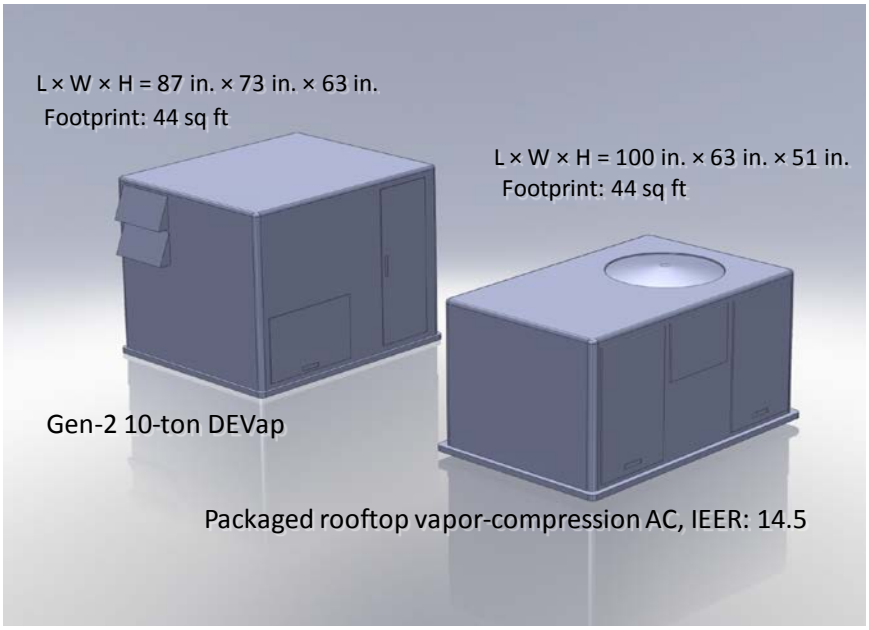

Figure 5–3 Gen-2 packaged AC compared to a packaged vapor compression AC with an IEER rating of 14.5

(Illustration by Jason Woods, NREL)

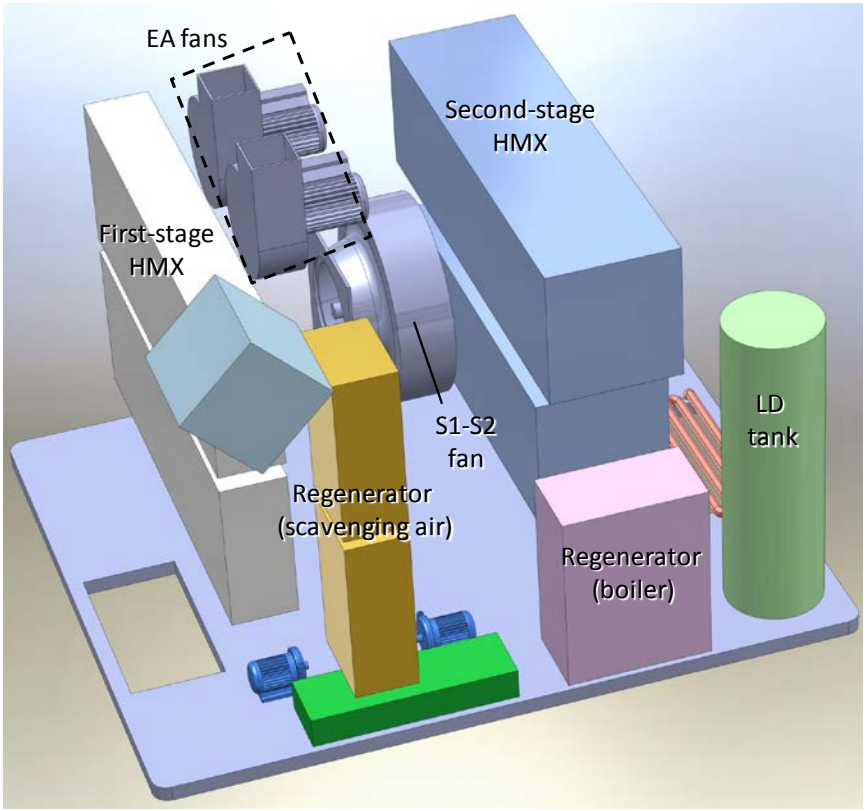

Figure 5–4 Components in the Gen-2 packaged AC, isometric view

(Illustration by Jason Woods, NREL)

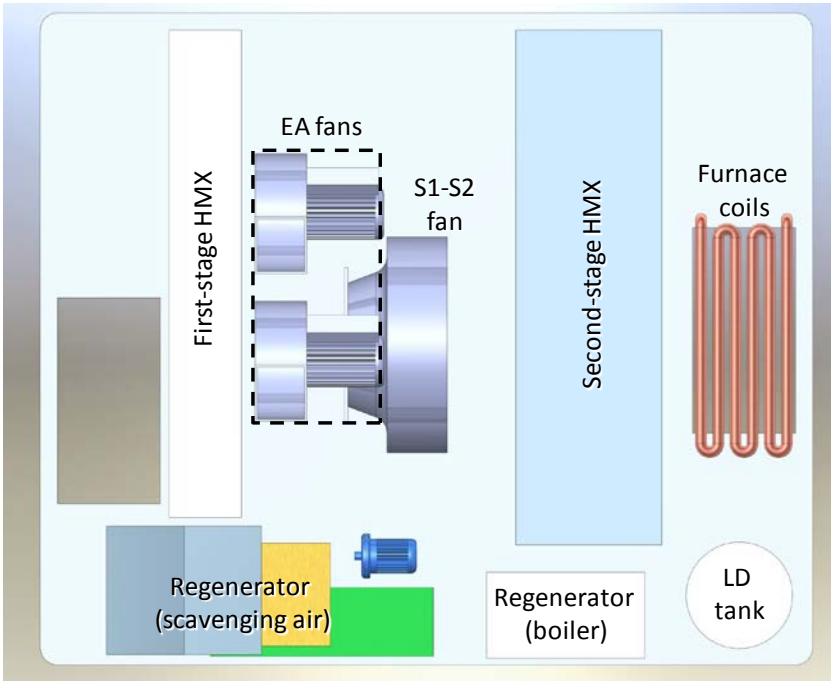

Figure 5–5 Components in the Gen-2 packaged AC, top view

(*Illustration by Jason Woods, NREL*)

Based on this packaged unit, the total weight of the DEVAP AC is compared to the weight of a vapor compression AC with a rated IEER of 14.5 (Figure 5–6). The weight of the DEVAP AC is calculated by summing the weights of the components (e.g., HMXs, regenerator, LD tank, fans). The weights of the HMXs are based on weights of each material used in their construction (e.g., Coroplast, wick, aluminum). The details of these calculations are included in Appendix D.

The estimated total cost of the DEVAP AC is about 25% higher than a typical 14.5 IEER rated AC (Figure 5–7). The DEVAP AC cost is based on estimates of all major components. The costs of the HMXs are based on information from suppliers about each material (e.g., the Celgard membrane); labor costs were estimated by AIL Research. The costs of the major balance-of-system components are from AIL Research quotes. Cost markups common in the AC industry are used to convert from wholesale to retail costs (single unit sale). Appendix E includes the details of these cost calculations.

Based on these cost estimates and the energy savings from Kozubal et al. (2011), we estimate a simple payback of less than two years in Phoenix and less than three years in Houston.

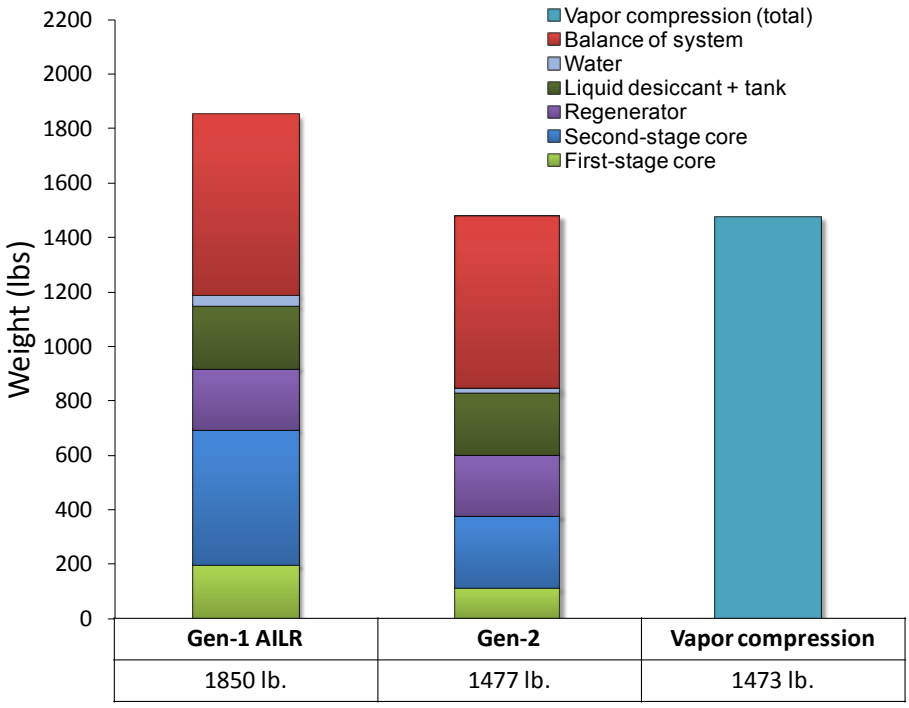

Figure 5–6 Weight of packaged 10-ton DEVAP AC compared to 10-ton packaged vapor compression AC with an IEER rating of 14.5

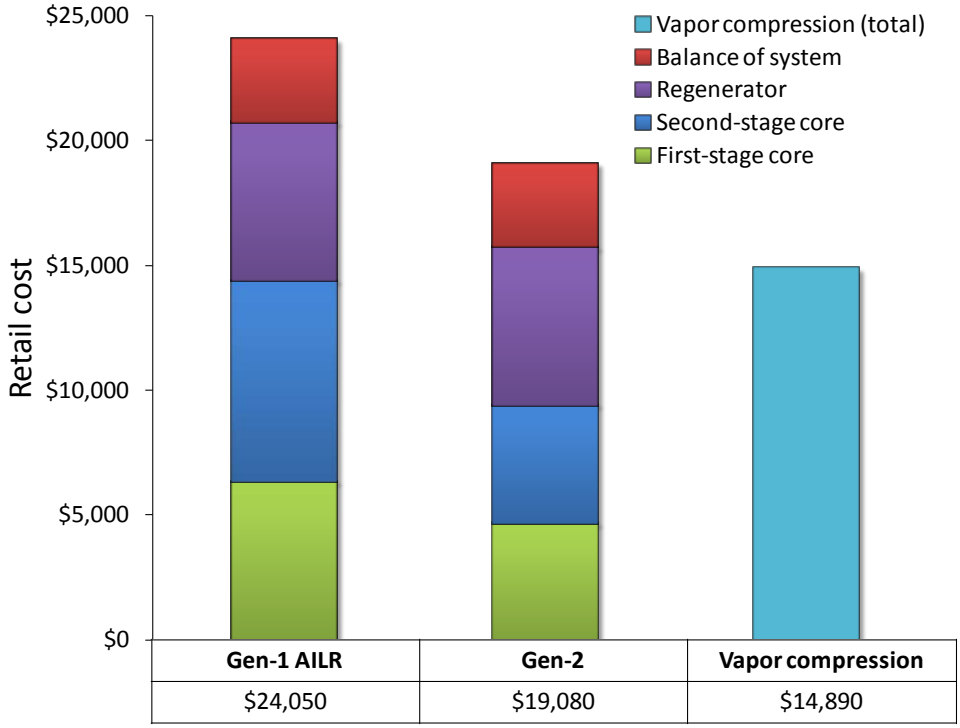

Figure 5–7 Estimated retail cost of packaged 10-ton DEVAP AC compared to 10-ton packaged vapor compression AC with an IEER rating of 14.5

6.0 Summary and Conclusions

In this report we described the development of two DEVAP AC prototypes and their tested performance. The design approach looked at all relevant variables in the design of the DEVAP AC HMXs. The approach focused on proving performance with the use of off-the-shelf components. Testing showed that cooling and energy use performance agree within 10% of predicted values for the Synapse first-stage and the AIL Research second-stage HMXs. The AIL Research first-stage HMX had latent cooling capacity about 22% less than predicted. Diagnosis revealed nonuniform desiccant distribution from plate to plate. Also, the lack of wicked surfaces in the Coroplast flutes in airstream 3-4 degraded the heat transfer. Despite the capacity issue, efficiency of the AIL Research first-stage HMX was still within 10% of predicted values. The Synapse second-stage HMX was not tested because manufacturing issues prevented the HMX from operating as designed. We also tested the AIL Research prototype at the conditions for rating IEER to compare the DEVAP AC to other technologies. An effective IEER was calculated to be 21.1 or 23.2 while using a 50% or 60% efficient fan respectively.

Testing of the two prototypes validates the numerical design approach and gives confidence in using the numerical model for:

- Energy estimation from building energy simulations (shown in the previous report)
- Use in a model-based design method to create a Gen-2 system.

We explored a Gen-2 DEVAP AC design with help from our vendors, and a design emerged that removed the constraints imposed on the Gen-1 design and included the aspects of each prototype that worked well. We then estimated the size, weight, and cost of a packaged DEVAP AC unit based on the Gen-1 and Gen-2 designs and compared them to those of a packaged vapor compression system with an IEER rating of 14.5. Using the Gen-2 design for comparison, the estimated DEVAP AC footprint and weight are about the same as a typical vapor compression AC; the cost is about 28% higher.

7.0 References

AHRI. (2007). *ANSI/AHRI Standard 340/360 2007 Standard for Performance Rating of Commercial and Industrial Unitary Air-Conditioning and Heat Pump Equipment.* Air-Conditioning, Heating, and Refrigeration Institute. *22 pp.*

ASHRAE. (2010). *ANSI / ASHRAE / IES Standard 90.1-2010: Energy Standard For Buildings Except Low-Rise Residential Buildings. pp.*

Deru, M. and P. Torcellini (2007). *Source Energy and Emission Factors for Energy Use in Buildings. pp.; National Renewable Energy Laboratory Report TP-550-3861*

Kozubal, E., J. Woods, J. Burch, A. Boranian and T. Merrigan (2011). *Desiccant Enhanced Evaporative Air-Conditioning (DEVap): Evaluation of a New Concept in Ultra Efficient Air Conditioning. 71 pp.; National Renewable Energy Laboratory Report No. TP-5500-49722*

Lowenstein, A. (2006). *Task 3C Report: Packaged 1.5-Effect Liquid Desiccant Regenerator. 6 pp.; AIL Research Task 3C Report: NREL Subcontract NO. NDJ-5-55010-01*

Lowenstein, A., S. Slayzak and E. Kozubal (2006). *A Zero Carryover Liquid-Desiccant Air Conditioner for Solar Applications.* Paper No. ISEC2006-99079. J. H. Morehouse and M. Krarti. Solar Engineering 2006: ASME 2006 International Solar Energy Conference (ISEC2006), 09-13, July, 2006, Denver, Colorado. 11 pp.

NREL (2005). *NREL's Advanced Thermal Conversion Laboratory at the Center for Buildings and Thermal Systems: On the Cutting-Edge of HVAC and CHP Technology (Revised). 4 pp.; National Renewable Energy Laboratory Report No. BR-550-34928*

Woods, J. and E. Kozubal (2012a). *A Desiccant-Enhanced Evaporative Air Conditioner: Numerical Modeling and Experiments*. Submitted to Energy Conversion and Management.

Woods, J. and E. Kozubal (2012b). *Heat Transfer and Pressure Drop in Spacer Filled Channels for Membrane Energy Recovery Ventilators*. Submitted to Applied Thermal Engineering.

Appendix A Schematics

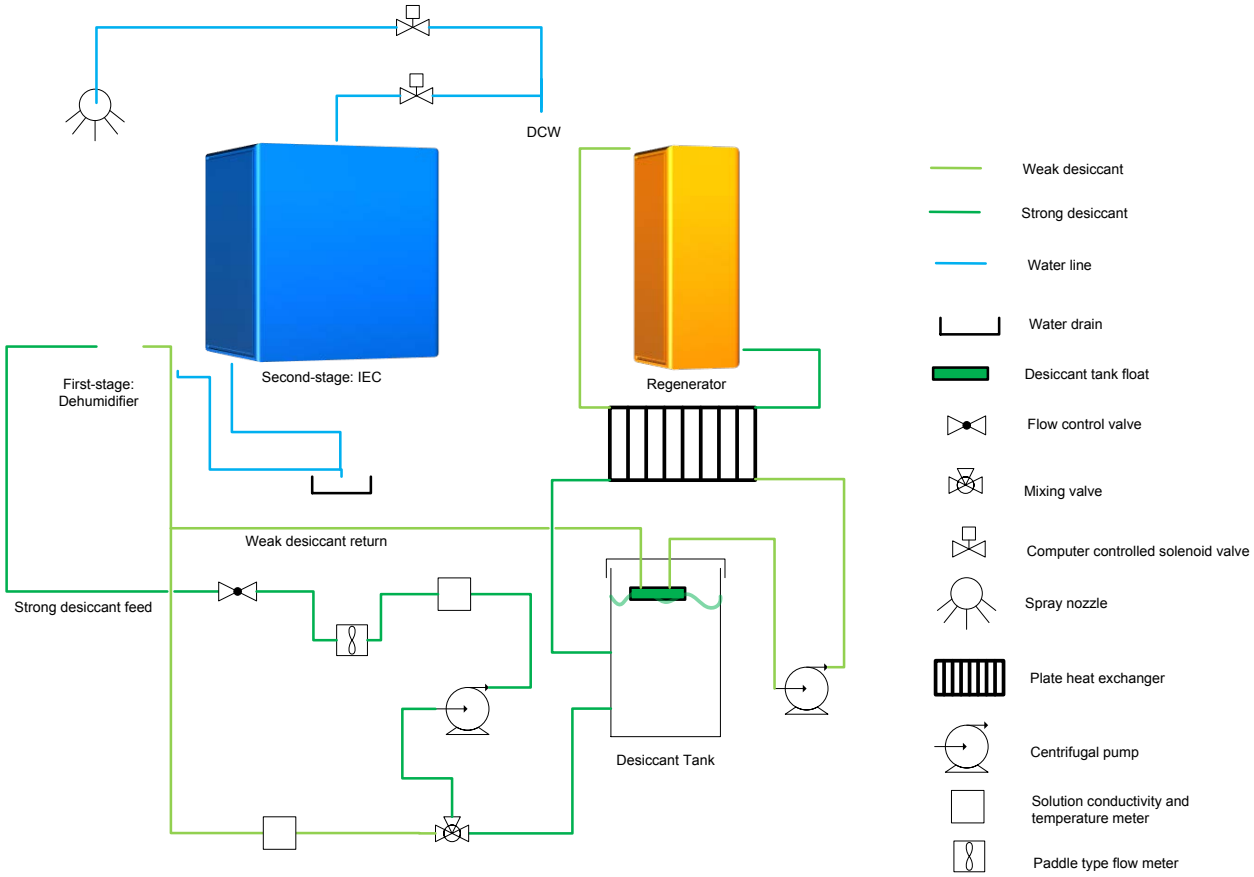

Figure A–1 Test schematic showing liquid flows and measurements

Illustration by Eric Kozubal, NREL

Appendix B Measured and Modeled Data for All AIL Research and Synapse Tests

The following pages show experimental and modeled data. They are presented in six tables, with each table in both IP and SI units. Symbols are defined in the Nomenclature section. The tables are in the following order:

Table B–1 AIL Research Prototype – Measured and Model Input Data (IP units)

	AILR - IP units													
	Input data (measured & modeled)													
Test number	**P_amb**	**Air Flow S12**	**Air Flow S34**	**Airflow S25**	**LD Flow**	**C_LD**	**T_LD**	**T S1**	**T S3**	**Tdp S1**	**w_s1**	**Tdp S3**	**S1 Water Duty**	**S2 Water Duty**
Full device	psi	SCFM	SCFM	SCFM	GPM	%	°F	°F	°F	°F	lb/lb	°F	%	%
1	12.0	275.5	137.8	-	0.22	38.0%	84.3	80.0	95.0	61.7	0.0144	68.5	100%	-
2	12.0	275.7	137.7	82.6	0.22	38.0%	90.1	80.0	95.0	61.7	0.0144	68.5	100%	7.7%
3	11.9	275.5	137.7	82.6	0.22	37.9%	87.5	81.7	95.0	61.7	0.0145	68.5	100%	11.1%
4	11.9	275.2	137.7	82.7	0.22	38.1%	87.6	81.7	95.0	61.7	0.0145	68.5	100%	11.1%
5	11.9	275.7	137.7	82.6	0.22	35.1%	85.9	81.7	95.0	61.7	0.0145	68.5	100%	11.1%
6	11.9	275.5	137.7	27.5	0.22	38.3%	89.1	77.9	95.0	59.4	0.0133	68.5	100%	11.1%
7	12.0	275.3	137.7	55.1	0.22	38.2%	87.9	79.8	95.0	60.6	0.0139	68.5	100%	11.1%
8	12.1	275.3	137.6	82.5	0.13	43.8%	88.0	81.7	95.0	61.7	0.0143	68.5	0%	14.3%
9	12.1	275.6	137.7	82.6	0.13	43.4%	94.5	81.7	95.0	61.7	0.0143	68.5	100%	14.3%
10	12.1	277.5	137.7	82.5	0.16	43.5%	103.2	95.0	95.0	68.5	0.0182	68.5	100%	14.3%
11	12.1	275.6	137.7	55.1	0.16	43.9%	104.5	95.0	95.0	68.5	0.0181	68.5	100%	14.3%
12	12.1	275.5	137.7	55.0	0.16	40.3%	96.5	95.0	95.0	68.5	0.0181	68.5	100%	14.3%
13	12.1	276.0	137.7	82.6	0.16	40.8%	97.7	95.0	95.0	68.5	0.0181	68.5	100%	14.3%
14	12.1	276.0	137.7	82.7	0.16	40.7%	91.3	81.7	95.0	61.7	0.0143	68.5	100%	14.3%
15	12.1	275.3	137.7	55.1	0.22	40.6%	94.3	81.7	95.0	61.7	0.0143	68.5	100%	14.3%
16	12.1	275.4	137.7	55.1	0.22	41.0%	93.3	79.8	95.0	60.6	0.0139	68.5	100%	14.3%
17	12.1	275.6	137.7	27.6	0.22	40.9%	92.6	77.9	95.0	59.4	0.0132	68.5	100%	14.3%
18	12.0	275.5	137.8	82.6	0.22	37.9%	87.4	76.3	77.0	61.7	0.0144	68.5	100%	11.1%
19	12.0	275.3	137.7	55.1	0.22	37.7%	87.1	76.2	77.0	60.6	0.0139	68.5	100%	11.1%
20	12.0	274.9	137.8	27.6	0.22	37.7%	86.1	76.1	77.0	59.4	0.0134	68.5	100%	11.1%
21	12.0	275.4	137.7	82.6	0.22	37.9%	83.8	76.3	77.0	58.5	0.0128	59.0	100%	11.1%
22	11.9	275.3	137.7	55.1	0.22	37.7%	83.1	76.2	77.0	58.4	0.0128	59.0	100%	11.1%
23	11.9	275.4	137.8	27.5	0.22	38.1%	83.9	76.1	77.0	58.3	0.0128	59.0	100%	11.1%
24	11.9	275.8	137.7	82.6	0.22	37.9%	86.1	81.7	95.0	58.5	0.0129	59.0	100%	11.1%
25	11.9	276.3	137.7	55.0	0.22	38.1%	85.6	79.8	95.0	58.4	0.0128	59.0	100%	11.1%
26	11.9	275.8	137.7	27.5	0.22	37.5%	83.4	77.9	95.0	58.3	0.0128	59.0	100%	11.1%
27	11.9	275.4	137.7	82.6	0.22	38.0%	88.5	81.7	95.0	61.7	0.0145	68.5	100%	11.1%
28	11.9	193.1	96.4	57.8	0.22	38.3%	87.8	81.7	95.0	61.7	0.0145	68.5	100%	11.1%
29	11.9	193.1	96.3	38.7	0.22	38.2%	88.1	79.8	95.0	60.6	0.0140	68.5	100%	11.1%
30	11.9	110.4	55.1	33.0	0.22	38.1%	85.3	82.8	98.6	59.6	0.0130	62.6	100%	11.1%
AILR stage 2														
1	11.7	275.5	-	82.7	-	-	-	95.0	-	26.6	0.0034	-	-	7.7%
2	11.7	275.5	-	55.2	-	-	-	95.0	-	50.0	0.0096	-	-	7.7%
3	11.7	275.4	-	27.6	-	-	-	95.0	-	50.0	0.0096	-	-	7.7%
4	11.8	192.8	-	57.9	-	-	-	95.0	-	50.0	0.0095	-	-	7.7%
5	11.8	110.2	-	33.0	-	-	-	95.0	-	50.0	0.0096	-	-	7.7%
6	11.8	275.5	-	82.6	-	-	-	95.0	-	64.4	0.0162	-	-	7.7%
7	12.0	270.0	-	80.7	-	-	-	84.0	-	51.2	0.0098	-	-	11.1%
8	12.0	270.0	-	80.8	-	-	-	95.0	-	51.1	0.0098	-	-	11.1%
9	12.0	270.0	-	80.6	-	-	-	110.0	-	51.5	0.0099	-	-	11.1%
10	12.1	269.0	-	25.8	-	-	-	77.0	-	53.6	0.0107	-	-	11.1%

Table B–2 AIL Research Prototype – Measured and Model Input Data (SI units)

Test number	P_amb	Air Flow S12	Air Flow S34	Airflow S25	LD Flow	C_LD	T_LD	T S1	T S3	Tdp S1	w_s1	Tdp S3	S1 Water Duty	S2 Water Duty
Full device	kPa	kg/s	kg/s	kg/s	LPM	%	°C	°C	°C	°C	kg/kg	°C	%	%
1	82.6	0.154	0.077	-	0.83	38.0%	29.1	26.7	35.0	16.5	0.0144	20.3	100%	-
2	82.9	0.154	0.077	0.046	0.83	38.0%	32.3	26.7	35.0	16.5	0.0144	20.3	100%	7.7%
3	82.4	0.154	0.077	0.046	0.83	37.9%	30.8	27.6	35.0	16.5	0.0145	20.3	100%	11.1%
4	82.3	0.154	0.077	0.046	0.83	38.1%	30.9	27.6	35.0	16.5	0.0145	20.3	100%	11.1%
5	82.2	0.154	0.077	0.046	0.83	35.1%	29.9	27.6	35.0	16.5	0.0145	20.3	100%	11.1%
6	82.2	0.154	0.077	0.015	0.83	38.3%	31.7	25.5	35.0	15.2	0.0133	20.3	100%	11.1%
7	82.8	0.154	0.077	0.031	0.83	38.2%	31.0	26.6	35.0	15.9	0.0139	20.3	100%	11.1%
8	83.5	0.154	0.077	0.046	0.50	43.8%	31.1	27.6	35.0	16.5	0.0143	20.3	0%	14.3%
9	83.4	0.154	0.077	0.046	0.50	43.4%	34.7	27.6	35.0	16.5	0.0143	20.3	100%	14.3%
10	83.4	0.155	0.077	0.046	0.60	43.5%	39.6	35.0	35.0	20.3	0.0182	20.3	100%	14.3%
11	83.4	0.154	0.077	0.031	0.60	43.9%	40.3	35.0	35.0	20.3	0.0181	20.3	100%	14.3%
12	83.3	0.154	0.077	0.031	0.60	40.3%	35.9	35.0	35.0	20.3	0.0181	20.3	100%	14.3%
13	83.4	0.154	0.077	0.046	0.60	40.8%	36.5	35.0	35.0	20.3	0.0181	20.3	100%	14.3%
14	83.4	0.154	0.077	0.046	0.60	40.7%	32.9	27.6	35.0	16.5	0.0143	20.3	100%	14.3%
15	83.4	0.154	0.077	0.031	0.83	40.6%	34.6	27.6	35.0	16.5	0.0143	20.3	100%	14.3%
16	83.3	0.154	0.077	0.031	0.83	41.0%	34.0	26.6	35.0	15.9	0.0139	20.3	100%	14.3%
17	83.4	0.154	0.077	0.015	0.83	40.9%	33.7	25.5	35.0	15.2	0.0132	20.3	100%	14.3%
18	82.6	0.154	0.077	0.046	0.83	37.9%	30.8	24.6	25.0	16.5	0.0144	20.3	100%	11.1%
19	82.7	0.154	0.077	0.031	0.83	37.7%	30.6	24.6	25.0	15.9	0.0139	20.3	100%	11.1%
20	82.5	0.154	0.077	0.015	0.83	37.7%	30.1	24.5	25.0	15.2	0.0134	20.3	100%	11.1%
21	82.4	0.154	0.077	0.046	0.83	37.9%	28.8	24.6	25.0	14.7	0.0128	15.0	100%	11.1%
22	82.3	0.154	0.077	0.031	0.83	37.7%	28.4	24.6	25.0	14.7	0.0128	15.0	100%	11.1%
23	82.3	0.154	0.077	0.015	0.83	38.1%	28.8	24.5	25.0	14.6	0.0128	15.0	100%	11.1%
24	82.2	0.154	0.077	0.046	0.83	37.9%	30.0	27.6	35.0	14.7	0.0129	15.0	100%	11.1%
25	82.2	0.154	0.077	0.031	0.83	38.1%	29.8	26.6	35.0	14.7	0.0128	15.0	100%	11.1%
26	82.3	0.154	0.077	0.015	0.83	37.5%	28.6	25.5	35.0	14.6	0.0128	15.0	100%	11.1%
27	82.2	0.154	0.077	0.046	0.83	38.0%	31.4	27.6	35.0	16.5	0.0145	20.3	100%	11.1%
28	82.2	0.108	0.054	0.032	0.83	38.3%	31.0	27.6	35.0	16.5	0.0145	20.3	100%	11.1%
29	82.2	0.108	0.054	0.022	0.83	38.2%	31.2	26.6	35.0	15.9	0.0140	20.3	100%	11.1%
30	82.3	0.062	0.031	0.018	0.83	38.1%	29.6	28.2	37.0	15.3	0.0130	17.0	100%	11.1%
AILR stage 2														
1	80.9	0.154	-	0.046	-	-	-	35.0	-	-3.0	0.0034	-	-	7.7%
2	81.0	0.154	-	0.031	-	-	-	35.0	-	10.0	0.0096	-	-	7.7%
3	81.0	0.154	-	0.015	-	-	-	35.0	-	10.0	0.0096	-	-	7.7%
4	81.0	0.108	-	0.032	-	-	-	35.0	-	10.0	0.0095	-	-	7.7%
5	81.0	0.062	-	0.018	-	-	-	35.0	-	10.0	0.0096	-	-	7.7%
6	81.1	0.154	-	0.046	-	-	-	35.0	-	18.0	0.0162	-	-	7.7%
7	82.6	0.151	-	0.045	-	-	-	28.9	-	10.7	0.0098	-	-	11.1%
8	82.6	0.151	-	0.045	-	-	-	35.0	-	10.6	0.0098	-	-	11.1%
9	82.6	0.151	-	0.045	-	-	-	43.3	-	10.8	0.0099	-	-	11.1%
10	83.2	0.150	-	0.014	-	-	-	25.0	-	12.0	0.0107	-	-	11.1%

Table B–3 AIL Research Prototype – Measured Output Data (IP units)

	AILR - IP units														
	Output data (measured)														
Test number	**ΔP 12**	**ΔP 34**	**ΔP 25**	**Fan power**	**T S2**	**w S2**	**h S2**	**Δw 12**	**ΔT 12**	**Δh 12**	**Q_cooling**	**Q_sensible**	**Q_latent**	**Q_th**	**COP_unit**
Full device	in WC	in WC	in WC	hp	°C	lb/lb	BTU/lb	lb/lb	°F	BTU/lb	BTU/hr	BTU/hr	BTU/hr	BTU/hr	-
1	0.169	0.472		0.044	83.9	0.0098	23.2	0.0046	-3.9	1.7	4956	-667	5623	5623	
2	1.096	0.460	0.395	0.158	58.4	0.0100	17.2	0.0044	21.6	4.3	8662	4868	3794	5419	1.18
3	1.058	0.460	0.395	0.155	58.7	0.0096	16.9	0.0049	23.0	4.7	9410	5194	4216	6023	1.18
4	1.064	0.460	0.395	0.156	58.4	0.0095	16.7	0.0050	23.2	4.8	9567	5247	4320	6174	1.18
5	1.062	0.460	0.395	0.156	59.1	0.0102	17.6	0.0043	22.6	4.4	8785	5072	3713	5302	1.22
6	1.085	0.460	0.102	0.145	70.1	0.0092	19.2	0.0041	7.8	2.8	7059	2496	4563	5070	1.03
7	1.097	0.460	0.234	0.150	63.5	0.0097	18.1	0.0042	16.4	3.7	8448	4293	4155	5195	1.20
8	1.038	0.460	0.394	0.150	59.7	0.0099	17.4	0.0044	20.3	4.2	8377	4593	3784	5404	1.16
9	1.067	0.460	0.395	0.153	57.3	0.0089	15.7	0.0054	22.7	4.9	9784	5166	4618	6596	1.14
10	1.077	0.460	0.394	0.160	61.0	0.0113	19.2	0.0069	34.1	6.9	13768	7777	5992	8537	1.28
11	1.106	0.460	0.234	0.155	65.0	0.0112	20.2	0.0069	30.0	6.4	14621	7856	6765	8455	1.37
12	1.102	0.460	0.233	0.155	65.9	0.0121	21.4	0.0060	29.1	5.9	13420	7559	5861	7325	1.43
13	1.075	0.460	0.395	0.160	61.9	0.0121	20.3	0.0061	33.1	6.4	12705	7465	5240	7480	1.32
14	1.042	0.460	0.395	0.152	58.4	0.0098	16.9	0.0045	23.6	4.6	9182	5304	3878	5538	1.24
15	1.076	0.460	0.234	0.147	63.1	0.0097	18.0	0.0046	18.9	4.2	9450	4916	4535	5669	1.26
16	1.071	0.460	0.234	0.146	62.7	0.0093	17.4	0.0047	17.2	4.0	9127	4523	4605	5756	1.20
17	1.073	0.460	0.102	0.142	71.3	0.0090	19.2	0.0042	6.6	2.7	6800	2174	4626	5140	0.99
18	1.070	0.461	0.395	0.154	57.9	0.0093	16.3	0.0051	17.1	4.2	8332	3956	4376	6250	1.02
19	1.089	0.460	0.234	0.148	62.7	0.0093	17.5	0.0045	12.6	3.4	7843	3401	4442	5553	1.06
20	1.110	0.460	0.102	0.146	70.0	0.0092	19.1	0.0042	5.7	2.6	6626	1942	4684	5207	0.95
21	1.063	0.460	0.395	0.153	55.8	0.0082	14.6	0.0047	17.9	4.1	8100	4082	4019	5741	1.06
22	1.080	0.460	0.234	0.147	61.1	0.0083	16.0	0.0045	13.3	3.5	8013	3565	4447	5560	1.08
23	1.109	0.461	0.102	0.147	68.0	0.0083	17.7	0.0045	7.1	2.9	7347	2348	4998	5554	1.00
24	1.064	0.460	0.395	0.156	57.2	0.0091	15.9	0.0038	24.5	4.3	8655	5422	3233	4616	1.35
25	1.094	0.460	0.233	0.151	62.3	0.0089	16.9	0.0039	17.5	3.7	8437	4541	3895	4865	1.27
26	1.116	0.460	0.102	0.148	69.9	0.0089	18.8	0.0039	8.0	2.7	6834	2536	4299	4776	1.05
27	1.057	0.460	0.395	0.155	58.4	0.0100	17.2	0.0045	23.3	4.6	9112	5219	3893	5561	1.22
28	0.705	0.328	0.248	0.073	57.5	0.0089	15.8	0.0056	24.2	5.2	7236	3850	3386	4832	1.22
29	0.717	0.327	0.152	0.070	62.4	0.0088	16.8	0.0052	17.4	4.3	6839	3235	3604	4506	1.23
30	0.374	0.220	0.126	0.023	56.6	0.0075	14.0	0.0055	26.2	5.3	4244	2356	1888	2695	1.34
AILR stage 2															
1	1.139	-	0.399	0.142	49.5	0.0036	8.1	0.000	45.5	10.8	9229	9404.21	-174.74	-	7.50
2	1.178	-	0.236	0.140	64.5	0.0094	18.1	0.000	30.5	7.6	7430	7311.39	118.80	-	6.15
3	1.199	-	0.102	0.138	76.2	0.0095	21.0	0.000	18.8	4.7	5119	5052.15	67.26	-	4.30
4	0.786	-	0.251	0.069	57.6	0.0095	16.5	0.000	37.4	9.2	5496	5481.68	14.16	-	9.25
5	0.429	-	0.126	0.021	57.4	0.0097	16.6	0.000	37.6	9.1	3101	3138.95	-37.50	-	16.86
6	1.169	-	0.399	0.148	66.8	0.0159	25.6	0.000	28.2	7.4	6324	5996.46	327.91	-	4.94
7	1.135	-	0.396	0.137	57.2	0.0098	16.7	0.000	26.8	6.6	5614	5613.88	0.34	-	4.73
8	1.015	-	0.397	0.126	58.1	0.0098	11.3	0.000	36.9	14.6	7721	7721.36	0.85	-	7.06
9	1.110	-	0.396	0.141	58.7	0.0099	11.4	0.000	51.3	18.3	10729	10729.10	1.02	-	8.81
10	1.186	-	0.096	0.128	69.8	0.0107	20.7	0.000	7.2	1.8	1933	1933.02	0.17	-	1.75

Table B–4 AIL Research Prototype – Measured Output Data (SI units)

	AILR - SI Units														
	Output data (measured)														
Test number	**ΔP 12**	**ΔP 34**	**ΔP 25**	**Fan power**	**T S2**	**w S2**	**h S2**	**Δw 12**	**ΔT 12**	**Δh 12**	**Q_cooling**	**Q_sensible**	**Q_latent**	**Q_th**	**COP_unit**
Full device	Pa	Pa	Pa	kW	°C	kg/kg	kJ/kg	kg/kg	°C	kJ/kg	kW	kW	kW	kW	-
1	42	118	-	0.033	28.8	0.0098	54.1	0.0046	-2.2	4.1	1.45	-0.20	1.65	1.65	
2	273	115	98	0.118	14.7	0.0100	40.1	0.0044	12.0	10.1	2.54	1.43	1.11	1.59	1.18
3	263	115	98	0.116	14.8	0.0096	39.3	0.0049	12.8	11.0	2.76	1.52	1.24	1.77	1.18
4	265	115	98	0.116	14.7	0.0095	38.8	0.0050	12.9	11.2	2.80	1.54	1.27	1.81	1.18
5	264	115	98	0.116	15.0	0.0102	41.0	0.0043	12.6	10.3	2.57	1.49	1.09	1.55	1.22
6	270	115	25	0.108	21.2	0.0092	44.7	0.0041	4.3	6.4	2.07	0.73	1.34	1.49	1.03
7	273	114	58	0.112	17.5	0.0097	42.2	0.0042	9.1	8.6	2.48	1.26	1.22	1.52	1.20
8	258	114	98	0.112	15.4	0.0099	40.5	0.0044	11.3	9.8	2.46	1.35	1.11	1.58	1.16
9	266	115	98	0.114	14.0	0.0089	36.7	0.0054	12.6	11.4	2.87	1.51	1.35	1.93	1.14
10	268	114	98	0.120	16.1	0.0113	44.8	0.0069	18.9	16.0	4.04	2.28	1.76	2.50	1.28
11	275	115	58	0.116	18.3	0.0112	46.9	0.0069	16.7	14.9	4.29	2.30	1.98	2.48	1.37
12	274	115	58	0.115	18.8	0.0121	49.7	0.0060	16.2	13.7	3.93	2.22	1.72	2.15	1.43
13	267	115	98	0.119	16.6	0.0121	47.3	0.0061	18.4	14.8	3.72	2.19	1.54	2.19	1.32
14	259	115	98	0.113	14.6	0.0098	39.4	0.0045	13.1	10.7	2.69	1.55	1.14	1.62	1.24
15	268	115	58	0.110	17.3	0.0097	41.9	0.0046	10.5	9.7	2.77	1.44	1.33	1.66	1.26
16	267	114	58	0.109	17.0	0.0093	40.6	0.0047	9.6	9.3	2.67	1.33	1.35	1.69	1.20
17	267	115	25	0.106	21.8	0.0090	44.8	0.0042	3.6	6.2	1.99	0.64	1.36	1.51	0.99
18	266	115	98	0.115	14.4	0.0093	38.0	0.0051	9.5	9.7	2.44	1.16	1.28	1.83	1.02
19	271	115	58	0.110	17.1	0.0093	40.8	0.0045	7.0	8.0	2.30	1.00	1.30	1.63	1.06
20	276	115	25	0.109	21.1	0.0092	44.5	0.0042	3.2	6.0	1.94	0.57	1.37	1.53	0.95
21	265	115	98	0.114	13.2	0.0082	33.9	0.0047	9.9	9.5	2.37	1.20	1.18	1.68	1.06
22	269	115	58	0.110	16.2	0.0083	37.3	0.0045	7.4	8.2	2.35	1.04	1.30	1.63	1.08
23	276	115	25	0.109	20.0	0.0083	41.3	0.0045	4.0	6.7	2.15	0.69	1.46	1.63	1.00
24	265	115	98	0.116	14.0	0.0091	37.1	0.0038	13.6	10.1	2.54	1.59	0.95	1.35	1.35
25	272	115	58	0.112	16.8	0.0089	39.4	0.0039	9.7	8.6	2.47	1.33	1.14	1.43	1.27
26	278	115	25	0.111	21.0	0.0089	43.8	0.0039	4.5	6.2	2.00	0.74	1.26	1.40	1.05
27	263	115	98	0.116	14.7	0.0100	40.0	0.0045	12.9	10.6	2.67	1.53	1.14	1.63	1.22
28	176	82	62	0.054	14.2	0.0089	36.8	0.0056	13.4	12.1	2.12	1.13	0.99	1.42	1.22
29	178	81	38	0.052	16.9	0.0088	39.2	0.0052	9.7	10.0	2.00	0.95	1.06	1.32	1.23
30	93	55	31	0.017	13.7	0.0075	32.7	0.0055	14.5	12.4	1.24	0.69	0.55	0.79	1.34
AILR stage 2															
1	284	-	99	0.106	9.7	0.0036	18.9	0.000	25.3	25.1	2.70	2.76	-0.05	-	7.50
2	293	-	59	0.104	18.0	0.0094	42.1	0.000	17.0	17.7	2.18	2.14	0.03	-	6.15
3	298	-	25	0.103	24.6	0.0095	48.9	0.000	10.4	10.8	1.50	1.48	0.02	-	4.30
4	196	-	62	0.051	14.2	0.0095	38.3	0.000	20.8	21.4	1.61	1.61	0.00	-	9.25
5	107	-	31	0.016	14.1	0.0097	38.6	0.000	20.9	21.1	0.91	0.92	-0.01	-	16.86
6	291	-	99	0.110	19.3	0.0159	59.7	0.000	15.7	17.2	1.85	1.76	0.10	-	4.94
7	282	-	99	0.102	14	0.0098	38.9	0.000	14.9	15.3	1.65	1.65	0.00	-	4.73
8	253	-	99	0.094	14.49	0.0098	26.3	0.000	20.5	34.0	2.26	2.26	0.00	-	7.06
9	276	-	99	0.105	14.85	0.0099	26.7	0.000	28.5	42.5	3.14	3.14	0.00	-	8.81
10	295	-	24	0.095	21.01	0.0107	48.2	0.000	4.0	4.1	0.57	0.57	0.00	-	1.75

Table B–5 AIL Research Prototype – Modeled Output Data (IP units)

	AILR - IP units														
	Output data (modeled)														
Test number	**ΔP 12**	**ΔP 34**	**ΔP 25**	**Fan power**	**T S2**	**w S2**	**h S2**	**Δw 12**	**ΔT 12**	**Δh 12**	**Q_cooling**	**Q_sensible**	**Q_latent**	**Q_th**	**COP_unit**
Full device	in WC	in WC	in WC	hp	°F	lb/lb	BTU/lb	lb/lb	°F	BTU/lb	BTU/hr	BTU/hr	BTU/hr	BTU/hr	-
1	1.21	0.33	-	0.040	84.0	0.0085	21.8	0.0059	-4.0	5.5	6719	-547	7266	7266	
2	1.19	0.33	0.07	0.143	55.6	0.0088	15.2	0.0057	24.4	12.2	10416	5538	4879	6968	1.15
3	1.20	0.33	0.08	0.146	55.6	0.0089	15.3	0.0057	26.1	12.6	10762	5886	4877	6966	1.20
4	1.20	0.33	0.08	0.146	55.5	0.0088	15.2	0.0057	26.2	12.7	10849	5913	4936	7054	1.19
5	1.20	0.33	0.08	0.147	57.2	0.0100	16.9	0.0045	24.5	11.0	9388	5484	3905	5577	1.25
6	1.20	0.33	0.03	0.143	72.6	0.0080	18.5	0.0053	5.2	7.1	7790	1926	5864	6516	0.93
7	1.19	0.33	0.05	0.142	61.8	0.0084	16.3	0.0055	18.1	10.5	10231	4797	5433	6793	1.17
8	1.17	0.33	0.07	0.141	58.5	0.0096	16.8	0.0047	21.5	10.4	8902	4851	4051	5786	1.16
9	1.18	0.33	0.07	0.141	53.3	0.0071	12.8	0.0072	26.7	14.4	12307	6110	6198	8852	1.11
10	1.24	0.33	0.08	0.153	57.2	0.0092	16.0	0.0090	37.8	19.2	16565	8717	7848	11182	1.21
11	1.24	0.33	0.05	0.151	63.7	0.0088	17.2	0.0093	31.3	17.9	17479	8352	9127	11407	1.26
12	1.24	0.33	0.05	0.151	64.8	0.0102	18.9	0.0079	30.2	16.1	15792	7983	7809	9759	1.31
13	1.23	0.33	0.08	0.152	58.3	0.0100	17.2	0.0081	36.7	17.9	15354	8367	6987	9973	1.24
14	1.18	0.33	0.07	0.143	54.6	0.0079	14.0	0.0063	27.4	13.6	11700	6225	5475	7817	1.18
15	1.19	0.33	0.05	0.141	61.7	0.0078	15.6	0.0065	20.3	12.1	11803	5407	6396	7996	1.17
16	1.18	0.33	0.05	0.140	61.3	0.0074	15.1	0.0065	18.6	11.7	11407	5006	6402	8002	1.13
17	1.18	0.33	0.03	0.139	73.2	0.0071	17.6	0.0061	4.7	7.8	8619	1863	6756	7506	0.91
18	1.17	0.32	0.07	0.140	54.1	0.0081	14.1	0.0063	20.9	12.0	10261	4834	5428	7752	1.04
19	1.18	0.31	0.05	0.139	60.7	0.0079	15.5	0.0059	14.7	10.1	9837	4002	5835	7294	1.06
20	1.18	0.32	0.03	0.139	70.8	0.0077	17.7	0.0057	4.9	7.4	8173	1861	6311	7015	0.91
21	1.17	0.31	0.07	0.138	51.3	0.0068	12.0	0.0060	22.4	12.0	10282	5105	5177	7397	1.09
22	1.17	0.31	0.05	0.138	58.4	0.0069	13.8	0.0059	16.1	10.4	10171	4326	5846	7308	1.09
23	1.18	0.31	0.03	0.139	68.1	0.0067	16.0	0.0061	7.1	8.4	9239	2491	6748	7498	0.97
24	1.20	0.33	0.07	0.145	53.4	0.0078	13.5	0.0051	28.3	12.5	10709	6305	4405	6290	1.30
25	1.20	0.33	0.05	0.144	60.1	0.0075	14.9	0.0053	19.7	10.6	10383	5170	5213	6511	1.23
26	1.20	0.33	0.03	0.142	70.4	0.0076	17.5	0.0052	7.5	7.5	8320	2525	5796	6438	0.99
27	1.20	0.33	0.08	0.146	55.5	0.0089	15.3	0.0056	26.2	12.6	10763	5901	4861	6945	1.20
28	0.83	0.23	0.05	0.071	52.8	0.0080	13.7	0.0065	28.9	14.2	8530	4588	3942	5627	1.25
29	0.83	0.23	0.04	0.070	60.2	0.0078	15.2	0.0062	19.6	11.6	7945	3659	4286	5358	1.22
30	0.47	0.13	0.03	0.023	48.5	0.0065	11.0	0.0064	34.3	15.4	5271	3059	2212	3158	1.43
AILR stage 2															
1	1.23	-	0.08	0.142	47.3	0.0034	7.3	0.0000	47.7	11.6	9894	9894	0	-	8.04
2	1.26	-	0.05	0.145	63.9	0.0096	18.1	0.0000	31.1	7.6	7402	7402	0	-	6.13
3	1.27	-	0.03	0.145	77.6	0.0096	21.4	0.0000	17.4	4.2	4651	4651	0	-	3.90
4	0.87	-	0.05	0.070	55.3	0.0095	15.9	0.0000	39.7	9.7	5829	5829	0	-	9.81
5	0.49	-	0.03	0.023	53.8	0.0096	15.6	0.0000	41.2	10.0	3434	3434	0	-	18.66
6	1.27	-	0.08	0.149	66.8	0.0162	26.0	0.0000	28.2	7.0	6024	6024	0	-	4.70
7	1.17	-	0.07	0.128	57.25	0.0098	16.7	0.0000	26.8	6.6	5617	5617	0	-	4.97
8	1.2	-	0.07	0.134	58.05	0.0098	16.9	0.0000	37.0	9.0	7707	7707	0	-	6.54
9	1.25	-	0.08	0.143	59.00	0.0099	17.2	0.0000	51.0	12.5	10687	10687	0	-	8.47
10	1.15	-	0.02	0.121	70.66	0.0107	21.0	0.0000	6.3	1.5	1646	1646	0	-	1.60

Table B–6 AIL Research Prototype – Modeled Output Data (SI units)

	AILR - SI Units														
	Output data (modeled)														
Test number	**ΔP 12**	**ΔP 34**	**ΔP 25**	**Fan power**	**T S2**	**w S2**	**h S2**	**Δw 12**	**ΔT 12**	**Δh 12**	**Q_cooling**	**Q_sensible**	**Q_latent**	**Q_th**	**COP_unit**
Full device	Pa	Pa	Pa	kW	°C	kg/kg	kJ/kg	kg/kg	°C	BTU/lb	kW	kW	kW	kW	-
1	301	82	-	0.030	28.8	0.0085	21.8	0.0059	-2.2	12.8	1.97	-0.16	2.13	2.13	
2	296	82	19	0.107	28.8	0.0088	15.2	0.0057	13.6	28.3	3.05	1.62	1.43	2.04	1.15
3	299	82	19	0.109	28.8	0.0089	15.3	0.0057	14.5	29.3	3.15	1.72	1.43	2.04	1.20
4	299	82	19	0.109	28.8	0.0088	15.2	0.0057	14.6	29.5	3.18	1.73	1.45	2.07	1.19
5	299	82	19	0.109	28.8	0.0100	16.9	0.0045	13.6	25.5	2.75	1.61	1.14	1.63	1.25
6	299	82	6	0.107	28.8	0.0080	18.5	0.0053	2.9	16.5	2.28	0.56	1.72	1.91	0.93
7	296	82	13	0.106	28.8	0.0084	16.3	0.0055	10.1	24.4	3.00	1.41	1.59	1.99	1.17
8	291	81	18	0.105	28.8	0.0096	16.8	0.0047	11.9	24.2	2.61	1.42	1.19	1.70	1.16
9	294	81	18	0.105	28.8	0.0071	12.8	0.0072	14.8	33.5	3.61	1.79	1.82	2.59	1.11
10	309	82	19	0.114	28.8	0.0092	16.0	0.0090	21.0	44.7	4.85	2.55	2.30	3.28	1.21
11	309	82	13	0.112	28.8	0.0088	17.2	0.0093	17.4	41.6	5.12	2.45	2.67	3.34	1.26
12	309	82	13	0.113	28.8	0.0102	18.9	0.0079	16.8	37.6	4.63	2.34	2.29	2.86	1.31
13	306	82	19	0.113	28.8	0.0100	17.2	0.0081	20.4	41.7	4.50	2.45	2.05	2.92	1.24
14	294	81	18	0.106	28.8	0.0079	14.0	0.0063	15.2	31.8	3.43	1.82	1.60	2.29	1.18
15	296	81	13	0.106	28.8	0.0078	15.6	0.0065	11.3	28.1	3.46	1.58	1.87	2.34	1.17
16	294	81	13	0.105	28.8	0.0074	15.1	0.0065	10.3	27.2	3.34	1.47	1.88	2.35	1.13
17	294	81	6	0.104	28.8	0.0071	17.6	0.0061	2.6	18.2	2.53	0.55	1.98	2.20	0.91
18	291	78	19	0.104	28.8	0.0081	14.1	0.0063	11.6	27.9	3.01	1.42	1.59	2.27	1.04
19	294	78	13	0.103	28.8	0.0079	15.5	0.0059	8.1	23.4	2.88	1.17	1.71	2.14	1.06
20	294	78	6	0.104	28.8	0.0077	17.7	0.0057	2.7	17.3	2.40	0.55	1.85	2.06	0.91
21	291	77	18	0.103	28.8	0.0068	12.0	0.0060	12.4	28.0	3.01	1.50	1.52	2.17	1.09
22	291	77	12	0.103	28.8	0.0069	13.8	0.0059	8.9	24.2	2.98	1.27	1.71	2.14	1.09
23	294	77	6	0.103	28.8	0.0067	16.0	0.0061	4.0	19.5	2.71	0.73	1.98	2.20	0.97
24	299	81	19	0.108	28.8	0.0078	13.5	0.0051	15.7	29.1	3.14	1.85	1.29	1.84	1.30
25	299	81	13	0.107	28.8	0.0075	14.9	0.0053	10.9	24.6	3.04	1.52	1.53	1.91	1.23
26	299	81	6	0.106	28.8	0.0076	17.5	0.0052	4.2	17.6	2.44	0.74	1.70	1.89	0.99
27	299	82	19	0.109	28.8	0.0089	15.3	0.0056	14.5	29.3	3.15	1.73	1.42	2.04	1.20
28	207	58	13	0.053	28.8	0.0080	13.7	0.0065	16.1	33.1	2.50	1.34	1.16	1.65	1.25
29	207	58	9	0.052	28.8	0.0078	15.2	0.0062	10.9	27.0	2.33	1.07	1.26	1.57	1.22
30	117	33	7	0.017	28.8	0.0065	11.0	0.0064	19.0	35.8	1.54	0.90	0.65	0.93	1.43
AILR stage 2															
1	306	-	19	0.106	47.3	0.0034	7.3	0.0000	26.5	26.9	2.90	2.90	0.00	-	8.04
2	314	-	13	0.108	63.9	0.0096	18.1	0.0000	17.3	17.6	2.17	2.17	0.00	-	6.13
3	316	-	7	0.108	77.6	0.0096	21.4	0.0000	9.7	9.8	1.36	1.36	0.00	-	3.90
4	216	-	13	0.053	55.3	0.0095	15.9	0.0000	22.0	22.6	1.71	1.71	0.00	-	9.81
5	122	-	8	0.017	53.8	0.0096	15.6	0.0000	22.9	23.3	1.01	1.01	0.00	-	18.66
6	316	-	20	0.111	66.8	0.0162	26.0	0.0000	15.7	16.4	1.77	1.77	0.00	-	4.70
7	291	-	18	0.095	57.25	0.0098	16.7	0.0000	14.9	15.3	1.65	1.65	0.00	-	4.97
8	299	-	19	0.100	58.05	0.0098	16.9	0.0000	20.5	21.0	2.26	2.26	0.00	-	6.54
9	311	-	19	0.107	59.00	0.0099	17.2	0.0000	28.3	29.1	3.13	3.13	0.00	-	8.47
10	286	-	6	0.090	70.66	0.0107	21.0	0.0000	3.5	3.5	0.48	0.48	0.00	-	1.60

Table B–7 Synapse Prototype – Measured and Model Input Data (IP units)

	Synapse - IP Units											
	Input data (measured & modeled)											
Test number	**P_amb**	**Air Flow S12**	**Air Flow S34**	**LD Flow**	**C_LD_in**	**T LD**	**T S12**	**T S33**	**Tdp S14**	**w S1**	**Tdp S3**	**S1 Water Duty**
	psi	SCFM	SCFM	GPM	-	°F	°F	°F	°F	lb/lb	°F	%
1	12.0	274.0	0.1	0.089	0.378	83.1	69.6	-	61.7	0.01440	-	0.0%
2	12.0	193.5	0.1	0.082	0.378	78.8	69.6	-	61.7	0.01436	-	0.0%
3	12.0	355.1	0.1	0.089	0.378	82.2	69.6	-	61.7	0.01441	-	0.0%
4	12.0	275.5	110.1	0.089	0.373	81.4	80.1	95.0	61.7	0.01440	68.5	9.1%
5	12.0	275.4	110.0	0.095	0.379	83.7	80.1	80.0	61.7	0.01441	68.5	9.1%
6	12.0	275.4	110.0	0.089	0.377	82.7	80.1	80.1	61.7	0.01439	59.0	9.1%
7	12.0	275.5	110.2	0.089	0.376	82.6	80.1	95.0	61.7	0.01437	59.0	9.1%
8	12.0	275.4	110.2	0.095	0.385	89.2	95.0	95.0	68.5	0.01832	68.5	9.1%
9	12.0	275.4	82.6	0.089	0.379	84.2	80.1	95.0	61.7	0.01440	68.5	9.1%
10	12.0	275.5	55.1	0.089	0.376	82.9	80.1	95.0	61.7	0.01441	68.5	9.1%
11	12.0	192.8	77.1	0.082	0.381	85.7	80.1	95.0	61.7	0.01444	68.5	9.1%
12	11.8	330.5	132.2	0.089	0.379	81.9	80.1	95.0	61.7	0.01464	68.5	9.1%
13	11.9	275.4	110.2	0.089	0.378	85.8	80.1	95.0	61.7	0.01459	68.5	9.1%
14	11.8	275.5	110.2	0.079	0.424	95.4	95.0	95.0	68.5	0.01868	68.5	9.1%
15	11.8	275.6	110.2	0.079	0.428	91.5	80.0	95.0	61.7	0.01462	68.5	9.1%
16	11.9	275.4	110.2	0.154	0.377	84.6	80.1	95.0	61.7	0.01458	68.5	9.1%
17	12.0	275.4	110.2	0.151	0.334	78.5	80.0	95.0	61.7	0.01417	68.5	9.1%
18	12.0	275.4	110.2	0.117	0.362	77.4	80.0	95.0	61.7	0.01435	66.2	9.1%
19	12.0	275.4	110.3	0.136	0.343	84.8	80.0	95.0	61.7	0.01431	61.7	9.1%
20	12.0	275.5	82.7	0.136	0.345	86.5	80.0	95.0	61.7	0.01427	59.0	9.1%

Table B–8 Synapse Prototype – Measured and Model Input Data (SI units)

	Synapse - SI units											
	Input data (measured & modeled)											
Test number	**P_amb**	**Air Flow S12**	**Air Flow S34**	**LD Flow**	**C_LD_in**	**T LD**	**T S12**	**T S33**	**Tdp S14**	**w_S1**	**Tdp S3**	**S1 Water Duty**
	kPa	kg/s	kg/s	LPM	-	°C	°C	°C	°C	kg/kg	°C	%
1	82.9	0.1531	0.0001	0.337	0.378	28.4	20.9	-	16.5	0.01440	-	0.0%
2	83.0	0.1081	0.0001	0.310	0.378	26.0	20.9	-	16.5	0.01436	-	0.0%
3	82.9	0.1984	0.0001	0.337	0.378	27.9	20.9	-	16.5	0.01441	-	0.0%
4	82.8	0.1540	0.0615	0.337	0.373	27.4	26.7	35.0	16.5	0.01440	20.3	9.1%
5	82.9	0.1539	0.0615	0.360	0.379	28.7	26.7	26.7	16.5	0.01441	20.3	9.1%
6	82.9	0.1539	0.0615	0.337	0.377	28.2	26.7	26.7	16.5	0.01439	15.0	9.1%
7	82.8	0.1540	0.0616	0.337	0.376	28.1	26.7	35.0	16.5	0.01437	15.0	9.1%
8	82.8	0.1539	0.0616	0.360	0.385	31.8	35.0	35.0	20.3	0.01832	20.3	9.1%
9	82.7	0.1539	0.0462	0.337	0.379	29.0	26.7	35.0	16.5	0.01440	20.3	9.1%
10	82.7	0.1539	0.0308	0.337	0.376	28.3	26.7	35.0	16.5	0.01441	20.3	9.1%
11	82.6	0.1078	0.0431	0.310	0.381	29.8	26.7	35.0	16.5	0.01444	20.3	9.1%
12	81.6	0.1847	0.0739	0.337	0.379	27.7	26.7	35.0	16.5	0.01464	20.3	9.1%
13	81.8	0.1539	0.0616	0.337	0.378	29.9	26.7	35.0	16.5	0.01459	20.3	9.1%
14	81.7	0.1539	0.0616	0.299	0.424	35.2	35.0	35.0	20.3	0.01868	20.3	9.1%
15	81.6	0.1540	0.0616	0.299	0.428	33.1	26.7	35.0	16.5	0.01462	20.3	9.1%
16	81.8	0.1539	0.0616	0.583	0.377	29.2	26.7	35.0	16.5	0.01458	20.3	9.1%
17	83.0	0.1539	0.0616	0.572	0.334	25.9	26.7	35.0	16.5	0.01417	20.3	9.1%
18	83.0	0.1539	0.0616	0.443	0.362	25.2	26.7	35.0	16.5	0.01435	19.0	9.1%
19	82.9	0.1539	0.0616	0.515	0.343	29.3	26.7	35.0	16.5	0.01431	16.5	9.1%
20	82.9	0.1540	0.0462	0.515	0.345	30.3	26.7	35.0	16.5	0.01427	15.0	9.1%

Table B–9 Synapse Prototype – Measured Output Data (IP units)

	Synapse - IP Units												
	Output data (measured)												
Test number	**ΔP1-1.5**	**ΔP S34**	**Fan power**	**T_S1.5**	**w_S1.5**	**h_S1.5**	**Δw 1-1.5**	**ΔT 1-1.5**	**Δh 1-1.5**	**Q_cooling**	**Q_sensible**	**Q_latent**	**Q_th**
	in WC	in WC	hp	°F	lb/lb	BTU/lb	lb/lb	°F	BTU/lb	BTU/hr	BTU/hr	BTU/hr	BTU/hr
1	0.23	0.0	0.10	86.7	0.0101	24.2	0.0043	-17.0	0.5	633	-4612	5245	5245
2	0.14	0.0	0.04	88.2	0.0099	24.3	0.0045	-18.2	0.4	378	-3491	3870	3870
3	0.31	0.0	0.16	85.9	0.0107	24.7	0.0037	-15.5	0.2	346	-5485	5830	5830
4	0.24	1.04	0.27	81.0	0.0098	22.5	0.0046	-1.0	4.8	5914	209	5705	6374
5	0.24	0.99	0.26	79.4	0.0092	21.5	0.0052	0.6	5.9	7155	750	6405	7319
6	0.23	0.99	0.26	76.6	0.0088	20.3	0.0056	3.4	7.0	8519	1627	6892	7979
7	0.24	1.01	0.27	78.9	0.0093	21.4	0.0051	1.1	5.8	7127	896	6231	6996
8	0.25	1.02	0.27	86.5	0.0123	26.6	0.0060	8.5	8.7	10619	3254	7365	8150
9	0.24	0.65	0.18	82.1	0.0101	23.1	0.0043	-2.0	4.2	5105	-135	5240	5732
10	0.24	0.37	0.13	82.7	0.0103	23.5	0.0041	-2.6	3.9	4714	-339	5053	5524
11	0.14	0.59	0.11	80.8	0.0093	21.9	0.0051	-0.7	5.4	4656	244	4412	4834
12	0.36	1.26	0.43	81.2	0.0103	23.1	0.0044	-1.2	4.5	6608	154	6455	6746
13	0.24	0.98	0.26	81.0	0.0099	22.6	0.0047	-1.0	4.9	6025	230	5795	6211
14	0.25	0.97	0.26	87.1	0.0108	25.1	0.0078	7.9	10.6	12937	3288	9648	10059
15	0.26	1.01	0.27	82.8	0.0084	21.4	0.0062	-2.8	6.1	7478	-146	7624	8189
16	0.25	0.99	0.27	81.0	0.0097	22.4	0.0049	-1.0	5.1	6246	229	6017	6448
17	0.26	1.06	0.28	79.1	0.0109	23.2	0.0033	1.0	3.8	4648	644	4004	4381
18	0.26	1.06	0.28	79.9	0.0102	22.6	0.0042	0.1	4.6	5647	492	5155	5638
19	0.26	1.04	0.28	78.6	0.0104	22.6	0.0039	1.4	4.6	5613	839	4773	5207
20	0.23	0.89	0.21	78.0	0.0101	22.1	0.0042	2.0	5.1	6232	1058	5174	5661

Table B–10 Synapse Prototype – Measured Output Data (SI units)

	Synapse - SI units												
	Output data (measured)												
Test number	**ΔP1-1.5**	**ΔP S34**	**Fan power**	**T_S1.5**	**w_S1.5**	**h_S1.5**	**Δw 1-1.5**	**ΔT 1-1.5**	**Δh 1-1.5**	**Q_cooling**	**Q_sensible**	**Q_latent**	**Q_th**
	Pa	Pa	kW	°C	kg/kg	kJ/kg	kg/kg	°C	kJ/kg	kW	kW	kW	kW
1	58	0	0.07	30.4	0.0101	56.4	0.0043	-9.4	1.2	0.19	-1.35	1.54	1.54
2	35	0	0.03	31.2	0.0099	56.7	0.0045	-10.1	1.0	0.11	-1.02	1.13	1.13
3	76	0	0.12	29.9	0.0107	57.5	0.0037	-8.6	0.5	0.10	-1.61	1.71	1.71
4	60	258	0.20	27.2	0.0098	52.3	0.0046	-0.6	11.3	1.73	0.06	1.67	1.87
5	59	246	0.19	26.3	0.0092	50.0	0.0052	0.3	13.6	2.10	0.22	1.88	2.14
6	58	245	0.19	24.8	0.0088	47.3	0.0056	1.9	16.2	2.50	0.48	2.02	2.34
7	59	252	0.20	26.0	0.0093	49.9	0.0051	0.6	13.6	2.09	0.26	1.83	2.05
8	63	253	0.20	30.3	0.0123	62.0	0.0060	4.7	20.2	3.11	0.95	2.16	2.39
9	60	162	0.13	27.8	0.0101	53.9	0.0043	-1.1	9.7	1.50	-0.04	1.54	1.68
10	60	92	0.10	28.2	0.0103	54.6	0.0041	-1.5	9.0	1.38	-0.10	1.48	1.62
11	35	146	0.08	27.1	0.0093	51.0	0.0051	-0.4	12.7	1.36	0.07	1.29	1.42
12	89	314	0.32	27.4	0.0103	53.7	0.0044	-0.7	10.5	1.94	0.05	1.89	1.98
13	60	245	0.19	27.2	0.0099	52.6	0.0047	-0.5	11.5	1.77	0.07	1.70	1.82
14	63	242	0.20	30.6	0.0108	58.5	0.0078	4.4	24.6	3.79	0.96	2.83	2.95
15	65	250	0.20	28.2	0.0084	49.9	0.0062	-1.5	14.2	2.19	-0.04	2.23	2.40
16	62	246	0.20	27.2	0.0097	52.1	0.0049	-0.6	11.9	1.83	0.07	1.76	1.89
17	64	263	0.21	26.1	0.0109	54.1	0.0033	0.5	8.8	1.36	0.19	1.17	1.28
18	64	264	0.21	26.6	0.0102	52.7	0.0042	0.1	10.8	1.66	0.14	1.51	1.65
19	64	260	0.21	25.9	0.0104	52.6	0.0039	0.8	10.7	1.64	0.25	1.40	1.53
20	58	221	0.15	25.6	0.0101	51.4	0.0042	1.1	11.9	1.83	0.31	1.52	1.66

Table B–11 Synapse Prototype – Modeled Output Data (IP units)

	Synapse - IP Units												
	Output data (modeled)												
Test number	**ΔP1-1.5**	**ΔP S34**	**Fan power**	**T_S1.5**	**w_S1.5**	**h_S1.5**	**Δw 1-1.5**	**ΔT 1-1.5**	**Δh 1-1.5**	**Q_cooling**	**Q_sensible**	**Q_latent**	**Q_th**
	in WC	in WC	hp	°F	lb/lb	BTU/lb	lb/lb	°F	BTU/lb	BTU/hr	BTU/hr	BTU/hr	BTU/hr
1	0.40	0.00	0.16	87.49	0.0103	24.7	0.0041	-17.9	0.1	124	-4870	4994	4994
2	0.22	0.00	0.06	88.01	0.0100	24.5	0.0043	-18.4	0.3	260	-3473	3733	3733
3	0.62	0.00	0.33	86.67	0.0107	24.9	0.0037	-17.0	0.1	111	-5785	5896	5896
4	0.41	0.74	0.29	82.41	0.0097	22.8	0.0047	-2.3	4.5	5545	-203	5747	6421
5	0.40	0.78	0.29	81.08	0.0092	21.9	0.0052	-1.0	5.5	6666	252	6414	7329
6	0.40	0.77	0.29	78.22	0.0089	20.8	0.0055	1.8	6.5	7948	1143	6805	7878
7	0.40	0.79	0.29	79.97	0.0092	21.6	0.0052	0.1	5.7	6978	583	6394	7179
8	0.41	0.81	0.30	88.57	0.0119	26.7	0.0064	6.4	8.7	10590	2691	7899	8740
9	0.40	0.49	0.23	83.84	0.0098	23.2	0.0046	-3.8	4.1	5057	-625	5682	6215
10	0.40	0.25	0.19	85.25	0.0102	24.0	0.0042	-5.2	3.3	4033	-1092	5125	5602
11	0.22	0.44	0.11	82.88	0.0090	22.0	0.0055	-2.8	5.3	4551	-166	4717	5169
12	0.55	1.10	0.49	82.56	0.0101	23.2	0.0046	-2.5	4.4	6453	-295	6747	7052
13	0.40	0.81	0.30	82.77	0.0097	22.9	0.0049	-2.7	4.6	5678	-293	5971	6400
14	0.42	0.82	0.31	90.23	0.0110	26.1	0.0077	4.8	9.6	11755	2337	9417	9819
15	0.40	0.81	0.30	84.68	0.0083	21.8	0.0063	-4.7	5.8	7065	-685	7750	8323
16	0.40	0.81	0.30	82.89	0.0094	22.5	0.0052	-2.8	5.0	6087	-293	6380	6836
17	0.40	0.80	0.30	80.65	0.0107	23.4	0.0035	-0.6	3.7	4497	195	4302	4707
18	0.40	0.79	0.30	81.18	0.0097	22.5	0.0046	-1.2	4.8	5827	158	5669	6201
19	0.40	0.79	0.29	79.66	0.0101	22.5	0.0042	0.3	4.7	5692	564	5129	5594
20	0.40	0.49	0.22	80.34	0.0102	22.8	0.0041	-0.3	4.4	5341	349	4992	5462

Table B–12 Synapse Prototype – Modeled Output Data (SI units)

	Synapse - SI units												
	Output data (modeled)												
Test number	**ΔP1-1.5**	**ΔP S34**	**Fan power**	**T_S1.5**	**w_S1.5**	**h_S1.5**	**Δw 1-1.5**	**ΔT 1-1.5**	**Δh 1-1.5**	**Q_cooling**	**Q_sensible**	**Q_latent**	**Q_th**
	99	0	kW	°C	kg/kg	kJ/kg	kg/kg	°C	kJ/kg	kW	kW	kW	kW
1	55	0	0.12	30.8	0.0103	57.4	0.0041	-9.9	0.2	0.04	-1.43	1.46	1.46
2	154	0	0.05	31.1	0.0100	57.0	0.0043	-10.2	0.7	0.08	-1.02	1.09	1.09
3	103	185	0.25	30.4	0.0107	57.9	0.0037	-9.5	0.2	0.03	-1.70	1.73	1.73
4	99	194	0.22	28.0	0.0097	53.0	0.0047	-1.3	10.6	1.62	-0.06	1.68	1.88
5	99	192	0.22	27.3	0.0092	50.9	0.0052	-0.6	12.7	1.95	0.07	1.88	2.15
6	99	197	0.22	25.7	0.0089	48.4	0.0055	1.0	15.1	2.33	0.33	1.99	2.31
7	103	200	0.22	26.7	0.0092	50.2	0.0052	0.0	13.3	2.04	0.17	1.87	2.10
8	99	123	0.23	31.4	0.0119	62.1	0.0064	3.6	20.2	3.10	0.79	2.31	2.56
9	99	62	0.17	28.8	0.0098	54.0	0.0046	-2.1	9.6	1.48	-0.18	1.67	1.82
10	54	109	0.14	29.6	0.0102	55.9	0.0042	-2.9	7.7	1.18	-0.32	1.50	1.64
11	137	274	0.09	28.3	0.0090	51.3	0.0055	-1.6	12.4	1.33	-0.05	1.38	1.51
12	100	201	0.37	28.1	0.0101	54.0	0.0046	-1.4	10.2	1.89	-0.09	1.98	2.07
13	104	204	0.22	28.2	0.0097	53.2	0.0049	-1.5	10.8	1.66	-0.09	1.75	1.88
14	101	202	0.23	32.3	0.0110	60.8	0.0077	2.7	22.4	3.45	0.69	2.76	2.88
15	100	202	0.22	29.3	0.0083	50.7	0.0063	-2.6	13.4	2.07	-0.20	2.27	2.44
16	99	198	0.22	28.3	0.0094	52.4	0.0052	-1.6	11.6	1.78	-0.09	1.87	2.00
17	99	198	0.22	27.0	0.0107	54.4	0.0035	-0.4	8.6	1.32	0.06	1.26	1.38
18	99	197	0.22	27.3	0.0097	52.3	0.0046	-0.7	11.1	1.71	0.05	1.66	1.82
19	99	121	0.22	26.5	0.0101	52.5	0.0042	0.2	10.8	1.67	0.17	1.50	1.64
20	0	0	0.17	26.9	0.0102	53.1	0.0041	-0.2	10.2	1.57	0.10	1.46	1.60

Appendix C Numerical Modeling and Experiments for the AIL Research First-Stage HMX

The purposes of this appendix are to (1) show the performance of the AIL Research HMX compared to the numerical model, and (2) illustrate the differences between the Synapse and AIL Research first-stage HMXs and how these differences impact their performance.

C.1 Experimental

The AIL Research HMX is a stack of 41 channel pairs. The dimensions are specified in Table C–1. In addition to slight differences in the dimensions between the AIL Research first-stage HMX and the Synapse first-stage HMX, five other differences relate to the stack structure, the LD distribution method, the water distribution method, the membrane, and the spacer.

Table C–1 Prototype Specifications for Dehumidifier

Dimension	Symbol	Value	Units
Process/supply channel thickness	δ_s	3	mm
Exhaust channel thickness	δ_e	3.67	mm
Plate length	L	190	mm
Plate height	W	560	mm
Total plate thickness	δ_{plate}	0.25	mm
Flocking thickness	$\delta_{flocking}$	0.3	mm
Membrane			
Property	**Symbol**	**Value**	**Units**
Membrane thickness	δ_{mem}	30	μm
Mean pore size	d_{pore}	0.1	μm
Porosity	ε	0.72	
Tortuosity[a]	τ	2.3	
Membrane diffusivity[b]	D_{mem}	0.02	cm^2/s
Membrane thermal conductivity[c]	k_{mem}	0.06	W/m-K

[a] Calculated with relation $\tau = \frac{(2-\varepsilon)^2}{\varepsilon}$

[b] Calculated as in Woods and Kozubal (2012a) for Synapse HMX, except membrane here is unbacked

[c] Calculated as in Woods and Kozubal (2012a) for Synapse HMX

Instead of laminated sheets that were bonded together to make up a channel pair in the Synapse HMX, the AIL Research HMX uses PP extrusions (inexpensive Coroplast sheets).

The LD distribution system, which is proprietary to AIL Research, was also different. The key difference is that the Synapse HMX used several high-pressure-drop holes feeding into the flocking, which ensured even distribution across the plate. The AIL Research HMX used the pressure applied to the stack from the external frame to ensure even distribution. This method, as shown below, was inconsistent; it worked for some plates but not for others.

The water method used in the AIL Research HMX did not use wicked surfaces on the exhaust side to help the water wet the wall surface. This required a higher water flow rate.

The AIL Research HMX used the unbacked version of the backed membrane used in the Synapse HMX. Thus, the properties of the microporous membrane layer are the same, but no correction is required for the membrane backing.

The spacer in the AIL Research HMX is different than that in the Synapse HMX. This spacer is proprietary to AIL Research, and thus the data are not shown, but the heat transfer was measured similarly to the Synapse spacers. The same methods that were used for the Synapse first-stage HMX were used to take the results of these tests and estimate the heat and mass transfer performance of the AIL Research spacer.

The experimental setup for the AIL Research first-stage HMX is the same as that for the Synapse first-stage HMX, except that a sump and a pump were used for the continuous water flow, rather than the mains water pressure used for the once-through, cycled water flow in the Synapse HMX. The test points are shown in Table B–1 (IP units) and Table B–2 (SI units). These include different process and EA flow rates, LD flow rates and concentrations, and inlet air temperatures and humidities.

C.2 Model

The model used for the AIL Research HMX was the same as that used for the Synapse HMX, which is outlined in a separate publication Woods and Kozubal (2012a), except for the different inputs for dimensions and transport coefficients.

C.3 Results and Discussion

C.3.1 Experimental Results

This section focuses on the first-stage of the AIL Research HMX, although some of the presented results are for the AIL Research first- and second-stage HMXs together. The data are used to show two issues with the AIL Research first stage that make the model-predicted values different from the experimentally measured values:

- The model assumes that the LD is distributed evenly from one plate to the next.
- The model assumes a completely wetted surface on the exhaust side, which is the case for the wicked surface in the Synapse HMX.

The Synapse HMX used wicks on the exhaust side. For ease of construction, the AIL Research HMX used the flutes of the Coroplast extrusions as the exhaust side channels. Applying a wick inside these flutes would be difficult, so the AIL Research HMX instead uses a high water flow with no wicked surface. This section shows the effect of this wicked surface by first showing a test point with dry cooling from the first-stage exhaust (no water flow), and then showing a point with evaporative cooling from the first-stage exhaust (with water flow).

Figure C–1 shows the test results for the AIL Research HMX with no first-stage water flow (Test 8). The model does not match the experiments because of the uneven LD distribution, as discussed in the main body of the report. Figure C–2 shows the test results for the AIL Research HMX with continuous first-stage water flow (Test 9). This test is even further from predicted because of the lack of wetting on the exhaust side in addition to the imperfect LD distribution.

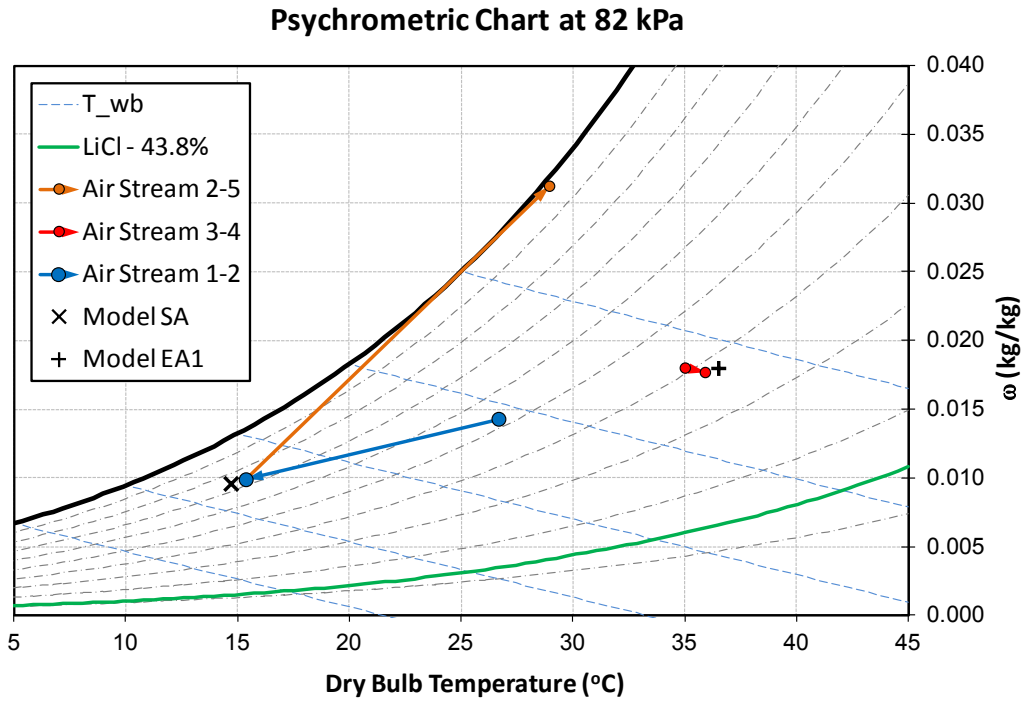

Figure C–1 Test #8, adiabatic test psychrometric chart at 82 kPa

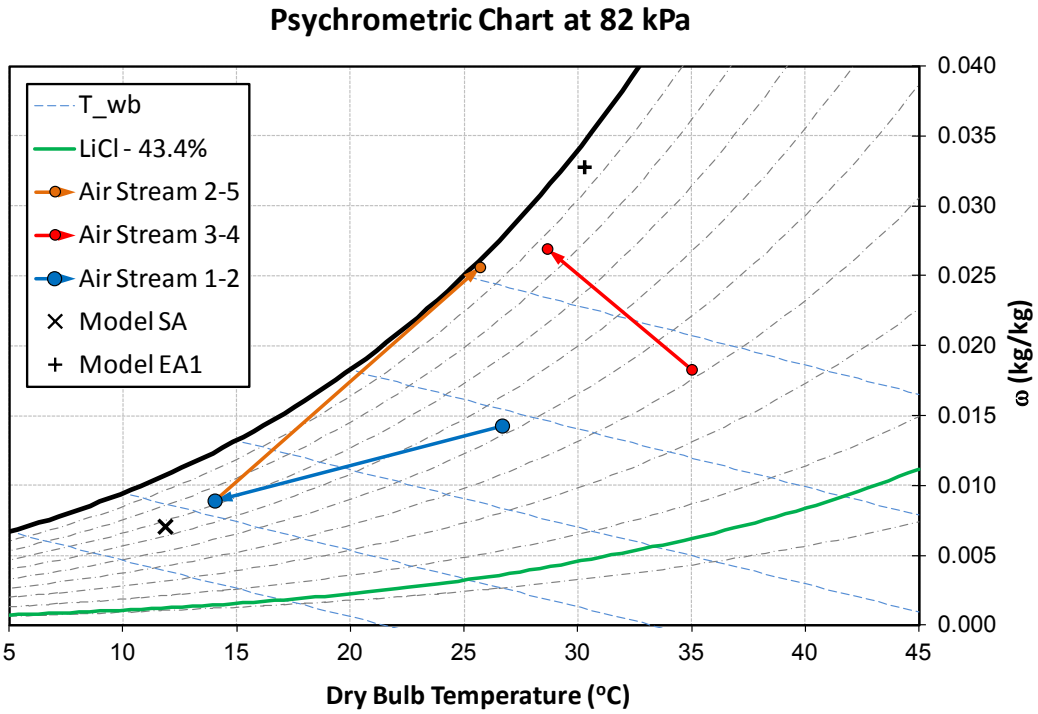

Figure C–2 Test #9 psychrometric chart at 82 kPa

C.3.2 Model-Experiment Comparison

This section compares the experiments and the model predictions for the key first-stage measurement ($\Delta\omega_s$) as well as the total enthalpy change (Δh_s) with the two stages combined.

The model over predicts the change in humidity ratio of the process air for the AIL Research HMX for the reasons discussed above (Figure C–3). On average, the experiments are 22% below the model predictions. This discrepancy is due to the reasons discussed in the previous section.

Figure C–4 shows the model-experiment agreement for the total enthalpy change of the first- and second-stages combined. The disagreement here is almost entirely from the first-stage HMX. As discussed in Section 3.1.2, the second-stage HMX matched the model predictions. On average, the experiments are 17% below the model predictions. This is primarily due to the lower latent cooling in the first-stage, but is also due to lower sensible cooling in the second stage. Even though the model and experiment match for the second stage, the sensible cooling in these tests in the second stage is less than the model prediction because of the higher humidity entering the second stage.

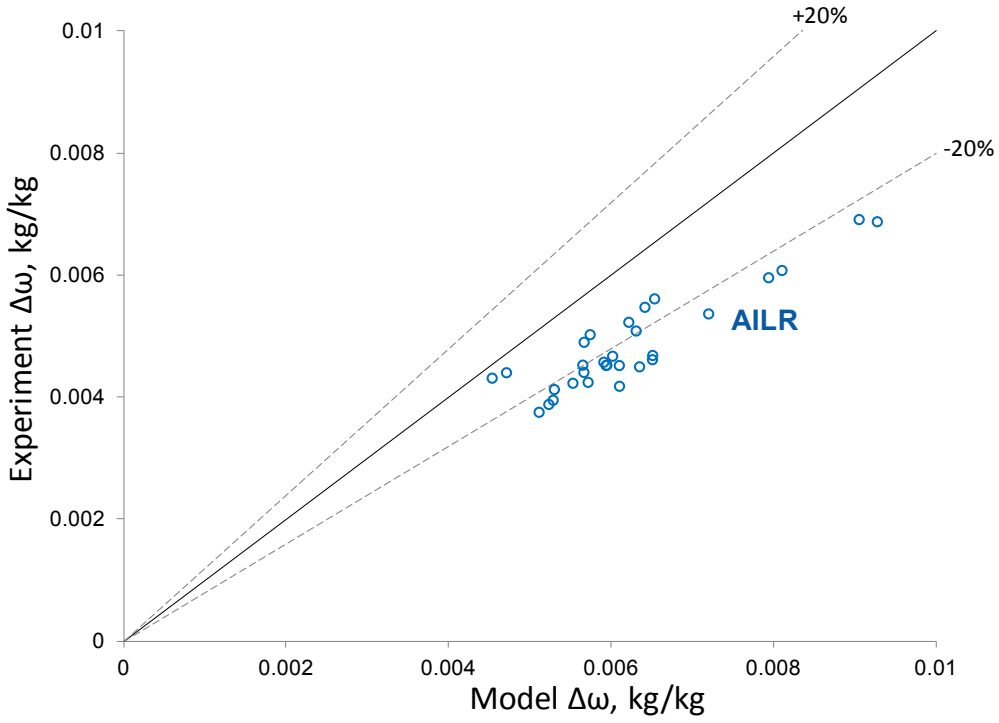

Figure C–3 Model-experiment comparison for change in humidity ratio for AIL Research first-stage

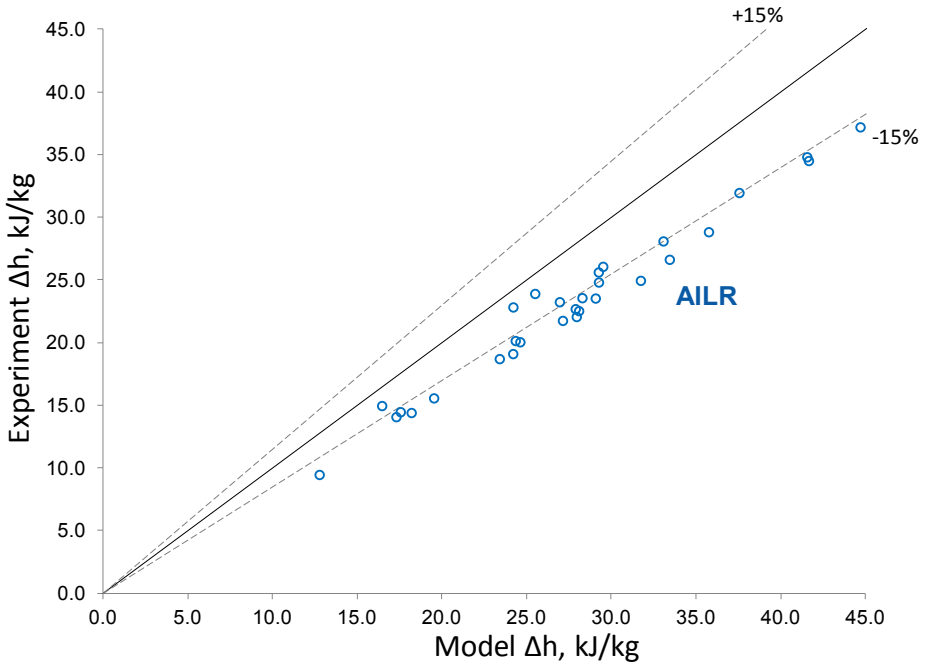

Figure C–4 Model-experiment comparison for change in enthalpy for AIL Research first- and second-stages combined

Appendix D Weight Calculations

Table D–1 Synapse Weights – HMXs
(not selected for packaged unit weight analysis)

	Synapse - stage 1		
Module specs	channel pairs	45	per ton
	Area / ton	10.9	m^2/ton
Headers	Custom synapse spacers		
	header weight	0.01	kg
	Weight / ton	0.9	kg / ton
Separation plate	PET sheet		
	Density	1400	kg/m^3
	Thickness	0.0002	m
	Weight / ton	3.052	kg
Membrane	Backed Celgard membrane		
	Density	225	kg/m^3
	Thickness	0.00008	m
	Weight / ton	0.1962	kg
Support / frame	Spacer (x2)		
	weigth / m^2	0.3896	kg/m^2
	Weight / ton	8.49328	kg
Flocking	Flocking / wick (x2)		
	Density	500	kg/m^3
	Thickness	0.00025	m
	Weight / ton	2.725	kg
Adhesive	Pressure-sensitive adhesive (x2)		
	Density	1000	kg/m^3
	Thickness	0.0001	m
	% area of application	100%	(for all of sheet)
	Weight / ton	2.18	kg
	Stage 1 total	**17.5**	**kg / ton**
		38.6	**lbs/ton**
	Synapse - stage 2		
	Area / ton	45.8	m^2/ton
Flocking	Flocking / wick		
	Density	500	kg/m^3
	Thickness	0.00025	m
	Weight / ton	5.725	kg
Separator	PET sheet		
	Density	1400	kg/m^3
	Thickness	0.00025	m
	Weight / ton	16.03	kg
Adhesive	Pressure sensitive adhesive (x2)		
	Density	1000	kg/m^3
	Thickness	0.0001	m
	% area of application	100%	(for all of sheet)
	Weight / ton	2.18	kg
	Stage 2 total	**23.9**	**kg / ton**
		52.7	**lbs/ton**
	Synapse total (stage 1 + stage 2)	**91.3**	**lbs / ton**

x2 - times 2 since applied to both sides
x1/2 - times 0.5 since 1 unit takes the place of two plates

Table D–2 AIL Research Weight – HMXs

	AILR - stage 1		
Module specs	channel pairs	51	per ton
	Area / ton	12.84	m^2/ton
Headers	Custom silicone headers (x2)		
	header weight	0.025	kg
	Weight / ton	2.55	kg / ton
Separation plate	*no additonal plate; coroplast serves as separator*		
Membrane	Celgard membrane		
	Density	225	kg/m^3
	Thickness	0.00003	m
	Weight / ton	0.08667	kg
Support / frame	coroplast (x1/2)		
	weigth / m^2	0.6	kg/m^2
	%extra for support	10%	
	Weight / ton	4.2372	kg
Flocking	Flocking / wick		
	Density	500	kg/m^3
	Thickness	0.00025	m
	Weight / ton	1.605	kg
Adhesive	Adhesive (x2)		
	Density	1000	kg/m^3
	Thickness	0.0001	m
	% area of application	5%	(around edges)
	Weight / ton	0.1284	kg
	Stage 1 total	**8.6**	**kg / ton**
		18.9	**lbs/ton**
	AILR - stage 2		
	Area / ton	48.63	m^2/ton
Flocking	Flocking / wick		
	Density	500	kg/m^3
	Thickness	0.00025	m
	Weight / ton	6.07875	kg
Separator	Coroplast (x1/2)		
	Density	0.6	kg/m^2
	% extra for support	5%	
	Weight / ton	15.31845	kg
Separator	Adhesive (x2)		
	Density	1000	kg/m^3
	Thickness	0.0001	m
	% area of application	5%	(around edges)
	Weight / ton	0.1284	kg
	Stage 2 total	**21.5**	**kg / ton**
		47.4	**lbs/ton**
	AILR total (stage 1 + stage 2)	**66.3**	**lbs / ton**

x2 - times 2 since applied to both sides

x1/2 - times 0.5 since 1 unit takes the place of two plates

Table D–3 AIL Research Packaged 10-Ton Unit Weight

DEVap, AILR Gen-1

Component	Weight (lbs)	comment
Liquid desiccant	215	20 gallons of 44% LiCl
Tank	15	30 gallon polypropylene cylindrical tank
Shell	201	20-gauge std. steel sheet metal, top and sides
Skid	100	Estimate
Supply fan	90	EBM Papst 6000 cfm plenum fan, K3G500 series
Exhaust fans	100	50 lbs each
Pumps	20	2 Desiccant pumps
Regenerator	225	Estimate from AIL Research for 2-stage regenerator
Stage 1 core	199	See table on AILR stage 1 weight per ton
Stage 2 core	497	See table on AILR stage 2 weight per ton
Water	38	Assuming 50% porous flocking with flocking half filled
Misc.	150	Tubing, plenums, filters, heating coils, hinged doors, fittings
Total	1850	

Table D–4 Gen-2 Weight – HMXs

	Gen-2 - stage 1		
Module specs	channel pairs	40	per ton
	Area / ton	7.53	m^2/ton
Headers	Synapse-design headers		
	header weight	0.01	kg
	Weight / ton	0.8	kg / ton
Separation plate	Polypropylene sheet		
	Density	900	kg/m^3
	Thickness	0.00025	m
	Weight / ton	1.69425	kg
Membrane	Celgard membrane		
	Density	225	kg/m^3
	Thickness	0.00003	m
	Weight / ton	0.0508275	kg
Support / frame	coroplast (frame)		
	weigth / m^2	0.6	kg/m^2
	amount removed	90%	
	Weight / ton	0.4518	kg
Flocking	Flocking / wick (x2)		
	Density	500	kg/m^3
	Thickness	0.00025	m
	Weight / ton	1.8825	kg
Adhesive	Adhesive (x2)		
	Density	1000	kg/m^3
	Thickness	0.0001	m
	% area of application	5%	(around edges)
	Weight / ton	0.0753	kg
	Stage 1 total	**5.0**	**kg / ton**
		10.9	**lbs/ton**

	Gen 2 - stage 2		
	Area / ton	21.31	m^2/ton
Flocking	Flocking / wick		
	Density	500	kg/m^3
	Thickness	0.00025	m
	Weight / ton	2.66375	kg
Separator	Aluminum		
	Density	2700	kg/m^3
	Thickness	0.00015	m
	Weight / ton	8.63055	kg
Separator	Adhesive (x2)		
	Density	1000	kg/m^3
	Thickness	0.0001	m
	% area of application	5%	(around edges)
	Weight / ton	0.0753	kg
	Stage 2 total	**11.4**	**kg / ton**
		25.0	**lbs/ton**
	Gen-2 total (stage 1 + stage 2)	**35.9**	**lbs / ton**

x2 - times 2 since applied to both sides

x1/2 - times 0.5 since 1 unit takes the place of two plates

Table D–5 Gen-2 Packaged 10-Ton Unit Weight

DEVap, Gen-2

Component	Weight (lbs)	comment
Liquid desiccant	215	20 gallons of 44% LiCl
Tank	15	30 gallon polypropylene cylindrical tank
Shell	167	20-gauge std. steel sheet metal, top and sides
Skid	100	Estimate
Supply fan	90	EBM Papst 6000 cfm plenum fan, K3G500 series
Exhaust fans	100	50 lbs each
Pumps	20	2 Desiccant pumps
Regenerator	225	Estimate from AIL Research for 2-stage regenerator
Stage 1 core	114	See table on Gen-2 stage 1 weight per ton
Stage 2 core	263	See table on Gen-2 stage 2 weight per ton
Water	18	Assuming 50% porous flocking with flocking half filled
Misc.	150	Tubing, plenums, filters, heating coils, hinged doors, fittings
Total	1477	

Table D–6 High-Efficiency 10-Ton Vapor Compression Unit Weight

Vapor Compression Unit With 14.5 IEER	
Component	**Weight**
Baseline	1372 lb
Economizer	36 lb
Hinged doors	12 lb
Reheat coil	53 lb
Total	1473 lb

Appendix E Cost Calculations

Table E–1 AIL Research Cost Spreadsheet – HMXs

	(Metric units)			(IP units)		
Design	1st stage	2nd stage		1st stage	2nd stage	
plate length	0.231	0.584	m	0.8	1.9	ft
plate height	0.546	0.457	m	1.8	1.5	ft
area / ton-modeled	12.84	48.63	m^2/ton	138	523	ft^2/ton
channel pairs / ton	51	91	# / ton	51	91	# / ton
Coroplast						
coroplast / plate	0.5	0.5		0.5	0.5	
m^2 / ton	6.4	24.3	m^2	69.1	261.7	ft^2
Aluminum						
sheets / plate	0	0		0	0	
m^2 / ton	0.0	0.0	m^2	0.0	0.0	ft^2
Membrane						
membranes / plate	1	0		1	0	
m^2 / ton	12.8	0.0	m^2	138.2	0.0	ft^2
Flocking / Wick						
wicked surfaces / plate	1	1		1	1	
m^2 / ton	12.8	48.6	m^2	138.2	523.4	ft^2
Desiccant headers						
# / channel pair	1	0		1	0	
# / ton	51	0		51	0	

Unit costs			% waste *
Coroplast	2.41	$/m^2	0.1
Aluminum sheet	1.5	$/m^2	0
Membrane	2.69	$/m^2	0.02
Flocking	1.02	$/m^2	0.02
Headers	2.52	$/header	0
Labor (stage1)	1.5	$/plate pair	* inactive area included in area/ton
Labor (stage2)	2.5	$/plate pair	

Costs per ton	1st stage	2nd stage	Total
Coroplast	$17	$64	$81
Aluminum	$0	$0	$0
Membrane	$35	$0	$35
Flocking	$13	$51	$64
Headers	$129	$0	$129
Total materials	$194	$115	$309
Total materials	$194	$115	$309
Labor	$77	$228	$304
Total costs	$271	$343	$613

shaded cells = inputs

unshaded cells = calculations

Table E–2 AIL Research Cost Spreadsheet – Full AC

A/C Mark-ups	Mark-up	Total Mark-up to retail	Total Mark down to mfg cost
1 - Manufacturer	1.23	2.35	1.23
2 - Distributer	1.49	1.91	1.83
3 - Retailer	1.28	1.28	2.35
4 - Retail cost	1.00	1.00	

Component cost estimates		Cost Estimate	Price Level	Markup		Retail Cost	Comments
$/ton, core	$	613	1	2.35	$	1,438	
$/kg LiCl	$	18	4	1.00	$	18	$/kg anhydrous
Total fixed costs					$	8,897	
2-stage regenerator	$	2,700	1	2.35	$	6,334	AILR Estimate -e-mail correspondance
Tank	$	100	4	1.00	$	100	30 gal tank
Supply/mixed-air fan	$	360	4	1.00	$	360	Based on AILR estimate
Exhaust fan	$	300	4	1.00	$	300	Based on AILR estimate
Gas furnace	$	400	4	1.00	$	400	
Electronics	$	400	4	1.00	$	400	Estimate from Coolerado
Packaging	$	600	3	1.28	$	768	Estimate from Coolerado distribution cost
2 desiccant pumps	$	60	4	1.00	$	60	pumps, 5 gpm each
Solenoid	$	75	4	1.00	$	75	retail estimate
Filters	$	25	4	1.00	$	25	retail estimate
Pressure regulator	$	75	4	1.00	$	75	retail estimate

System size		10.0	*tons*
LiCl storage density		7.3	kg/tonh_L
LiCl storage		0.6	*0.5 hours + 20% for pipe volumes*
LiCl required		43.8	kg
LiCl cost	$	771	

System Retail Cost	$	24,052	*10-ton system cost with 30-min storage*
Mark-up level to estimate cost		4	
Mark-up factor		1.00	
Total system cost at level shown above	$	24,052	

shaded cells = inputs

unshaded cells = calculations

Table E–3 Gen-2 Cost Spreadsheet – HMXs

	(Metric units)			(IP units)		
Design	1st stage	2nd stage		1st stage	2nd stage	
plate length	0.186	0.4	m	0.6	1.3	ft
plate height	0.5	0.45	m	1.6	1.5	ft
area / ton (modeled)	7.53	21.31	m^2/ton	81	229	ft^2/ton
channel pairs / ton	40	59	# / ton	40	59	# / ton
Coroplast						
coroplast / plate	1	0		1	0	
m^2 / ton	7.5	0.0	m^2	81.1	0.0	ft^2
Aluminum						
sheets / plate	0	1		0	1	
m^2 / ton	0.0	21.3	m^2	0.0	229.4	ft^2
Membrane						
membranes / plate	1	0		1	0	
m^2 / ton	7.5	0.0	m^2	81.1	0.0	ft^2
Flocking / Wick						
wicked surfaces / plate	2	1		2	1	
m^2 / ton	15.1	21.3	m^2	162.1	229.4	ft^2
Desiccant headers						
# / channel pair	2	0		2	0	
# / ton	80	0		80	0	

Unit costs		
Coroplast	2.41	$/m^2
Aluminum sheet	1.5	$/m^2
Membrane	2.69	$/m^2
Flocking	1.02	$/m^2
Headers	1	$/header
Labor (stage1)	1.5	$/plate pair
Labor (stage2)	2.5	$/plate pair

% waste + inactive area
0.15
0.02
0.05
0.05
0

Costs per ton	1st stage	2nd stage	Total
Coroplast	$21	$0	$21
Aluminum	$0	$33	$33
Membrane	$21	$0	$21
Flocking	$16	$23	$39
Headers	$80	$0	$80
Total materials	$138	$55	$194
Total materials	$138	$55	$194
Labor	$60	$148	$208
Total costs	$198	$203	$401

shaded cells = inputs

unshaded cells = calculations

Table E–4 Gen-2 Cost Spreadsheet – Full AC

A/C Mark-ups	Mark-up	Total Mark-up to retail	Total Mark down to mfg cost
1 - Manufacturer	1.23	2.35	1.23
2 - Distributer	1.49	1.91	1.83
3 - Retailer	1.28	1.28	2.35
4 - Retail cost	1.00	1.00	

Component cost estimates	Cost Estimate	Price Level	Markup	Retail Cost	Comments
$/ton, core	$ 401	1	2.35	$ 941	From HMX core calculations
$/kg LiCl	$ 18	4	1.00	$ 18	$/kg anhydrous
Total fixed costs				$ 8,897	
2-stage regenerator	$ 2,700	1	2.35	$ 6,334	AILR Estimate -e-mail correspondance
Tank	$ 100	4	1.00	$ 100	30 gal tank
Supply/mixed-air fan	$ 360	4	1.00	$ 360	Based on AILR estimate
Exhaust fan	$ 300	4	1.00	$ 300	Based on AILR estimate
Gas furnace	$ 400	4	1.00	$ 400	
Electronics	$ 400	4	1.00	$ 400	Estimate from Coolerado
Packaging	$ 600	3	1.28	$ 768	Estimate from Coolerado distribution cost
2 desiccant pumps	$ 60	4	1.00	$ 60	pumps, 5 gpm each
Solenoid	$ 75	4	1.00	$ 75	retail estimate
Filters	$ 25	4	1.00	$ 25	retail estimate
Pressure regulator	$ 75	4	1.00	$ 75	retail estimate

System size	10.0	*tons*
LiCl storage density	7.3	kg/tonh_L
LiCl storage	0.6	*0.5 hours + 20% for pipe volumes*
LiCl required	43.8	kg
LiCl cost	$ 771	

System Retail Cost	$ 19,079	*10-ton system cost with 30-min storage*
Mark-up level to estimate cost	4	
Mark-up factor	1.00	
Total system cost at level shown above	$ 19,079	

shaded cells = inputs
unshaded cells = calculations